QC
918
B37

UC-NRLF
$B 60 822

LIBRARY
OF THE
UNIVERSITY
OF
CALIFORNIA

PHYSICS

PHYSICS LIBRARY

CONDENSATION OF VAPOR AS INDUCED BY NUCLEI AND IONS

FOURTH REPORT

By CARL BARUS
Hazard Professor of Physics, Brown University

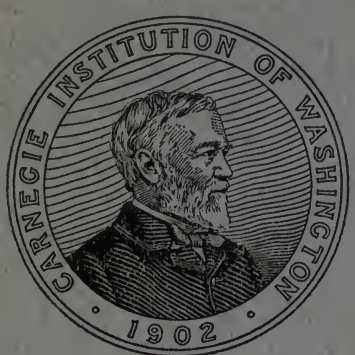

WASHINGTON, D. C.:
Published by the Carnegie Institution of Washington
1910

CONDENSATION OF VAPOR AS INDUCED BY NUCLEI AND IONS

FOURTH REPORT

By CARL BARUS
Hazard Professor of Physics, Brown University

WASHINGTON, D. C.:
Published by the Carnegie Institution of Washington
1910

PHYSICS LIBRARY

CARNEGIE INSTITUTION OF WASHINGTON
PUBLICATION NO. 96 (PART 2)

B37
PHYSICS
LIBRARY

PREFACE.

In Chapter I of the present publication the investigations on the residual nuclei of pure water (compare Carnegie Institution of Washington Publication No. 96, Chapter V, 1908) have been resumed with regard to the size and persistence of such nuclei. These are obtained by the precipitation of water on the nuclei of pure water vapor, in a dust-free fog chamber, by sudden cooling. The fog particles so produced evaporate to water nuclei on compression, the number of the latter as compared with the former being greater as the evaporation of fog particles is more rapid and as their size is larger. In the extreme case nearly 50 per cent of the fog particles were represented by these residual water nuclei. It is a curious observation that whereas the relatively enormous fog particles of pure water evaporate at once beyond the range of visibility, such evaporation stops in cases of certain of the invisible water particles (0.5 to 50 per cent of the total number of fog particles) as the evaporation is more rapid in the manner specified. The remaining fog particles evaporate completely. It was impossible to detect any electrical effect due to rapid evaporation. The cause of these phenomena is difficult to ascertain, but it may be suspected that it is associated with the composite nature of the molecule of liquid water.

The first part of Chapter II contains further studies of the optics of coronas. It was shown that the interference phenomenon superimposed upon the diffraction phenomenon in the case of coronas may be treated in a way similar to the lamellar grating, consisting of a uniform succession of alternate strips of thin and thicker transparent glass. Given types of coronas are reproduced in successively increasing size, when the respective fog-particle diameters are in the ratio of . . . . 5, 4, 3, 2, 1, 0. The ratio of fog-particle diameters d and interference plate thickness D for the same color minimum in the interferences and a film of water is $d/D=n(n-1)$, where n is the index of refraction of water. The experimental value of d/D agrees well with this. It must therefore be possible to compute the nucleation corresponding to a given corona purely from optical considerations of diffraction and interference, as indicated. To further verify the theory suggested, special study was made of the axial or interference colors of coronas by the aid of large drum-shaped chambers 2 meters long.

The coronas obtained with electric light are almost too complicated for practice, for which reason a part of the mantle of a Welsbach burner

M6634?5

has usually been used as a source of light. Much better results are obtained, however, by the use of the virtually monochromatic mercury lamp as a source. This is sufficiently intense and admits a more definite optical interpretation. Experiments are therefore given in the second part of Chapter II, with a view to standardizing these simplified coronas by the method of successive exhaustions and phosphorus nuclei.

The third part of the chapter gives an account of further progress made in increasing the efficiency of the fog chamber by reducing its size compatibly with the use of a new type of goniometer.

In an endeavor to standardize the coronas in terms of the nucleation involved, by the aid of separate small sealed aluminum tubes containing radium, used singly or in groups, very little progress was made, because the coronal diameter varies as the sixth root of the intensity of ionization. The experiments of Chapter III, however, lead to certain remarkable results on the distribution of ionization with reference to the position within the fog chamber of the sealed aluminum tubelets (beta and gamma rays being in question, largely the latter).

If the parts of the fog chamber consist of different materials or not, the maximum ionization due to primary and secondary radiation rarely coincides with the position of the radium. In a horizontal cylindrical fog chamber, closed at one end and open for exhaustion at the other, the maximum ionization is found to move from the closed end to the exhaustion end as the radium moves from the closed end to the middle of the chamber. As the radium moves further the maximum remains near the exhaustion end, but the ionization diminishes in marked degree throughout the whole chamber. The ratios of ionization are frequently greater than 2 to 1. To obtain maxima of ionization near the middle of the chamber the sealed radium tube must be near the closed end. In other adjustments even minimum ionization was produceable in the middle, as compared with the ends. It appears from the results that it is possible to appreciably displace the ions during the period of exhaustion, the rate of reproduction being insufficiently rapid as compared with the displacement.

In a final investigation, Chapter IV, the endeavor is made to standardize the coronas in relation to the number of fog particles represented under given circumstances of exhaustion by aid of Thomson's electron and correlative constants. After a number of trials the first successful method consisted in making a closed aluminum tube, containing an even distribution of radium, the core of a cylindrical condenser, leaded to an inch or more in thickness without. This core was suspended axially from fine wire leading to Dolezalek's electrometer for the measurement of the small voltages and currents involved. The core in question was then removed from the electrical condenser and put into the axis of a dust-

free fog chamber, where the nucleation (ionization) was found from the constants of the coronas obtained upon exhaustion, or *vice versa.*

Using the method which depends essentially on the known velocity of the ions in the unit electric field and my earlier values of the constants of coronas, a few rough tests of the charge of the electron gave consistent values. There was, however, an inherent difficulty of great importance, the nature of which has already been referred to—the ionization differs in different parts of the fog chamber and the extreme ratios may exceed 2 to 1. It does not follow, therefore, that the mean ionization observed in the fog chamber is the same as that obtaining within the heavy leaded electrical condenser. To secure this identity the fog chamber itself must be the condenser.

The method was, therefore, varied by using the cylindrical fog chamber (glass wet within, put to earth) with its axial core of charged aluminum tube both as an electrical condenser for the measurement of current and as a fog chamber for the measurement of ionization. The end of the aluminum tube within the fog chamber is hermetically sealed; the other is open without for the introduction of the sealed tubelets containing radium. By properly adjusting these along the axis an approximately uniform ionization within the fog chamber is obtainable. The trials made seemed promising enough to make it worth while to repeat the determination of e by Thomson's method, using, however, the mercury lamp as a source of light and a purely optical method for the measurement of the nucleation as suggested above. Results will be given in a later report.

The correlative method of determining e in terms of the decay constant of the ionization has also been tried. If N be the number of ions in the fog chamber due to the radium in the aluminum tube when the latter is not charged and n the number when it is charged the constant e may be written

$$e = C\dot{V}/(b(N^2 - n^2)v)$$

where C is the capacity and v the volume of the cylindrical condenser fog chamber and $\dot{V}$ the (constant) fall of potential of the core per second, due to the current passing through the ionized air within the chamber. In this case very large potentials (250 volts) may be used, and a graduated Exner electroscope suffices for the measurement of $\dot{V}$.

The experiments by the decay method in the second part of Chapter IV, made for the present merely to test the standardization of the fog chamber, as detailed in the earlier publications of the Carnegie Institution of Washington, nevertheless lead to very acceptable values of e, even at the enormous ionizations (exceeding 500,000 nuclei per cubic centimeter) employed.

The values for e in Chapter IV were too high, even with the admission that negative ions only are caught in the fog chamber employed. The

method is, therefore, repeated in Chapter V with greater detail. Condenser and fog chamber are now identical, and the data obtained are of reasonable value.

In Chapter VI, finally, the effect of incidental voltaic contacts occurring in Chapter V is critically studied, with a view to using a condenser whose parts are of different metals separated by an ionized medium for the measurement of voltaic potentials.

My thanks are due to Miss Laura C. Brant for efficient assistance throughout the course of this work.

Carl Barus.

Brown University,
Providence, R. I., August 1, 1909.

CONTENTS.

CHAPTER I.—*Nuclei of Pure Water.*

Page.

1. Introductory 1
2. Rapid evaporation of fog particles. Phosphorus nuclei. Table 1; fig. 1 1
3. Spontaneous evaporation of fog particles. Phosphorus nuclei. Table 2 3
4. Slow spontaneous evaporation of fog particles. Vapor nuclei. Table 3 4
5. Rapid evaporation of fog particles. Vapor nuclei. Table 4 7
6. Evaporation retarded as the diameter of fog particles decreases 8
7. Time losses. Table 5 8
8. Effect of changes of the drop of pressure 10
9. Exceptionally rapid evaporation 11
10. Conclusion 11
11. The same, continued 12
12. The same, continued 13
13. The same, continued 13
14. Statistical hypothesis 14

CHAPTER II.—*Standardization and Efficiency of the Fog Chamber.*

AXIAL COLORS AND INTERFERENCES.

15. Introductory 15
16. Causes of axial colors. Table 6 15
17. The lamellar grating 16
18. Disk colors of coronas 16
19. Experiments with long tubes. Table 7; fig. 2 17
20. Short tubes. Table 8 19

CORONAS WITH MERCURY LIGHT.

21. Preliminary survey 20
22. Apparatus 21
23. Equations 21
24. Data with white light. Table 9; fig. 3 22
25. Data with green mercury light. Tables 10 and 11; figs. 4 to 9 24
26. Inferences. Interference and diffraction. Table 12 31

EFFICIENCY OF LARGE AND SMALL FOG CHAMBERS ATTACHED TO THE SAME VACUUM CHAMBER.

27. Fog chambers 33
28. Data. Table 13; fig. 10 34
29. Data for apertures. Table 14; fig. 11 37
30. Results 39
31. Conclusion 39

CHAPTER III.—*Regions of Maximum Ionization and Miscellaneous Experiments.*

REGIONS OF MAXIMUM IONIZATION DUE TO GAMMA RADIATION.

32. Introductory 41
33. Short fog chamber 41
34. Behavior after removal of radium 42
35. Long fog chamber 43
36. Data. Table 15; figs. 12 to 15 43
37. Inferences 47

MISCELLANEOUS EXPERIMENTS. Page.

38. Experiments to detect the region of positive ions. Table 16; fig. 16..... 48
39. Radium within the fog chamber. Sealed tubes. Table 17..... 50
40. Distance effect. Table 18..... 51
41. Attempt to calibrate the fog chamber with five separate sealed tubelets of radium. Tables 18 and 19..... 51

CHAPTER IV.—*The Standardization of the Fog Chamber by Aid of Thomson's Electron.*

THE CONSTANT *e*, EXPRESSED IN TERMS OF VELOCITIES OF THE IONS.

42. Advantages..... 54
43. Plate. Fig. 17..... 54
44. Cylinder. Fig. 18..... 55
45. The same. Preliminary data. Table 20..... 56
46. The same. Wires surrounded by earthed pipes..... 57
47. Conclusion..... 58

THOMSON'S CONSTANT *e*, EXPRESSED IN TERMS OF THE DECAY CONSTANT OF IONS WITHIN THE FOG CHAMBER.

48. Introductory..... 59
49. Electrical condenser fog chamber..... 59
50. Auxiliary condenser..... 60
51. Methods..... 61
52. Data disregarding external gamma rays. Table 21..... 61
53. Further data. Table 22..... 63

CHAPTER V.—*The Elecíron Method of Standardizing the Coronas of Cloudy Condensation in Terms of the Velocities of the Ions.*

54. Introductory..... 65
55. Apparatus. Fig. 19..... 65
56. Auxiliary electrical condensers..... 66
57. Methods pursued..... 67
58. Data. High ionization currents. Table 23..... 69
59. The same. Coronas..... 70
60. The same. Summary. Figs. 20 and 21..... 71
61. Data. Moderate ionization. Electrical currents..... 72
62. The same. Coronas..... 72
63. The same. Summary. Figs. 22 and 23..... 72
64. Data. Small ionizations. Electric currents..... 74
65. The same. Coronas..... 74
66. The same. Summary. Figs. 24 and 25..... 74
67. Conclusion..... 75

CHAPTER VI.—*Electrometric Measurement of Voltaic Potential Difference between the Conductors of the Condenser Separated by an Ionized Medium.*

68. Introductory. Fig. 26..... 76
69. Theory..... 78
70. Data. Origin of the electrometer current. Fig. 27..... 80
71. Aluminum core charged with radium tubelets. Table 24; fig. 28..... 82
72. Results. Ionization and voltaic contact potential difference..... 82
73. Voltaic contacts: aluminum-zinc, aluminum-copper, aluminum-aluminum. Table 25; fig. 29..... 82
74. Further experiments and conclusion..... 83

CHAPTER I.

NUCLEI OF PURE WATER.

1. Introductory.—In case of a fog chamber but 4 cm. high and broad and lined with wet cloth, I was surprised to find that if each of a succession of fogs precipitated on phosphorus nuclei is allowed to (apparently) subside, *i. e.*, to be completely dissipated without influx of air before the next exhaustion is made, it nevertheless takes about 10 or 12 exhaustions before all the nuclei are precipitated. It follows, therefore, that for very small fog particles the dissipation by evaporation in originally* saturated air is enormously more important than the dissipation by subsidence. The fog particles do not, however, vanish completely, but the evaporation terminates in persistent solutional water nuclei, large enough to keep the air bluish or hazy.

If the same experiment is made with rigorously dust-free air and vapor nuclei, the fog particles vanish almost completely in a single slow evaporation, so that but one additional exhaustion is needed to quite clear the fog chamber. Very few water nuclei (several per cent) are left behind in this case. The number increases when the evaporation is more and more accelerated by the rapid influx of dust-free air.

It is this feature of the experiment, the tendency of the water nuclei left after precipitation of dust-free wet air on the vapor nuclei of its own medium to persist in proportion as the evaporation is faster (more or less compression or rise of temperature), that is the chief burden of the present paper. The fact that water nuclei may persist, while the enormously larger fog particles from which they have been obtained all but evaporate, is the interesting part of this result. Some restraining tendency† must therefore be evoked by which the accelerating effect of convexity is much more than canceled, for the nuclei here in question are produced in rigorously dust-free air by the precipitation of water vapor on water vapor. A solutional effect is therefore absent.

To investigate the question it is expedient to begin with a medium of phosphorus or solutional nuclei, to subject the fogs thereupon to more or less rapid evaporation, and thereafter to compare these results with the corresponding case for vapor nuclei.

2. Rapid evaporation of fog particles. Phosphorus nuclei.—In the following experiments I have endeavored to trace these results quantita-

*Probably the rise of temperature is sufficiently rapid to render saturated air from which a fog has been precipitated temporarily unsaturated.

†The earlier work has been quoted in Part I of Publication No. 96, Carnegie Institution of Washington.

tively. For this purpose fog particles precipitated on phosphorus nuclei were successively evaporated as rapidly as possible by compression (influx of air), so as to make the loss by subsidence negligible except at the end of the series, when so few nuclei are present that the precipitate is rain-like. In such a case the only loss of nuclei is due to the exhaustion, as the normal time loss* is relatively small. In table 1, taken from an earlier report,† I have given a typical case, the exhaustion ratio being $y=0.78$, nearly. As dust-free air is introduced after each exhaustion the successive nucleations are clearly in geometric progression. As long as the nucleation is less than 100,000, subsidence may be disregarded, as the

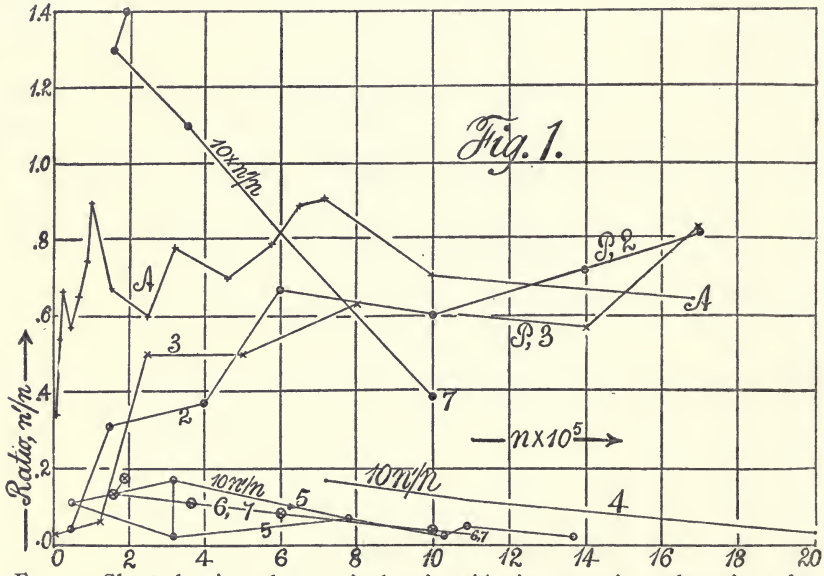

FIG. 1.—Chart showing the survival ratio, n'/n, in successive exhaustions, for phosphorus nuclei (A, 2, 3,) and water nuclei (4, 5, 6, 7). Scale of latter magnified ten times.

curves A in fig. 1 show. The table also contains the angular diameters $\phi=s/30$ of the coronas and the nucleations n computed therefrom. Finally the ratios n'/n of the successive nucleations n and n' are given in each case. These should be equal to the exhaustion ratio if no other loss of nuclei occurs. In fact, if we take the data above $n=100{,}000$ the mean ratio of the ten cases is $n'/n=0.76$, agreeing practically with $y=0.78$.

If we plot the successive ratios n'/n in terms of n, the results show a jagged curve oscillating about $n'/n=0.78$, but descending rapidly below $n=10^5$ as the result of subsidence. (Compare curve A, fig. 1.) The irregularity of the curve is inevitable, as it corresponds to a ratio between two large coronas whose outlines are no longer sharp; but there is compensation in the successive values, as the curve, taken as a whole, indicates.

*Compare chapter II.

†Carnegie Institution of Washington Publication No. 96, chap. III, table 17, 1908.

TABLE 1.—Quick evaporation. (Reproduced from Carnegie Institution of Washington Publication No. 92, chap. III, table 17, 1908.) $y=0.779$.

SERIES A.

Corona.	s.	$n\times10^{-3}$.	Ratio n'/n.	Corona.	s.	$n\times10^{-3}$.	Ratio n'/n.
w r	....	1500	0.67	g	7.8	100	0.69
w v	....	1000	.71	o	7.5	89	.74
s b	....	715	.91		6.8	66.5	.65
b p	....	650	.89		5.9	63.0	.57
g	....	580	.79		4.9	24.6	.66
g y	13	460	.70		4.2	16.3	.53
w o	11.7	320	.78		3.4	8.7	.35
w r	10.5	250	.60		2.4	3.0	.40
w p	9.0	152	.67		1.8	1.2	....

3. Spontaneous evaporation of fog particles. Phosphorus nuclei.—With the above data one may now compare the corresponding cases for very slow evaporation, in which the fog has disappeared spontaneously in the lapse of time, apparently by subsidence, but in greater measure by evaporation. Part 1 of table 2 shows the results obtained in a very long (2 meters) brass tube, lined with wet cloth but 4 cm. high and broad. Twelve exhaustions are needed for removing the nucleation, in spite of the spontaneous disappearance of each individual fog. The disappointing feature about these experiments with 2-inch tubes is the total absence of disk or axial color throughout. They were made in the hope that such colors would appear.

In parts 2 and 3 of the table these observations are continued, but now, with a glass fog chamber, where the line of vision passes through but 8 cm. of fog as compared with 200 cm. above. The exhaustion ratio is $y=0.78$, as in table 1. Besides the disk color of coronas, the successive nucleations n and the nucleation ratios n'/n are given. These ratios are also constructed in fig. 1 in terms of n, in the curves 2 and 3 of the chart. Notwithstanding the complete apparent subsidence, nine exhaustions are needed to clean the fog chamber of these solutional nuclei; but the effect of subsidence is here unmistakable at least below $n=10^6$ nuclei per cubic centimeter. From a smooth curve, embodying series 2 and 3, the subsidence effect, together with other permanent loss, may be stated as follows ($y=0.78$). The approximate diameter is d.

10^6d	$10^{-3}n$	Exhaustion loss.	n'/n.	Subsidence loss.	Evaporation to water nuclei.
cm.					
164	1500	0.22	0.76	0.02	0.98
189	1000	.22	.68	.10	.90
203	800	.22	.63	.15	.85
225	600	.22	.56	.22	.78
255	400	.22	.48	.30	.70
320	200	.22	.30	.48	.52

From these data it appears that above $n = 200{,}000$ nuclei dissipation is due more and more largely to evaporation; below $n = 2 \times 10^5$ more and more largely to subsidence. Above $n = 10^5$ or $d = 0.003$ cm., moreover, the tube in part 1 remains permanently hazy and the fogs (if seen through some thickness) quite black.

TABLE 2.—Persistence of solutional water nuclei. Shows number of exhaustions to clean with complete (apparent) subsidence.

Exhaustion No.	Corona.	$n \times 10^{-3}$	Ratio.	Exhaustion No.	Corona.	$n \times 10^{-3}$	Ratio.
Part 1.—Phosphorus emanation. Long brass tube; length 200 cm.; diameter 5 cm.; cloth lined. Barometer 77.15 at 20°. $\delta p_3 = 17$ cm., about. Each fog apparently falls out. Time consumed, about 30 minutes.							
1	black	....	....	7	corona	....	....
2	black	....	....	8	corona	....	....
3	black	....	....	9	corona	....	....
4	translucent	....	....	10	faint cor.	....	....
5	fawn	....	....	11	very faint	....	....
6	fog	....	....	12	very faint	....	....
Part 2, series 2.—Glass fog chamber (observations transverse); length 45 cm.; diameter 12 cm.; height of cloth 8 cm. Each fog allowed to fall out or dissipate. Two sources. Barometer 77.75 at 20°. $\delta p_3 = 17$; $\delta p_3/p = 0.205$. Time consumed, 27 minutes. Fogs dissipate into blue haze.							
1	Fog r′	....	....	7	$s = 9$; g	150	0.31
2	Fog r′	1700	0.82	8	$s = 5$; cor.	46	.04
3	Fog c′	1400	.72	9	$s = 15$; cor.	2	....
4	Fog v	1000	.60	10	....	....	....
5	g	600	.67	11	....	....	....
6	$s = 12$; o	400	.37	12	....	....	....
Part 3, series 3.—Repeated. Same glass fog chamber. Same time, about. No. 4 still evaporates to blue haze.							
1	Fog	....	....	6	$s = 105$; c	250	0.50
2	$s = 163$; r	1700	0.83	7	$s = 70$; cor.	125	.06
3	$s = 147$; c	1400	.57	8	$s = 27$; cor.	7	.03
4	$s = 143$; g b	800	.63	9	$s = 10$; cor.	2	....
5	$s = 130$; g y	500	.50				

4. Slow spontaneous evaporation of fog particles. Vapor nuclei.—We may now contrast with the preceding the evaporation of fog particles precipitated on the vapor nuclei of dust-free air. Table 3 contains the results arranged on a plan similar to the above. A slight difference of procedure is necessary, because the vapor nuclei are not caught in sufficient quantity except at very high exhaustion. Moreover, these exhaustions have no effect in removing vapor nuclei, as these are instantly reproduced by the kinetic mechanism. The water nuclei, however, should be precipitated at an exhaustion less than the fog limit of dust-free air. Beyond this the exact value of the exhaustion ratio $y = 0.71$ to 0.77 is of no importance, because the ratio of successive nucleations, n'/n is usually less than

1 per cent, showing that almost all nuclei have vanished in the first evaporation of the corresponding fog particles. The curves Nos. 4 and 5, fig. 1, give these results on a scale *ten times larger* than the preceding, to bring out the small values n'/n, which would vanish on the scale adopted for the solutional nuclei. For reasons which do not clearly appear, the data in series 4 are larger than corresponding results in series 5, possibly

TABLE 3.—Persistence of water nuclei when fogs are precipitated on vapor nuclei. Glass fog chamber. $\delta p_3 = 32$ for vapor nuclei; $\delta p_3 = 22$ or 23 for water nuclei. Lower $\delta p = 22$ or 23 is above fog limit, but vapor nuclei are inactive.

δp_3	Corona.	$n \times 10^{-3}$	Ratio.	δp_3	Corona.	$n \times 10^{-3}$	Ratio.
Part 1, series 4.—Barometer 77.75 at 20°.							
32	$s_1 = 108$; o	720	0.017	42	$s_1 = 150$; g	2170	0.003
22	$s_2 = 30$	12.4		23	$s_2 = 25$	6.9	
36	$s_1 = 120$; y	1080	0.012				
	$s_2 = 31$	13.3					
Part 2, series 5.—Repeated in glass fog chamber. Barometer 75.77 at 22°.							
39	$s_1 = 130$; g	1370		27	$s_1 = 45$	47	
17	$s_2 = 20$	3.0	0.002	17	$s_2 = 12$	.5	0.001
36	$s_1 = 120$; g	*1090		28	$s_1 = 84$; p	320	
17	$s_2 = 24$	5.1	.005	17	$s_2 = 12$	.5	.002
32	$s_1 = 122$; g	†1030		28	$s_1 = 85$; p	326	
17	$s_2 = 19$	2.6	.002	17	$s_2 = 25$	5.5	.007
29	$s_1 = 111$; r o	780					
17	$s_2 = 25$	5.5	.007				

*Long waiting (30^m) for s_2. †No waiting (1^m) for s_2.

because the exhaustion in the former case was above the fog limit of dust-free air and would therefore catch the smaller order of water nuclei than occur in series 5. These water nuclei, in fact, are reduced appreciably in number in the lapse of time, as will be seen by comparing the two experiments for $n = 320{,}000$ nuclei in series 5. The following exhibit may be regarded as a smoothed curve for about the same period of dissipation. The curves rise for smaller nucleation; the exhaustion loss is 0.23.

$10^6 d$	$10^{-3} n$	n'/n	Complete evaporation.	Number completely evaporating per cm³.	Subsidence loss above.
cm.					
160	1500	0.003	0.75	1050	0.02
190	1000	.006	.66	660	.10
200	800	.007	.61	490	.15
220	600	.008	.54	320	.22
250	400	.009	.46	185	.30
320	200	.010	.28	56	.48

This accentuates the effect of subsidence, which with the exhaustion evaporation must account for the total number of nuclei removed. At first sight it would appear that the number of residual nuclei is independent of the number of vapor nuclei present, as if some other nuclei which may accompany the vapor nuclei were responsible for residual water nuclei.

TABLE 4.—Case of rapid evaporation by compression (influx of dust-free air).

δp	Corona.	s	Corona dissipated by—	$\delta p/p$	$n \times 10^{-3}$	Ratio.
Part 1, series 6.—Barometer 76.86 at 23.5°. Time between exhaustions, 5 minutes, usually. Curve No. 6, fig. 1.						
35.7	r o	11.8	Compression.....	0.465	600	0.082
18.5	corona	6.0		.240	49	
28.7	w b p	9.0	Slow evaporation.	·373	220	.023
18.5	corona	2.8		.240	5	
28.7	w b p	8.5	Compression.....	·373	190	.175
18.5	corona	5.3		.240	33	
28.7	y	8.0	....Do.....	·373	160	.130
18.5	corona	4.5		.240	21	
30.5	p	11.0	....Do.....	·397	355	.110
18.5	corona	5.6		.240	39	
30.5	p	10.0	Evaporation*....	·397	*270	.037
18.5	corona	3.5		.240	*10	
32.2	r	10.5	Compression*.....	.420	*320	.115
18.5	corona	5.5		.240	*37	
32.2	r	10.7	.....	.420	340	.091
18.5	corona	5.2	.....	.240	31	
*Time interval between observations 3 minutes. $y=0.75$						
Part 2, series 7.—Green coronas. No subsidence. Barometer 76.70 at 22°. Time between exhaustions, 3 to 5 minutes. Temperature 25°. Curve No. 7, fig. 1.						
δp	Corona.	s	Fog dissipated by	$\delta p/p$	$n \times 10^{-3}$	Ratio.
36	g	16.0	Compression or	0.470	1000	0.039
18	br b p	5.6	influx.....	.240	39	
36	g	16.0	....Do.....	.470	1000	.039
18	g b p	5.6		.240	39	
36	g	16.0	....Do.....	.470	1000	.039
18	g b p	5.6		.240	39	
36	g	16.5	Slow evaporation;	.470	1000	.001
18	corona	1.8	no influx.....	.240	1	
36	g	16.0	.....	.470	1000	.021
18	corona	4.5	.....	.240	21	

5. Rapid evaporation of fog particles. Vapor nuclei.—Finally, the fog particle precipitated on vapor nuclei may be rapidly evaporated by compression (influx of air). In order that all results may be comparable, it is necessary to allow the same time interval between the first exhaustion (capture of vapor nuclei) and the second (capture of residual water nuclei). Since filtered air enters in the same way here as in the foregoing section 4, its effect (if any) is eliminated from the results. Subsidence, however, is essentially reduced by the present method, since the time for subsidence is but one-third to one-fifth as large as in section 4. The results are given in table 4 on the same plan as in table 3. In part 1 two control experiments with gradual exhaustions are introduced to indicate the difference. The nucleations are as a rule low. In part 2 they are high and there is one control experiment. The curve is shown in Nos. 6 and 7 in fig. 1.

The data taken from smoothed curves will therefore be about as follows, d being the approximate diameter of fog particles, subsidence being ignored and the exhaustion loss 0.25.

$10^6 d$	$10^{-3} n$	n'/n	Complete evaporation.	Number of nuclei evaporating ($n \times 10^{-3}$).	Number of residual nuclei ($n \times 10^{-3}$).
cm.					
16	1500	....	....	....	....
19	1000	0.039	0.71	710	39
20	800	.060	.69	550	48
22	600	.082	.67	400	49
25	400	.105	.65	260	42
32	200	.126	.62	125	25

The apparently greater persistence of water nuclei on rapid evaporation is thus sustained. Subsidence is in excess in section 4; and though of the same order as the number of persistent nuclei, it always refers to the total charge of nuclei. As the number to be accounted for in the present instance can not well be estimated, it is safe to conclude that about 95 per cent of the fog particles precipitated on vapor nuclei evaporate without residue, when about 10^6 fog particles are suspended in each cubic centimeter; and that this percentage decreases with the number of fog particles or vapor nuclei caught, or as their size increases. Conversely the number of residual water nuclei persistent within 5 minutes increases as the number of fog particles decreases (*i. e.*, as their size increases) from a persistence of about 0.054 at $n = 10^6$ to over 0.17 at $n = 2 \times 10^5$. One would thus be tempted to conclude that larger fog particles take a longer time to evaporate completely; but that the case is far more subtle will appear in the next paragraph.

6. Evaporation retarded as the diameter of fog particles decreases.—A suggestive inference may be drawn from the results obtained. The visible part of the fog vanishes within less than a minute after the compression, or the (necessarily slow) influx of dust-free air begins. Here, then, by far the greater bulk of the particle vanishes. In the ensuing 5 minutes or more, optically quite inappreciable water nuclei are still present, to the extent of 5 to 20 per cent of the original charge of vapor nuclei. In other words, whereas the tendency to evaporate increases rapidly with the diameter of the fog particle, there must be, in case of the fog particles in question, some counteracting tendency in action, by which this evaporation is retarded much in excess of the accelerating effect of convexity. All this occurs in rigorously dust-free air, in which water vapor and the ions (less than 1,000 per cubic centimeter, whereas there are from 25,000 to 50,000 water nuclei) inseparable from air and due to natural causes, are alone present. It therefore becomes interesting to endeavor to ascertain the reason of this complete inversion of the behavior usually characteristic of these exceptionally small droplets.

7. Time losses.—The effect of lapse of time between the exhaustions has already been shown to be of minor importance within intervals like those of the above observations. It is important, however, to add quantitative work, and table 5 supplies relevant data, δp being the drop of pressure on exhaustion, n the nucleation, n'/n the ratio of successive nucleations. Table 5 shows that the nucleation is spontaneously reduced by diffusion to about one-half, in the interval between the second and tenth minutes, and so far as may be observed the decrease is fairly uniform. One may therefore estimate a time loss of about 6 per cent per minute. Consequently the coronas obtained in the second and third minutes (or even later) are liable to show no discernible difference comparable with the other possible complications involved. Thus, for instance, the loss of water nuclei proper can not begin before all the fog particles have evaporated, a process which must consume a minute at least if an influx of strictly dust-free air is to be assured.

Table 5 also gives evidence to the effect that no nuclei come through the filter. If the partial vacuum is *gradually* raised to $\delta p = 36$ cm. without sudden exhaustion, *i. e.*, without initial coronas, and filtered air is then passed in the identical way through the filter into the fog chamber, no water nuclei whatever are detected by the sudden exhaustion at $\delta p = 18$ cm. This is conclusive proof that the evaporation of fog particles is the sole cause of nucleation.

Again, table 5 shows that by keeping the influx cock open, nearly 9 per cent of the fog particles may be represented by water nuclei even when $n = 10^6$. It is not safe to admit a more rapid influx at the filter, but the sudden introduction of previously filtered air suggests itself as a means to the same end, and will be tried in turn.

TABLE 5.—Water nuclei from evaporation of fog particles precipitated on vapor nuclei in dust-free air. Effect of lapse of time and of drop of pressure.

Time elapsed between exhaustions (minutes).	δp	Corona.	s	Fog dissipated by—	$\delta p/p$	$n \times 10^{-3}$	Ratio n'/n
Part 1.—Effect of lapse of time between exhaustions. Barometer 75.26 at 26°. δp=36 and δp=18 or $\delta p/p$=0.475 and 0.245.							
2m	....	g r g	 72	Slightly open influx cock.	....	1000 86	0.86
3m	....	g r g	 72		....	1000 86	.86
5m	....	g	 70		....	1000 79	.79
10m	....	g	 56		....	1000 40	.40
2m	....	g r g	 72		....	1000 86	.86
5m	....	g r g	 66		....	1000 65	.65
10m	....	g	 55	....	....	1000 37	.37
2m	....	none none	 0	....	....	0 0	....
Part 2.—Effect of different drops of pressure δp. Barometer 75.26 at 26°.							
2m	36.0 19.9	g	 72	Slightly open influx cock.	0.475 .265	1000 90	....
2m	36.0 21.6	g	 72		.475 .290	1000 98	....
2m	36.0 27.0	g	 60		.475 .360	1000 66	....
Part 3.—Very rapid evaporation (0.25 minute). Barometer 76.22 at 24°.							
1.5m	36.0 20.0	g g b p	 80	Rapid influx from tank of dust-free air.	....	1000 123	0.123
1.5m	36.0 20.0	g v b p	 80		....	1000 145	.145
1.5m	36.0 20.0	g ! g b p	 80		....	1000 123	.123

TABLE 5.—Water nuclei from evaporation of fog particles precipitated on vapor nuclei in dust-free air—Continued.

Time elapsed between exhaustions (minutes).	δp	Corona.	s	Fog dissipated by—	$\delta p/p$	$n \times 10^{-3}$	Ratio n'/n
Part 4.—Larger particles. Rapid evaporation (less than 0.25 minute). Barometer 76.69 at 23°.							
1.5m	29.8	y o	....		0.388	540	0.20
	17.3	r b p	8.0		.225	108	
1.5m	29.8	y o	....		.388	540	.18
	17.3	r b p	7.7		.225	97	
1.5m	28.0	c	9.0	Influx of filtered air from reservoir.	.365	290	.38
	17.3	y b	8.0		.225	108	
1.5m	28.0	r	9.5		.365	260	.37
	17.3	g ! b p	7.7		.225	97	
1.5m	26.2	corona	5.7		.342	54	.30
	17.3	....	4.2		.225	16	
1.5m	27.0	corona	7.6		.352	130	.25
	17.3	....	5.4		.225	33	

*All conditions identical to the above, except that there is no primary exhaustion or fog precipitation on vapor nuclei. The absence of all condensation at 18 shows that no nuclei come through the filter.

8. Effect of changes of the drop of pressure δp.—The second part of table 5 contains results in which residual water nuclei are captured at drops of pressure from $\delta p = 18$ to 27 cm. At first the coronas do not change; eventually they decrease in a way to be referred to the increased amount of water precipitated. Vapor nuclei are inefficient in the presence of water nuclei.

The constancy of coronas after all nuclei have been caught through a considerable range of values of δp, occurs here as elsewhere and has not yet been fully explained. As the nucleation n varies with the precipitation (m grams per cu. cm.), while n increases with δp, the computed values of n must also do so, thus conflicting with the observed fixed coronal aperture. It is difficult to conjecture where the excess of water precipitated goes to, even if we recall the slow change of s implied in $d \propto \sqrt[3]{m}$ or $s\sqrt[3]{m} = \text{const}$. In some way, probably coincident with the rise of temperature after adiabatic cooling, the excess of precipitation is again removed before coronas can be observed. The efficiency of the fog chamber virtually breaks down, as no more water is deposited when δp increases.

It follows in general that neither by the time loss nor by the effect of a varying drop of pressure is the tendency of rapid evaporation to produce persistent water nuclei materially influenced. It must, therefore, be an occurrence of its own kind.

9. Exceptionally rapid evaporation.—In the third and fourth parts of table 5 the influx of dust-free air was increased in a marked degree, by withdrawing the influx of dust-free air from a large independent reservoir. In this way the time of evaporation was reduced to about 15 seconds. Nevertheless it required about 1.5 minutes to reduce the pressure from $\delta p = 36$ cm., to $\delta p = 20$ cm., so that some water nuclei vanished by decay. The yield of water nuclei has been materially increased. Thus even when $n = 10^6$ or $d = 0.00019$ cm., rapid evaporation will convert at least 18 per cent of the fog particles of pure water into persistent water nuclei. The case is most pronounced for $n = 300{,}000$ to 400,000 nuclei per cubic centimeter, or $d = 0.00027$ cm., when 48 per cent of the nuclei (about one-half), persist. Beyond this, $n = 10^5$, the persistence decreases, a result doubtless referable to the increasing importance of subsidence. Within reasonable limits persistence increases as the original number of nuclei decreases, which result is identical with the character of the earlier series.

Naturally all these data are lower limits. In appropriate apparatus the time of evaporation, the interval of observation, etc., might be made much shorter; but this would not change the general trend of the data. Again, many particles must be washed out by contact with the sides of the vessel or by coalescence, during the turbulent motion which accompanies the influx of air. The following is a digest of the data found:

$d \times 10^6$	$n \times 10^{-3}$	Exhaustion loss.	Subsidence loss.	Evaporation loss.	Residual water nuclei.	Ratio residual water nuclei to total water nuclei.	Corrected number of residual water nuclei ($n \times 10^{-3}$).
cm.							
190	1000	0.23	0	0.64	0.13	0.17	170
240	500	.23	0	.58	.19	.25	125
270	350	.23	0	.40	.37	.48	168
410	100	.23	0	.49	.28	.36	36

10. Conclusion.—For very small fog particles suspended in dust-free air saturated with water vapor and left without interference, the dissipation by evaporation is enormously more important than that by subsidence. In the above plug-cock fog chambers the transition occurs when the number of nuclei per cubic centimeter, $n = 200{,}000$, or the diameter of fog particles, $d = 0.0003$ cm., when about half evaporate and half subside.

Fog particles precipitated on solutional nuclei (phosphorus), evaporate to persistent water nuclei without other loss than is attributable to subsidence and in a small degree to time losses (diffusion). There is no loss by complete evaporation.

Fog particles precipitated on the nuclei of water vapor in dust-free air, in contrast with the preceding case, evaporate under the same circumstances almost without residue, the yield of water nuclei (after allowing for subsidence and in the absence of all interference) being but 0.004 when $d = 0.00016$ cm., increasing to 0.0036 when $d = 0.00032$ cm. These fog particles evaporate into the wet air from which they were precipitated, and the experiment may be repeated indefinitely. Relatively more water nuclei persist as the fog particles evaporated are larger.

11. The same, continued.—The persistence of water nuclei obtained in the last case from the nuclei of water vapor is much increased by *accelerating* the evaporation of the fog as soon as formed. Such forced evaporation is produced by the rise of temperature due to the compression accompanying the influx of dust-free air after the exhaustion which precipitated the fog. This result can not be associated with losses due to subsidence.

When the rate of evaporation is increased by compression, moreover, the number of water nuclei (derived from the reasonably rapid evaporation of fog particles precipitated on vapor nuclei and persisting within 5 minutes after the evaporation) may be as large as 5 per cent to over 20 per cent, depending upon the size ($d = 19 \times 10^{-5}$ to $d = 32 \times 10^{-5}$ cm., respectively) of the fog particles evaporated. Again, relatively more water nuclei persist when the fog particles evaporated are larger within limits given. By keeping the influx cock for dust-free air slightly open on sudden exhaustion, 10 per cent of the fog particles evaporated may be represented by persistent water nuclei, even when $d = 19 \times 10^{-5}$ cm. or $n = 10^6$. If it were safe* to make use of more rapid evaporations, this limit could unquestionably be much increased. Thus on the rapid evaporation of fog particles by the influx of filtered air from a large independent reservoir into the fog chamber, about 18 per cent of the fog particles were converted into residual water nuclei when $n = 10^6$ and actually 48 per cent when $n = 10^5$. All such values or lower limits, because the loss of fog particles at the walls of the vessel and by coalescence is not included, but tests under most rapid evaporation possible showed that a limit had been practically reached.

The loss of nuclei by decay (diffusion) in the lapse of time (say 6 per cent per minute within the given interval of observation) and the effect of changes in the drop of pressure on sudden exhaustions have no causal bearing on the production of water nuclei by rapid evaporation. They merely modify the number. Similarly the effect of subsidence is secondary. Hence the cause of the production of persistent water nuclei in rigorously dust-free air must be associated with the speed of evaporation or with the motion of the fog particles during evaporation. It is a curious

*Naturally the efficiency of the filter must be tested before each experiment.

fact that whereas the relatively enormous fog particle evaporates at once beyond the range of visibility, this process stops in case of certain of the invisible particles making about 0.5 to 50 per cent of the total number as the evaporation is more rapid in the manner specified. The remaining fog particles evaporate completely.

12. The same, continued.—J. J. Thomson, Langevin and Bloch, and others* have referred the persistence of pure water nuclei of about 10^{-6} cm. in diameter, to the minimum of surface tension discovered by Reinold and Rücker† for thicknesses of films of about the same value. Since all fog particles are so much larger than this order of values, it is difficult to see why, under quiet evaporation without any interference, they do not *all* terminate in water nuclei, allowance being made for subsidence. Yet under these circumstances the yield of water nuclei is least, being usually within 1 per cent. Whatever losses may be due to coalescence should be increased when the rate of evaporation is increased, because there is more motion of the air relatively to the fog particles. Again, precisely the reverse occurs, inasmuch as an increased rate of evaporation enormously increases the yield of water nuclei.

Moreover, the residual water nuclei may, on rapid evaporation, exceed the order of 10^{-6} cm. in diameter two or three times; or on slow evaporation they may fall below 5×10^{-7} cm. and yet persist for half an hour or more. Under any circumstances they are graded. They appear to diminish in size with extreme slowness in the lapse of time, so that an appropriate interval of waiting will yield any size.

13. The same, continued.—Since the fog particles are absolutely pure water (water condensed on water vapor), it is tempting to suggest electrical charge as the cause of the observed persistence, such charge being acquired either by friction during the motion of particles undergoing rapid evaporation (influx of air) or by the mere act of evaporation. The latter, like the minimum of surface tension, would require the same persistence of all fog particles under conditions of quiet evaporation. As has frequently been shown, this is not the case. A frictional mechanism, suggested in view of the occurrence of convection during the period of evaporation and influx of air, if in action, would account for the discrimination between fog particles as to survival. Thus drops of larger size are stirred about for a longer time before complete evaporation, and they are therefore more favorably circumstanced to persist, as they have been found to do; water nuclei should not be of the same size and they are not; etc. But all my experiments have failed to detect the amount of charge commensurate with the persistence of nuclei.

*J. J. Thomson: Conduction of Electricity through Gases, p. 152, 1903; C. T. R. Wilson, Trans. St. Louis Electrical Congress, vol. 1, pp. 364–378, 1904.

†Reinold and Rücker: Proc. Roy. Soc., vol. 40, p. 441, 1886.

If the radius of residual water nuclei be taken as 10^{-6} cm., the charge needed would be roughly $e = 6.3 \times 10^{-8}$ electro-static units per particle and its potential would be about 18 volts. If about 200,000 of these droplets or residual water nuclei are present per cubic centimeter (as were found above), the charge would be about 4 coulombs for a cube each side of which is 100 meters. If all the particles of the cubic centimeter were brought to coalescence the size of the drop would be 58×10^{-6} cm. at its potential of about 63,000 volts. Finally, the electric contents of my fog chamber should be about 30 electro-static units of quantity, and ought thus, in spite of the moisture present, to be easily determinable. The experiments showed only about 0.50×10^{-6} electro-static units per cubic centimeter, less than the contents (0.88×10^{-6}) in the room air without, at the time; that is, the average charge per nucleus was about 5×10^{-12} electro-static units, or less than 1 electron. Hence the electrical hypothesis must be abandoned. It would in any case be improbable for the charge to show so small a coefficient of decay as do the water nuclei.

14. Statistical hypothesis.—Under the circumstances it seems permissible to suggest an hypothesis of a statistical character; namely, that the molecule of liquid water is composite, consisting of virtually more volatile and less volatile constituents. Such a view is quite compatible with the composite molecule observed in water vapor, where millions of nuclei may be captured long before the molecule proper is reached, the evidences of which are now beyond question. In case of fog particles, when the evaporation is reduced to extreme slowness, we may conceive that all groups of molecules evaporate together at about the same rate, and that therefore the residue, *i. e.*, the persistent water nuclei, are present in least amount. On the other hand, when the evaporation is forced, or accelerated by the heat due to compression, the more volatile constituents of the fog particles evaporate faster than the less volatile, and there is a correspondingly greater residue of persistent water nuclei, because of this concentration of the less volatile molecular aggregates of water in each fog particle. It follows also that relatively more persistent nuclei are obtained by the evaporation of large fog particles than by the evaporation of small particles, because a greater relative number of these droplets would contain a sufficient number of the less volatile groups to persist; *i. e.*, the opportunities for concentrating the less volatile aggregates are enhanced. Finally, it should never be possible to replace all fog particles by the water nuclei derived from them. All of these deductions are in keeping with the experimental evidence, as pointed out.

CHAPTER II.

STANDARDIZATION AND EFFICIENCY OF THE FOG CHAMBER.

AXIAL COLORS AND INTERFERENCES.

15. Introductory.—The axial colors of the steam jet and of coronas overlie the source of light when looked at through a long column of wet air in which uniform cloud particles are suspended. It makes no difference whether the source is a point simply or a disk (say) 4 inches in diameter; it appears uniformly colored, as if seen through colored glass, so long as the cloud lasts. The order of colors, beginning with particles of extreme smallness, is the same as that of Newton's interferences seen by transmitted light. In case of the steam jet, however, on passing the transition from crimson to violet in the first order, the field becomes opaque, while the steady flow of the jet usually breaks down and becomes turbulent. In the case of coronas I have thus far failed to reach this transition, the medium showing mere fogs of uncertain character.

To produce the actual colors vividly, and especially the tints of the second and third orders for relatively large particles, the columns of fog must be long and very uniform. The steam jet soon fails in this respect, but a wide drum 1 to 2 meters long used as a fog chamber shows saturated colors surrounded by coronas. In the case of hydrocarbon vapors the columns may be shorter, because the particles throughout are larger for like numbers per cubic centimeter than is the case with water vapor.

16. Causes of axial color.—In my earlier work* I was inclined to regard these colors as interferences superimposed on the coronas, regarding the small field of refraction possible with small particles as in keeping with the long columns needed for observation. The explanation at best is purely tentative. Later in my work, when the size of particles was estimated from data given by successive exhaustions,† it appeared that the sizes of the fog particles were of an order about ten times larger than would be needed to produce interferences of the same kind. The interference hypothesis was therefore abandoned. In my more recent results the diameter of fog particles d and the ratio in question are somewhat reduced but remain of the same order. Thus if n be the number of fog particles per cubic centimeter, D the thickness of an air plate giving like interference colors, the results given in table 6 may be selected at random. They show that the strong axial blues of the first order must belong to particles even larger than 0.0001 cm. in diameter, and that all particles are more than six times larger than would be demanded for interferences.

*Phil. Mag. (5), XXXV, p. 315, 1893; Bull. U. S. Weather Bureau No. 12, 1895.
†Phil. Mag. (6), IV, p. 26, 1902; Smiths. Contrib. No. 1373, 1903; No. 1651, 1905.

TABLE 6.—Data for axial colors. $m = 3.6 \times 10^{-6}$ grams; $\sqrt[3]{\frac{6m}{\pi}} = 1.90 \times 10^{-2}$.

$D \times 10^6$	Corona.	Axial.	s	$d \times 10^5$	$d \times 10^5$	$n \times 10^{-3}$	$d \times 10^5$ computed.	Ratio d/D.
14	....	v	....	....	36	....	....	....
17	....	b	....	....	....	....	....	....
27	....	g y	....	....	46	....	....	....
29	b g	y	14.5	22	47	650	22	7.7
33	....	....	....	....	51	....	....	....
36	....	....	....	....	53	....	....	....
41	g y	p	13.0	25	55	460	25	6.1
42	y	v	12.0	27	60	360	26	6.4
45	....	b	11.0	29	65	280	29	6.5
55	p	g	10.0	32	67	213	32	5.8
57	....	y	9.0	36	70	152	36	6.3
69	g y	v	8.0	40	79	108	40	5.8

17. The lamellar grating.—Recently I have considered the case of coronas in relation to the lamellar grating, in which diffractions are obtained from a uniform succession of alternately different thicknesses of clear glass. Experiments with such gratings were originally made by Quincke and there is a full theoretical treatment by Verdet. The behavior of this grating differs from that of the usual kind in the occurrence of an additional factor

$$\cos^2(\pi d(n-1) + \pi a \sin \delta)/\lambda$$

where n is the index of refraction, d the difference in thickness between thin strips of width a and thick strips of width b, δ the angle of diffraction. Hence since for axial color, $\delta = 0$, minima occur at $(n-1)d = (2m+1).\lambda/2$, whereas for Newton's interferences, the mimima occur for a thickness D in the case of transmitted light where $2\mu D = (2m+1).\lambda/2$; whence

$$d/D = \frac{2n}{n-1}$$

In case of water $n = 0.133$, or $d/D = 8.0$. This result applied to a grating of transparent strips is so near the above datum $d/D > 6$ for a medium of transparent particles (for which there is no theory), that it seems reasonable to conclude that the actual colors are referable to the same type of phenomenon in both cases. The need of observations through long columns in case of fog particles suspended in air is additionally confirmative, since the contribution of color due to one particle must be exceedingly small.

18. Disk colors of coronas.—One might be tempted to explain the disk colors in the same way, for in case of deviation δ from the axial ray

$$D/d = (n-1)/2n + a \sin \delta/2\, dn$$

But here there are several insuperable difficulties which refer the disk color to a different origin. In the first place, they are much more intense

than the axial colors and are seen distinctly through very small thicknesses of fog; disk colors are apparently abruptly complementary to the axial colors and there is certainly no continuous transition; finally, there is no incident light of the requisite obliquity.

The appearance is, therefore, as if, corresponding to the interferences by transmission, there were complementary interference by reflection toward the source of light. This phenomenon could then be reversed in direction at any fog particle in its path, and thus turned again toward the observer. But apart from the complementary nature of disk and axial color, no other evidence bears on this explanation. Moreover, any such theory must account for the intensity of disk colors in general, and in particular for the vividness of the greens.

19. Experiments with long tubes.—In a long chamber and intense illumination the axial colors may be extended over a considerable area and intensified by strong illumination. It did not seem improbable that they might then be serviceable for spectroscopic investigation, in which case the mean wave-length of the interference bands would serve for their identification. Thus they might afford a means of further investigating the fog phenomenon at a degree of fineness beyond which the coronas cease to be available. Unexpected difficulties were, however, encountered, as will presently appear, and the endeavor to remove them has not been successful.

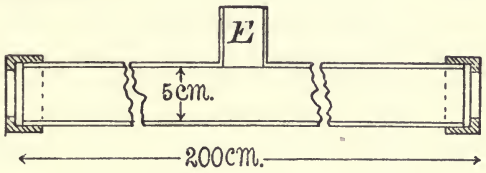

FIG. 2.—Section of brass tube for observing axial color.

Experiments of this kind were begun by using long brass tubes (fig. 2) with plate glass ends, carefully put together. Sometimes wet cloth linings were introduced; but they had no other effect than to dispel the horizontal columnar vortices seen on each side of the axis after exhaustion. With a naked tube the fog observed rises on the outside and falls in the center of the field, so that the axes of the two vortical columns are eccentrically placed parallel to the axis of the tube. Phosphorus nuclei, ions, and vapor nuclei were tried, and incidentally some fog and rain limits determined.

The following summary of results with vapor nuclei or with ions (δp being the drop in pressure), shows that in no case was there any color obtainable. In these narrow tubes the only manifestation is a more or less densely black fog.

TABLE 7.—Observations for axial color. Dust-free air, vapor nuclei, and ions. Long brass tube, 5 cm. diameter, 200 cm. long.

δp	Precipitate.
Part 1.—Barometer 77.28 at 18°.	
21.0	Fog
22.6	Fog
24.6	Fog
26.3	Fog
28.0	Fog
Part 2.—Barometer 77.37 at 19°.	
15.4	None
16.2	None
17.6	None
*19.4	None
21.3	Light fog
20.4	None
23.0	Fog
24.5	Fog†
26.4	Fog†
28.0	Fog†
29.9	Fog†
31.6	Fog†
33.1	Fog†
35.0	Fog†

δp	Precipitate.
Part 3.—Barometer 77.34 at 18°.	
*19.8	Just seen
19.4	None
20.4	None
20.9	Just dim.
21.0	Faint fog
Part 4.—Small round hole; sharper seeing; barometer 77.34.	
*21.1	Rain
20.4	Rain, faint
Part 5.—Radium on tube, outside; barometer 77.34.	
*20.4	Fog dense
19.4	Rain !
19.3	Rain !
20.3	Dense
21.1	Fog
Part 6.—Cloth hung in brass tubes; barometer 76.24 at 21°.	
17.6	None
19.2	Fog ?
21.0	Fog ?
23	Fog !
24	Fog !
26	Fog !
28	Fog !
30	Fog ! ‡

δp	Precipitate.
Part 7.—Barometer 77.65 at 20°	
*18.0	Darkness
18.0	Darkness !
19.4	Darkness !
20.3	Darkness !
21.3	Rain
22.4	Corona
Part 8.—Barometer 77.65 at 20°.	
21.4	Corona
20.6	Corona
19.4	(?)
18.5	Darkness
Part 9.—Radium on tube.	
18.0	(?)
18.9	Rain ?
19.5	Corona !
20.4	Corona !
24.3	Dense
25.0	Dense
Part 10—Dust-free air again. ‡	
24.5	Corona
26.4	Corona
28.0	Corona
No color appears.	

*Fog limits. †Dense but no color. ‡Dense fog but no color.

The same is true of phosphorus nuclei put into the identical (now cloth-lined) apparatus. Thus in case of long brass tubes 200 cm. in length and 5 cm. in diameter with the barometer at 77.15 cm. at 20°, thirteen successive exhaustions of air charged with phosphorus nuclei showed no color effects, but merely fogs gradually decreasing in density. The drop of pressure lay between 10 and 16 cm.

Again, four exhaustions with fresh charges of phosphorus nuclei behaved similarly. The nucleated air was usually fawn-colored by transmitted light and bluish by reflected light. Finally, when many successive charges of phosphorus nuclei were introduced, densely black fogs appeared without color, gradually lifting.

The endeavor to clean the fog chamber by successive exhaustion and apparently complete subsidence failed utterly. Fog particles evaporate before subsidence to persistent water nuclei, so that for small particles (above the middle green corona), subsidence is negligible as compared with evaporation, even in a long brass channel lined with a square tube of wet cloth 4 cm. high and 4 cm. wide.

20. Short tubes.—Believing that any irregularity in the size of the fog particles might be particularly harmful in the case of tubes 2 meters long, short tubes of the same diameter were next tried in the endeavor to obtain axial color effects with vapor nuclei. The results are given in table 8.

TABLE 8.—Observations for axial color. Dust-free air. Vapor nuclei. Short brass tube, 5 cm. diameter, 75 cm. long. Tube not cloth-lined. Part 15.—Barometer 77.00 at 21°.

δp	Precipitate.	δp	Precipitate.	δp	Precipitate.
*18.5	Rain	*20.9	Corona	35.7	Dense
*18.0	Rain	21.6	Corona	40.6	Dense
*17.5	None	23.4	Corona	43.1	Dense
*17.0	None	25.3	Corona	46.6	Dense
*18.0	None	†28.7	Dense		
*19.9	None	32	Dense		

*The difference of fog limit or rain limit for descending and ascending δp is noteworthy.
†No colors seen. Subsidence with a horizontal plane on top.

The attempt again failed. No colors were observed, merely an evenly subsiding, gradually (increasing δp) more intensely black fog.

These results are disappointing. To obtain axial colors (coronas are not observable longitudinally in tubes); it therefore seems essential that drums of considerable equatorial diameter be used. In other words, the vessel must not only be long but *voluminous* to obviate the radiation effect from the walls after exhaustion, as much as possible. In fact, the external layers of foggy air seem effectually to screen the interior from the radiation.

Incidentally a number of fog limits and rain limits were obtained, which, however, present nothing new, except that on diminishing pressure differences δp, the rain limit falls at a lower δp than on ascending differences. The appearance is as if the fine droplets generated nuclei. But more probably very fine nuclei escape capture in the presence of coarse.

Summarizing the above results, we may therefore conclude that the fog particles producing the axial colors of coronas are of such a size as to recall the interference phenomena of the lamellar grating, with which their constants agree.

The disk colors of coronas can not be similarly explained.

The observation of axial color fails unless long, capacious fog chambers are used. Tubes show opaque fields only.

CORONAS WITH MERCURY LIGHT.

21. Preliminary survey.—The inferences of the preceding papers* gave the promise that on judiciously using monochromatic light as the source of illumination the optical nature of the coronas might be fully brought out. Such light must be strictly homogeneous and at the same time very intense. Hence the usual methods of obtaining it are unsatisfactory. The strong green line of a mercury lamp, however, fulfills the requirements admirably, and this was therefore used. The results show that the green disk and the first green ring alternately vanish as the result of the interference phenomenon superimposed on the diffraction phenomenon. If, therefore, the nucleation of a highly charged medium is systematically reduced, a series of angular diameters may be obtained, both for the green disk and the inner or outer edge of the first green ring. From the loci of these values the position of the *first diffraction minimum* for green light may be inferred, and the size of droplets computed from the usual equation for small opaque particles.

If the reduction of the nucleation is accomplished by successive partial exhaustions, all of them identical, while filtered air is allowed to enter the receiver systematically between the exhaustions, the nucleations of any two consecutive exhaustions should show a constant ratio. Allowance must, however, be made for the subsidence during the later fogs and for time losses, if any. This is the method used hitherto in my work and the results seem to have been trustworthy.

In the case of mercury light, however, it is now possible to compare the latter with the former (diffraction) method of obtaining the diameter of particles, with a view to throwing definite light on the optical phenomenon. Subsidence methods are out of the question for large coronas, as these are invariably fleeting in character and pass at once into smaller coarse coronas.

The results of the two methods may be regarded as coincident as long as not more than 300,000 nuclei per cubic centimeter, or diameters of particles not smaller than 0.0003 cm. are in question. For larger numbers and smaller diameters the divergence rapidly increases. Indeed, for particles larger than the size given, the optically measured loss per exhaustion exceeds the exhaustion ratio, a result which is satisfactorily explained by the contemporaneous subsidence of these relatively large particles. For particles smaller than the limit in question, however, the loss computed by the optic method is larger than the exhaustion loss, as if fresh nuclei were produced or rather made available at each exhaustion. It is this result which the present paper purposes to bring out in detail and to consider in its bearings on the optical phenomenon.

*Amer. Journ. Sci., xxv, 1908, p. 224; xxvi, 1908, p. 87; xxvi, 1908, p. 324.

22. Apparatus.—The fog chamber was of the usual pattern, cylindrical in form, with its axis horizontal. The clear walls, being of blown glass, showed some refraction disturbances, not, however, of a serious character. The fog chamber was connected with a large vacuum chamber by a short, wide passageway, though width is of little consequence here. The cylinder was lined with wet cloth, closely adhering, except at the narrow horizontal windows for observation.

For exhaustion the stopcock was suddenly opened at the beginning of the first second, closed after 5 seconds, and the corona quickly measured. Filtered air was then at once introduced and the next exhaustion made at the beginning of the sixtieth second. This rhythm is essential. The isothermal value of a drop of pressure $[\delta p_2]$ was carefully predetermined. It fixes the ratio y of the geometric progression of nucleations, since

$$y = (p - \pi - [\delta p_2]) / (p - \pi)$$

where p is the barometric pressure and π the vapor pressure at the given temperature. If the cock were left open for a longer time than 5 seconds $[\delta p_2]$ would increase to the limit δp_3.

The goniometer was of the usual type, the eye being at the center or apex, while two needles on radii 30 cm. long registered the angular diameter of the coronal disks or annuli. Formerly the whole instrument was placed on the *near* side of a fog chamber, the eye being about 30 cm. from the nearest wall. It conduces to much greater sharpness of vision, however, and admits of a measurement of larger coronas, *caet. par.*, if the eye is placed all but in contact with the nearer wall and the needles (or in this case preferably the inner edges of round rods) beyond the further wall. In such a case the refraction errors are also diminished. In addition to these advantages I may mention the decidedly increased (about 25 per cent) value of the aperture obtained. These excessive apertures show, however, that the ordinary diffraction equation for coronas is not fully applicable; for aperture varies with the position of the eye along the line of sight. It is often surprising how large a corona can be measured by the second method, in a small fog chamber scarcely 6 inches long. The distance between lamp and chamber is kept about $D = 250$ cm.

23. Equations.—The equations needed in the present work are derived in my last report* and need merely be summarized here. If y is the exhaustion ratio, the nucleation n_z of the zth exhaustion in terms of the original nucleation n_0 will be

$$n_z = n_0 y^z (1 - S/s_0^2)(1 - S/s_1^2) \ . \ . \ . \ . \ . \ (1 - S/s_{z-1}^2)$$

where S is a subsidence constant and s the chord of angular diameter of the coronal disk on a radius of 30 cm.

*Carnegie Institution of Washington Publication No. 96, 1908, chapters I, III (equat. 1 to 12).

To find S, two consecutive values of s suffice, or

$$S = s_z^2(1 - s_{z+1}^3/y\, s_z^3)$$

approximately. The diameter of particles d is, in terms of n

$$d^3 = 6m/\pi n$$

If $\lambda = 54.6 \times 10^{-6}$ cm. is the wave-length of green mercury light and θ the angular radius of the first green minimum of the coronas, $\sin\theta = 0.61\ \lambda/(d'/2)$. Since $\sin\theta = s/2R$, R being the radius of the goniometer of which s is the chord, d' the diameter of fog particle (the primes referring to optic measurements),

$$d' = 0.004/s$$

for mercury light. Hence optically the nucleation is

$$10^{-6}n' = 29.8ms^3$$

where m grams of water are precipitated per cubic centimeter on exhaustion, and found in the exhausted fog chamber.

24. Data with white light.—The results in the following tables are reported in accordance with the same plan throughout. The fog chamber is initially at atmospheric pressure p, the vacuum chamber exhausted to $p - \delta p'$. When the exhaustion cock is closed 5 seconds after exhaustion, the pressure in the fog chamber, after the original temperature is reestablished, will be $p - [\delta p_2]$. The common isothermal pressure in vacuum and fog chambers when communicating after the exhaustion is eventually $p - \delta p_3$. If π is the vapor pressure at the given (isothermal) temperature, the exhaustion ratio is

$$y = (p - \pi - [\delta p_2])/(p - \pi)$$

The amount of water precipitated per cubic centimeter is m at the temperature and pressure given.

TABLE 9.—Standardization of the fog chamber. Welsbach burner and phosphorus. Cock open 5 sec. Observation interval 60 sec. Bar. 75.9 cm. at 22°. Temp. 26°. $[\delta p_2] = 16.5$ cm.; $\delta p_3 = 17.4$ cm.; $\delta p' = 18.6$ cm.; $y = (p - \pi - [\delta p_2])/(p - \pi) = 0.775$; $\delta p_3/p = 0.229$; $10^6 m = 3.77$ grams at 20°; 4.22 grams at 26°; $\pi = 2.5$ cm. Goniometer in front. Distances of eye and lamp 30 cm. and 250 cm., on opposite sides of fog chamber. Radius of s, $R = 30$ cm.

z	Corona.	s	z	Corona.	s	z	Corona.	s
1	Fog	25	9	g	14	17	Cor.	6.8
2	Fog	22	10	g y	13.5	18	Cor.	5.8
3	Fog	18	11	y	12.5	19	Cor.	5.1
4	r′	17	12	o	11.5	20	Cor.	4.0
5	r	16	*13	r	10.5	21	Cor.	3.0
6	v	15	14	p	9.5	22	Cor.	2.0
7	g′	..	15	g′	7.5	23	Cor.	1.0
8	g	14	16	g′	7.0			

*Two identical series beyond this.

To facilitate comparison with the later work, where mercury light is used, a series of coronas in geometric sequence is given in table 9, in which the Welsbach mantle still furnishes the light. Here s denotes the chord of the angular diameter of the coronal disk on a radius of $R = 30$ cm., when

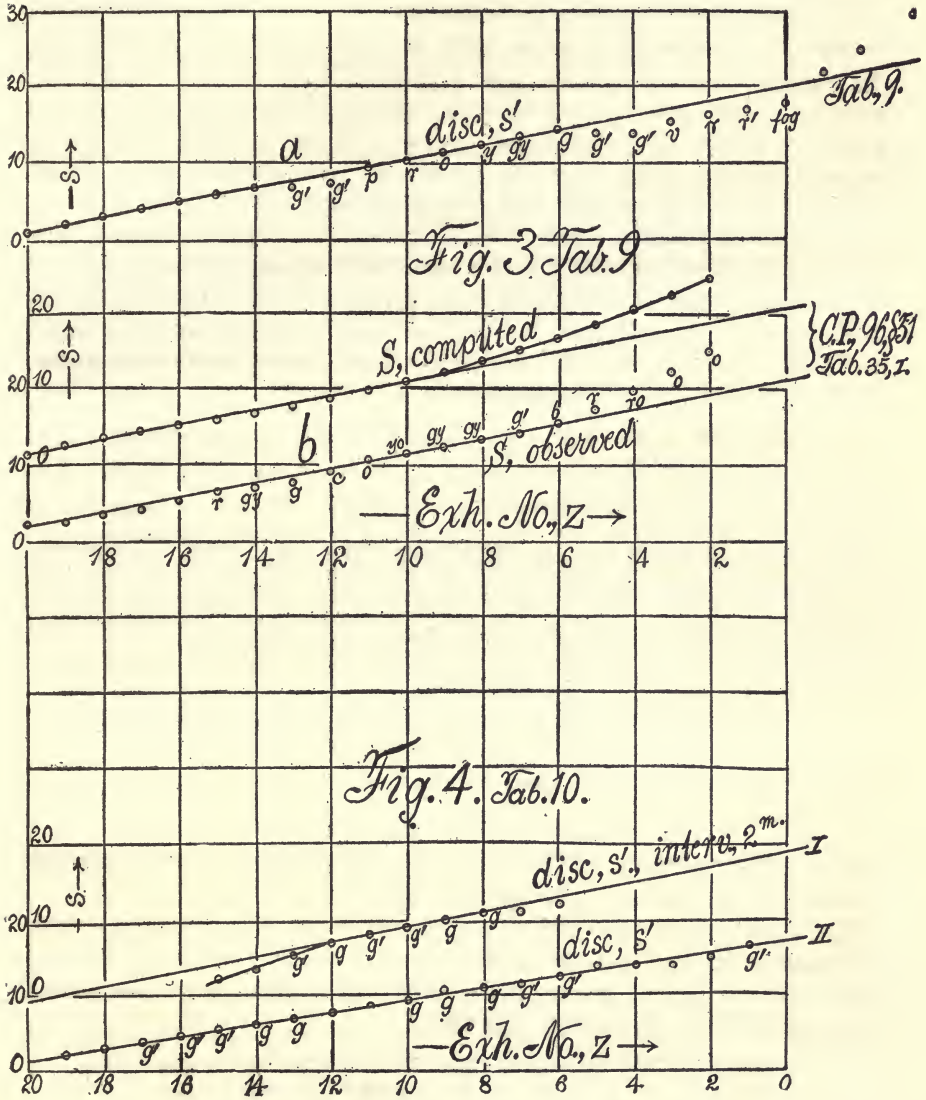

FIG. 3.—Charts for white light (Welsbach burner), $s/30$, of the reddish edge of the disk of coronas, in terms of a number, z, of the successive identical partial exhaustions in the series.

FIG. 4.—Charts for green mercury light, showing the coronal apertures, $s/30$, of the edges of the greenish disks of coronas, in terms of the series number z of the partial exhaustions. Series I for 2-minute intervals between exhaustions, series II for 1-minute intervals.

eye and lamp are at distances 30 and 250 cm. on opposite sides of the fog chamber. The colors of the edge of the disk are denoted by *r* red, *v* violet, *g* green, etc. The number of identical exhaustions made is equal to $z = 23$. Beyond $z = 13$ the series was obtained twice with identical data.

No attempt at computing nucleations from these data need be made, as they are practically identical with the earlier series given in the preceding report. In fact, in fig. 3 the *s* values or apertures have been constructed in the curve *a* in terms of the number of the exhaustion *z* in the geometric series. At *b* corresponding data (Carnegie Institution of Washington Publication No. 96, table 35, series 1) are taken from the report in question and represented in the same manner.

The feature of these results which I wish to accentuate is this, that after the tenth exhaustion, *i. e.*, for small and moderately large coronas, the *s*-data lie nearly on a straight line. In curve *a* this is the case almost throughout, or at least until the coronas become so large as to be vague and filmy, while the ends of the fog chamber interfere with the measurements. The slopes of these lines are:

In case *a*, ds/dz ..... $= 0.95$
In case *b*, ds/dz ..... $= 0.95$

or about the same in both cases.

25. Data with green mercury light, $10^6\lambda = 54.6$ cm.—Table 10 and figs. 4, 5, contain corresponding results obtained with a mercury arc lamp as the source of light. Different annuli are measured and the chords *s*, on a radius of 30 cm. are distinguished by accents as follows:

s' is the chord of the green disk,
s'' is the chord of the inner edge of the first green ring,
s''' is the chord of the outer edge of the first green ring.

The edges are fairly sharp. Hence

$$s = (s' + s'')/2$$

may be taken as the chord of the first green minimum. Optically the diameter of the particle is then $d' = 0.004/s$.

The water precipitated per cubic centimeter, *m*, differs with the drop of pressure $\delta p_3/p$ and the temperature. Putting n' as the optical value of the number of nuclei per cubic centimeter in the successive seven parts of the tables the data are:

	$10^6 m$	n'
Table 10:	*Grams.*	
Parts I and II.....	4.1	$122\, s^3$
Parts III and IV...	4.12	$123\, s^3$
Table 11:		
Parts V to VIII.....	4.02	$120\, s^3$

TABLE 10.—Standardization of fog chamber. Coronal disks. Mercury lamp. Phosphorus nuclei. Cock open 5 sec. Temperature 24°. $[\delta p'_2]=17.0$ cm.; $\delta p_3=17.6$ cm.; $\delta p'=18.9$ cm.; $y=(p-\pi-[\delta p_2])/(p-\pi)=0.770$; $\delta p_2/p=0.231$; $\pi=2.2$ cm. $m=4.1\times10^{-6}$g.

No.	Corona.	Interpolated s'	Observed s'	s
Part I.—Interval between observations 2 min. Barometer 76.17 cm. at 26°. Eye and lamp distances 30 cm. and 250 cm. Goniometer in front.				
1	Vague	13.0	12 ?	11.5
2	Vague	12.0	11 ?	10.6
3	g	11.0	10.8	9.8
4	g	10.0	9.9	8.9
5	g′	9.0	9.0	8.1
6	g′	8.0	8.0	7.2
7	g	7.0	7.0	6.4
8	g′	6.0	5.4	5.5
9	....	5.0	3.4	4.7
10	....	4.0	2.2	3.8
Part II.—The same. Interval between observations 1 min. More rapid filter.				
1	Vague g	16.4	16.5	14.2
2	Vague v	15.6	15 ?	13.5
3	Vague v	14.8	14 ?	12.8
4	Vague v	14.0	14 ?	12.1
5	Vague v	13.2	13.9	11.5
6	Vague v	12.4	12.5	10.8
7	g′	11.6	11.6	10.1
8	g′	10.8	11.2	9.5
9	g	10.0	10.8	8.8
10	g	9.2	9.5	8.1
11	Dull	8.4	8.9	7.5
12	Dull	7.6	7.9	6.8
13	g	6.8	7.0	6.1
14	g	6.0	6.2	5.5
15	g′	5.2	5.5	4.8
16	g′	4.4	4.7	4.1
17	g′	3.6	4.0	3.5
18	....	2.8	2.8	2.8
19	....	2.0	2.0	2.1

No.	Corona.	Interpolated s'	Observed s'	s
Part III.—Goniometer beyond fog chamber, eye at wall. Barometer 75.82 cm. at 25°. $y=0.769$; $\delta p_2/p=0.233$; $m=4.1\times10^{-6}$g.				
1	g	23.0	23	25
2	g	21.8	22	24
3	g	20.7	21	22.6
4	Vague	19.5	20	21.4
5	Vague	18.4	19	20.1
6	Vague	17.2	16	18.9
7	Vague	16.1	15	17.7
8	g	14.9	14	16.5
9	g	13.8	13.5	15.2
10	g	12.6	13.0	14.0
11	g′	11.5	11.7	12.8
12	Vague	10.3	10.5	11.6
13	Vague	9.2	9.4	10.3
14	g	8.0	8.4	9.1
15	Vague	6.9	7.3	7.9
16	g	5.7	6.3	6.7
17	....	4.6	5.2	5.4
18	....	3.5	4.0	4.2
19	....	2.3	2.3	3.0
Part IV.—The same, repeated.				
1	g	21.7	24	23.6
2	g	20.6	19	22.4
3	Vague	19.5	....	21.2
4	Vague	18.3	....	20.0
5	Vague	17.2	16	18.8
6	Vague	16.1	....	17.6
7	g	14.9	15	16.4
8	g	13.8	14.5	15.2
9	g	12.7	13.3	14.0
10	Vague	11.5	12	12.8
11	Vague	10.4	10	11.6
12	g	9.3	9.0	10.4
13	g	8.1	8.0	9.2
14	g′	7.0	7.0	8.0
15	g	5.9	6.0	6.8
16	g	4.8	5.0	5.6
17	....	3.6	4.0	4.4
18	....	2.5	2.5	3.2

In parts I to IV of table 10 the angular diameter s' of the green disks only was measured. The diameter s of the corresponding first minima may, however, be obtained by using the method of reduction found in parts V and VI, where $s=0.44+0.85\ s'$.

In parts V and VI the data for s' and s'', the angular diameter of the inner edge of the first ring are both observed, while in parts VII and VIII data for s' and s''', the outer diameter of the first ring, appear.

Turning specifically to parts I and II, in which the goniometer is in front of the fog chamber, it will be noticed that in series I a two-minute interval between exhaustions has been (exceptionally) introduced. The result is not good; for, as fig. 4 shows, there is a sudden break of the curve after the seventh exhaustion, probably due to time losses in the extra minutes. The reason, however, is by no means obvious. In series II, for 1-minute intervals, there is no break and the locus passing through the points for green disks (the others, not marked *g*, are to be disregarded) is persistently straight throughout. The curves show for series I, $ds/dz = 1.00$, green points only, and for series II, $ds/dz = 0.80$, suggesting a time loss in the first case. Compared with table 9, the values of ds/dz should be in the ratio of red and green minima, or

$$ds_r/dz : ds_g/dz = 0.95 : 0.80 \text{ correspond to } \lambda_r/\lambda_z = 63.0/54.6$$

The last ratio, 1.15, is somewhat short of the former, 1.19.

In series III and IV the pins of the goniometer are behind the fog chamber, the eye being at the front wall. In series III the relation

$$s' = 2.30 + 1.15(19 - z)$$

is remarkably well sustained throughout, and in series IV

$$s' = 2.50 + 1.13(18 - z)$$

gives a good account of the green coronas, if the dull cases are ignored.

The most interesting results are given in parts V and VI of table 11 and fig. 6, and the computations have been fully carried out. In these cases the chords on a radius of 30 cm. of the edge of the green disk s', and the inner edge of the first green ring s'', were successively observed. Fig. 6 contains both pairs of curves and their linear character is again astonishing. We may write

Part V: $s' = 2.0 + 1.10(19 - z)$ $\qquad s'' = 3.4 + 1.21(19 - z)$

$$s = 0.59 + 1.06s' = -0.56 + 0.96s''$$

Part VI: $s' = 2.0 + 1.13(18 - z)$ $\qquad s'' = 3.3 + 1.30(18 - z)$

$$s = 0.50 + 1.07s' = -0.44 + 0.93s''$$

where the minimum is located midway between s' and s'', both of which are fairly well demarcated.

From both series the mean value

$$s = 0.55 + 1.06 \qquad s' = -0.50 + 0.93\, s''$$

may be derived for the general reductions in this and other cases where s' is observed.

With the given value for s, the optical data for the diameters of the particles, $d' = 0.004/s$, and for the nucleation, $n' = 120\, s^3$ were computed.

The subsidence constant

$$S = s_z^2(1 - s_{z+1}^3/y\, s_z^3)$$

was obtained from the observations between $z = 13$ and $z = 19$ and a mean datum, $S = 12$, accepted as most satisfactory. It is, then, possible to compute n_0, the original nucleation, as

$$n_0 = n_z/\{y^z(1 - S/s_0^2) \ . \ . \ . \ . \ (1 - S/s_{z-1}^2)\}$$

from each of the groups of values specified. The mean results are: in part V, $n_0 = 4{,}540{,}000$; in part VI, $= 3{,}430{,}000$.

Knowing n_0, the series of data for nucleation given under $n \times 10^{-3}$, table 11 follow. From these the diameter $10^4 d = 199 n^{-1/3}$ of fog particles and the apertures $s = 0.004/d$ are finally computed. In other words, n and d are the data obtained in view of the occurrence of geometric series of nucleations with allowance for subsidence.

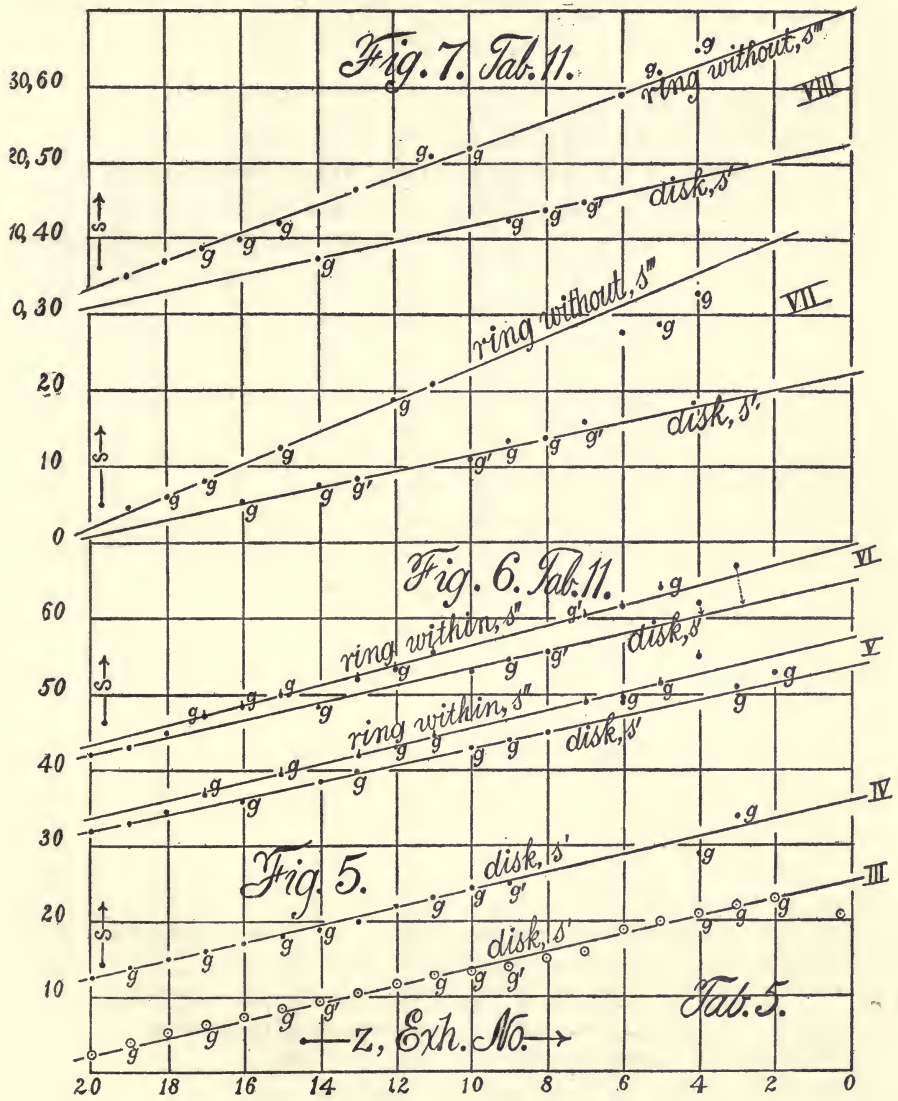

FIGS. 5, 6, 7.—Charts for mercury light, including measurements of the aperture of the disks s', of the aperture of the inner edge s'', and of the aperture of the outer edge s''', of the first green ring, in terms of the number z of the partial exhaustion. Vivid greens marked g, greenish g'; dull not marked. Apertures $s/30$ often displaced vertically for clearness.

TABLE 11.—Standardization of fog chamber. Mercury lamp. Phosphorus nuclei. Cock open 5 sec.; 60 sec. between observations. Barometer 76.4 cm. at 25°. Temperature 23°. Distance to lamp 250 cm. Goniometer behind. $\pi = 2.1$ cm. $S = 12$. $[\delta p_2] = 17.0$ cm.; $\delta p_3 = 17.6$ cm.; $\delta p' = 18.9$ cm.; $y = 0.771$; $\delta p_2/p = 0.231$; $m = 4.0 \times 10^{-6}$g.

Part V.—Coronal green disks and *inner* green edge of first rings.

No. z	Obs. s'	Interp. s'	Obs. s''	Interp. s''	s	$10^4 \times d'$	$10^{-3} \times n'$	$10^{-3} \times n$	$10^4 d = 199 n^{-1/3}$	$s = 0.2 \sqrt[3]{n}$ computed from n.
1	g_1 23	21.8	....	25.2	23.6	1.7	1580	4540	1.20	33
2	g_1 21	20.7	....	24.0	22.4	1.8	1350	3420	1.32	30
3	....	19.6	g 25	22.8	21.3	1.9	1160	2580	1.45	28
4	....	18.5	g 22	21.5	20.1	2.0	974	1940	1.60	25
5	....	17.4	g 20	20.3	18.9	2.1	810	1450	1.76	22.8
6	....	16.3	g′ 19	19.1	17.8	2.25	677	1080	1.93	20.8
7	g′ 15	15.2	....	17.9	16.6	2.4	549	800	2.14	18.8
8	g 14	14.1	....	16.7	15.5	2.6	447	589	2.37	16.9
9	g 13	13.0	....	15.5	14.3	2.8	350	432	2.62	15.3
10	g y	11.9	g 15.5	14.3	13.1	3.05	270	313	2.93	13.7
11		10.8	g 13	13.1	12.0	3.3	208	225	3.27	12.2
12	g′	9.7	g′ 12	11.9	10.8	3.7	151	159	3.67	10.9
13	g 8.5	8.6	....	10.7	9.7	4.1	110	110	4.16	9.6
14	y′	7.5	g 9.5	9.4	8.5	4.7	73.7	73.8	4.74	8.4
15	6.0	6.4	g′	8.2	7.3	5.5	46.7	47.4	5.50	7.3
16	y′	5.3	g 6.8	7.0	6.2	6.4	28.6	28.3	6.52	6.1
17	g y 4.5	4.2	....	5.8	5.0	8.0	15.0	14.9	8.10	5.0
18	y 3.0	3.1	....	4.6	3.9	10.3	7.1	....	....	....
19	2.0	2.0	....	3.4	2.7	14.8	2.4	....	....	....

Part VI.—The same, repeated.

No. z	Obs. s'	Obs. s''	s	$10^4 \times d'$	$10^{-3} \times n'$	$10^{-3} \times n$	$10^4 d = 199 n^{1/3}$	$s = 0.2 n^{1/3}$ computed.
1	g′ 27	....	23.3	1.7	1520	3430	1.32	30.2
2	g 22	....	22.1	1.8	1300	2580	1.46	27.4
3	....	g 24	20.9	1.9	1100	1940	1.60	25.0
4	....	g 22	19.7	2.0	918	1460	1.76	22.7
5	g′ ..	g′ 20	18.5	2.2	760	1090	1.94	20.6
6	g′ 15.5	....	17.3	2.3	622	811	2.14	18.7
7	g 14.5	....	16.0	2.5	492	600	2.37	16.9
8	13	....	14.8	2.7	389	441	2.62	15.2
9	g y !	g′ 15.5	13.6	2.9	301	321	2.92	13.7
10	....	g 13.5	12.3	3.3	226	232	3.25	12.3
11	g′	g′ 12	11.2	3.6	168	164	3.66	10.9
12	g 8.2	....	9.9	4.0	118	115	4.12	9.7
13	y	g 10	8.7	4.6	79	77.7	4.68	8.5
14	g′	8.5	7.5	5.4	50	50.4	5.42	7.4
15	....	7.2	6.3	6.4	30	30.5	6.56	6.3
16	y′ 4.9	g′	5.1	7.9	16	16.5	7.84	5.1
17	3.0	....	3.8	10.5	6.8	6.9	10.5	4.0
18	2.0	....	2.7	14.8	2.4	1.0	....	....

TABLE 11.—Standardization of fog chamber—Continued.

No. z	Obs. s'	Interp. s'	Obs. s'''	Interp. s'''	s	$d'=0.004/s$	$10^{-3}\times n'$
Part VII.—The same. Coronal green disks and outer green edge of first ring.							
1	....	18.6	g 33	35.6	20.3	1.97	1000
2	....	17.5	g 29	33.5	19.1	2.09	836
3	....	16.3	? 28	31.3	17.9	2.23	688
4	g′ 16	15.2	....	29.2	16.7	2.40	559
5	g 14	14.1	....	27.1	15.5	2.58	446
6	g 13.5	12.9	....	24.9	14.3	2.80	350
7	g′ 11.1	11.8	....	22.8	13.1	3.05	270
8	....	10.7	g 21	20.7	11.9	3.36	202
9	g′	9.5	? 19	18.5	10.7	3.74	147
10	g 8.5	8.4	....	16.4	9.5	4.21	103
11	g g 7.6	7.3	....	14.3	8.3	4.82	68.6
12	g′	6.2	12.5	12.2	7.1	5.63	43.0
13	g 5.5	5.0	....	10.0	5.9	6.78	24.6
14	g′	3.9	g 8.0	7.9	4.7	8.51	12.5
15	....	2.8	6.0	5.8	3.5	11.4	5.1
16	....	1.6	4.5	3.6	2.3	17.4	1.5
17	....	.5	3.0	1.5	1.1	36.4	.2
Part VIII.—The same repeated.							
1	g 22.5	19.2	.....	35.8	21.0	1.90	1110
2	....	18.1	g 35	33.9	19.8	2.02	930
3	....	17.1	g 32	32.0	18.7	2.13	785
4	....	16.0	29	30.0	17.6	2.27	654
5	g′ 15	14.9	....	28.1	16.4	2.43	529
6	g 13.8	13.8	....	26.2	15.3	2.61	430
7	g 12.5	12.8	....	24.2	14.1	2.84	336
8	g y	11.7	g 22	22.3	13.0	3.08	264
9	....	10.6	g 21	20.4	11.9	3.35	202
10	....	9.6	....	18.4	10.7	3.74	147
11	g′	8.5	g′ 16.5	16.5	9.6	4.17	106
12	g 7.5	7.4	....	14.6	8.4	4.76	71.2
13	g′	6.4	g 12.1	12.7	7.3	5.48	46.7
14	g y	5.3	g 10	10.7	6.2	6.45	28.6
15	....	4.2	g 8.7	8.8	5.0	8.00	15.0
16	....	3.1	6.8	6.9	3.9	10.3	7.1
17	....	2.1	5.0	4.9	2.7	14.8	2.4
18	....	1.0	3.5	3.0	1.6	23.5	.5

All the results shown in table 11 have been constructed graphically in figs. 8 and 9 for parts V and VI of the tables, respectively. The observed and computed apertures s are first given; then the observed or optically computed d', and the computed d from sequences appear, and finally the observed or optic n' and the computed nucleation n from sequences. The corresponding data coincide very closely after nine or eleven exhaustions, *i. e.*, for moderately small and small coronas; but in the case of large coronas and nucleations there is marked systematic divergence. A discussion of these results will be given presently.

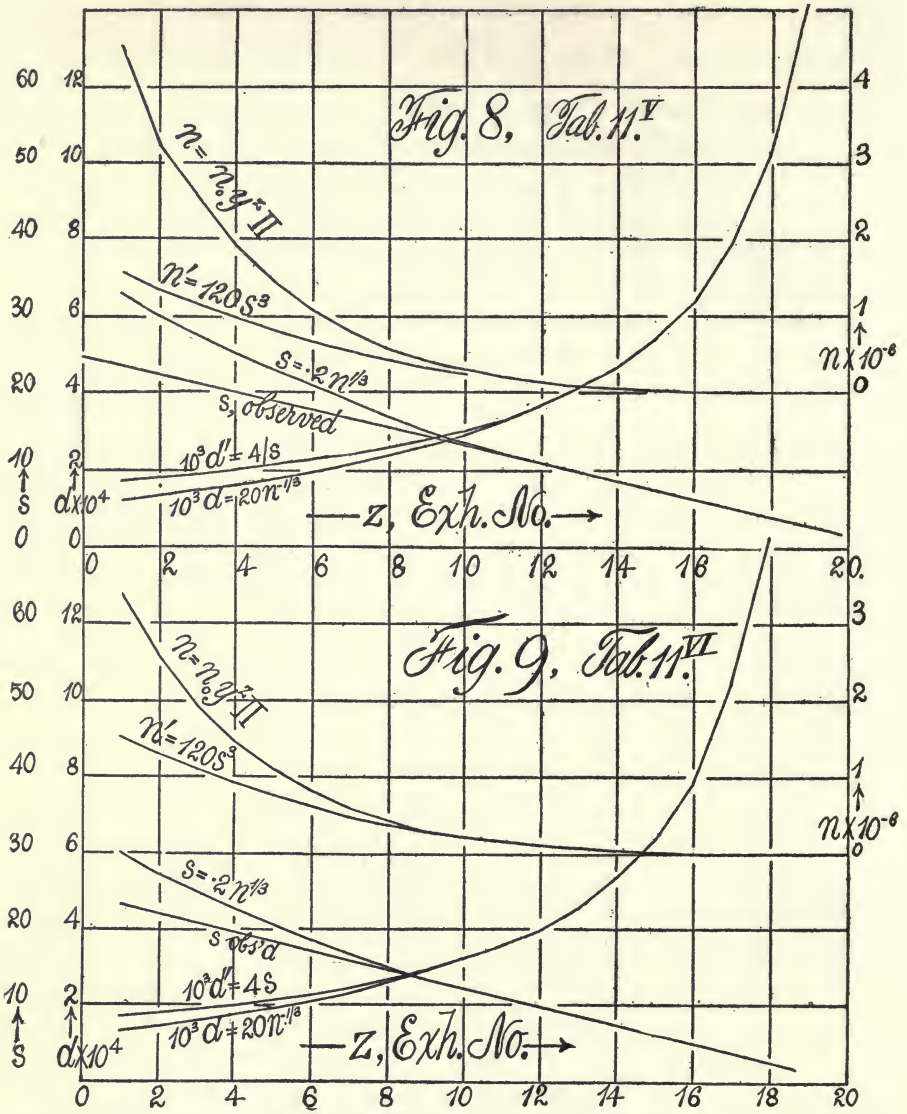

FIGS. 8, 9.—Nucleations n, n', coronal apertures $s/30$, and diameters d, d', of fog particles observed and computed for the successive partial exhaustion, number z.

Finally, parts VII and VIII of table 11 contain measurements of the chord of the angular diameter (radius of 30 cm.) of the outer edge of the green disk s' and the outer edge of the first ring s'''. The minimum may be deduced from s', since $s = 0.54 + 1.06s'$ has been accepted. From s the optic value of diameter of fog particle d' and the nucleation n' has been computed. The apertures are very fully given in fig. 7, in relation to the

number z of the exhaustion. The curves are again linear in character, but in case of the outer edge s''', the insufficient size of my fog chambers and the greater vagueness of definition interferes with close measurement. The results are—

Part VIII: $s' = 1.00 + 1.07\,(18 - z)$ $\qquad s''' = 3.00 + 1.93\,(18 - z)$
$\qquad\qquad s = 1.61 + 1.14\,(18 - z)$

Part VII: $s' = 0.50 + 1.13\,(17 - z)$ $\qquad s''' = 1.50 + 2.13\,(17 - z)$
$\qquad\qquad s = 1.08 + 1.20\,(17 - z)$

As a rule s''' is less than twice s'. The data for s' and s are obtained alternately, as the table shows, the green color passing from the disk of the first ring and returning again in succession.

26. Inferences. Interference and diffraction.—The tables and charts show, in the first place, that the disk and first ring of the coronas are alternately vivid green, other colors being dull because the remaining lines of the mercury spectrum are faint. At intervals neither disk nor ring are quite green. Hence there is a periodic term impressed on the diffractions, which may be identified as an interference similar to the case of the lamellar grating referred to in another paper.*

When monochromatic light is used it is necessary, therefore, to observe both the edge of the disk and the inner edge of the first ring, for neither appear vividly at the same time. The chord s on a radius of 30 cm., for the minimum in terms of the corresponding chords, s' and s'', of the first and second edges specified, may then be written

$$s = 0.55 + 106\,s' \qquad s = -0.50 + 93\,s'$$

Probably the ratio s/s' and s/s'' should be constant and the absolute term in these equations is an error of observation; but as it is small little depends upon it, millimeters only being significant.

If we summarize all the observations for ds/dt, the agreement as a whole is in keeping with the nature of the observations and reasonably satisfactory. Thus in

Series I, II,	$ds'/dz = 0.90$	$s = 0.44 + 0.85s'$ (goniometer in front)
III,	1.15	
IV,	1.13	
V,	1.10	$s = 0.55 + 1.06s'$ (goniometer behind)
VI,	1.13	mean $ds'/dz = 1.12$
VII,	1.13	
VIII,	1.07	

*Amer. Jour. Sci., xxv, p. 224, 1908.

The astonishing feature of these data is the occurrence of linear loci for s and z nearly throughout the extent of the curves. It is as difficult to even conjecture a reason for this as it is easy to find reasons against it. The presumptive equation for s is

$$s = 0.004(\pi/6m)^{1/3} n^{1/3} \qquad \propto \sqrt[3]{n}$$

and for n_z if π denotes the product

$$n_z = n_0 y^z \prod$$

Hence

$$s = 0.004(\pi n_0/6m)^{1/3} (y^z \prod)^{1/3}$$

If we disregard the subsidence correction $\prod$ for large coronas

$$ds/dz \propto y^{z/3}$$

in which there is no suggestion of a sustained constancy of the coefficient ds/dz such as the experiments show.

To come to some conclusion as to the cause of the discrepancy between the optic value of the nucleation n' and the presumable value n (geometric progression), we may, as in table 12, compare the successive value $n'_{z+1}/n'_z = s_{z+1}{}^3/s_z{}^3$ in their relation to $y = 0.771$, the exhaustion applied. The table shows that for very large coronas $n'_{z+1}/n'_z > y$, whereas for very small coronas $n'_{z+1}/n'_z < y$. For the intermediate coronas (g_3), *i. e.*, from the seventh to the tenth exhaustion among twenty, the ratio is nearly equal to y. Ratios smaller than y may be reasonably interpreted as due to subsidence and the subsidence constant S is actually of the order of values to be computed from the viscosity of the medium and the size of the vessels and fog particles. Within this range (coronas smaller than g_3) the optic and the presumptive nucleation may in fact be brought into agreement.

In case of the large coronas, however, subsidence is virtually absent and the occurrence of $n'_{z+1}/n'_z > y$ calls for some apparent production of nuclei at each exhaustion, which is naturally altogether improbable. In table 12 I have therefore additionally inserted n' and $n - n'$, the latter showing the number of nuclei not registered by condensation.

For, no matter whether condensation on a given group of nuclei occurs or not, no matter how many nuclei have failed of catching a charge of water, the removal of nuclei by partial exhaustion must take place in the same way. Such removal is independent of condensation and would occur in a dry atmosphere under similar treatment. Consequently y can not be too large. It may be too small not only from subsidence, but from time losses (decay) or as the result of the purification of air due to turbulent motion across a solid or liquid surface. Consequently n may be regarded as an inferior limit of the nucleation with a probably close

approximation to the true value. A comparison of n and $n-n'$ would in such a case show the percentage of nuclei of irregular size which have failed of capture, the number being $n-n'$.

At the same time it must always be recalled that no adequate theory of coronas exists and that therefore the meaning of n' is obscure. We must in any case place a part, if not all, the discrepancy between n and n' within the province of such a theory. The need of it is particularly manifest for the large coronas, in which there is accentuated superposition of interference and diffraction. Small coronas may be tested by coincident results obtained from subsidence, and the agreement is then well within the errors of observation.

TABLE 12.—Comparison of nucleations.

Part V.					Part VI.				
z	$s_{z+1}^3/s_z^2 y$	s_{z+1}/s_z	$10^{-3}n'$	$10^{-3}(n-n')$	z	$s_{z+1}^3/s_z^2 y$	s_{z+1}/s_z	$10^{-3}n'$	$10^{-3}(n-n')$
1	0.90	0.86	1580	2960	1	1.11	0.86	1520	1910
2	.89	.86	1350	2070	2	1.10	.84	1300	1280
3	.92	.84	1160	1420	3	1.09	.84	1000	940
4	.93	.83	974	966	4	1.08	.83	918	542
5	.92	.84	810	640	5	1.06	.82	760	330
6	.95	.81	677	403	6	1.03	.79	622	189
7	.95	.81	549	251	7	1.03	.79	492	108
8	.98	.79	447	142	8	1.01	.77	389	52
9	1.00	.77	350	82	9	.97	.75	301	20
10	1.00	.77	270	43	10	.96	.74	226	6
11	1.06	.73	208	17	11	.91	.70	168	−4
12	1.06	.72	151	8	12	.87	.67	118	−3
13	1.14	.67	110	0	13	.83	.64	79	−1
14	1.22	.63	74	0	14	.77	.59	50	0
15	1.26	.61	47	0	15	.68	.53	30	0
16	1.46	.53	29	−1	16	.56	.43	16	0
17	1.63	.48	15	0	17	.45	.34	7	0
18	2.32	.33	7	....	18	....	....	2	−1
19	....	....	2.4	....					
In the first eight exhaustions there is an apparent production of nuclei.					In both cases V and VI there is accession of nuclei at first and withdrawal finally.				

EFFICIENCY OF LARGE AND SMALL FOG CHAMBERS, ATTACHED TO THE SAME VACUUM CHAMBER.

27. Fog chambers.—The large apparatus used in the experiments* for the displacements of ions showed relatively low degree of condensational efficiency. It was therefore thought worth while to compare fog chambers both larger and smaller than the normal size (No. 1) with regard to their powers in catching nuclei. In addition to the large receiver (No. 2) specified, an exceptionally small fog chamber (No. 3) was specially constructed. Experiments were made with each in turn, both for the case of the vapor nuclei of dust-free air and of ions.

*See chapter III, fig. 12.

The dimensions of the three fog chambers were:

Number.	Apparatus.	Length.	Diameter.
		cm.	*cm.*
1	Old cylindrical.....	45	12
2	Large conical.....	110	14 to 22
3	Small cylindrical....	16	11

The axes were in all cases horizontal and care was taken to insure the occurrence of saturated air.

It is interesting to note that immediately after the small fog chamber was put together, there was an internal source of high nucleation active throughout 10 or 20 exhaustions, a result frequently obtained in other similar cases. It is none the less difficult to detect the reason for its occurrence. It vanishes completely in the course of time. It is probably identical with the emanation obtained by Russel* from metals and resins; at all events its eventual evanescence renders it harmless.

28. Data.—The preliminary data are given in table 13, where in the case of small apparatus the color of the corona was chiefly used to determine the nucleation. The ordinary form of goniometer would have been useless, as most of the larger coronas transcend the limits of the apparatus. The barometer is as usual denoted by p and the sudden drop of pressure after the return of isothermal conditions with both chambers in communication, by δp; n is the estimated nucleation per cubic centimeter.

These results are given with sufficient detail graphically in fig. 1, and are compared with the curves holding for the normal apparatus, No. 1, taken from a preceding report for identical exhaustions. In case of the large vessel, No. 2, it was impracticable to carry the exhaustions very high because of the danger of breaking the vessel.

The results show that fog and rain limits are not materially changed, no matter whether large or small apparatus is used. But few experiments were made.

The efficiencies of the apparatus, however, differ in marked degree. In case of the large apparatus, No. 2, less than 150,000 vapor nuclei respond, even at the highest exhaustions. The number of nuclei caught increases pretty uniformly with $\delta p/p$, even beyond the limits tested, but the efficiency is enormously lower than obtained for No. 1, where 1,500,000 to 2,000,000 is the maximum number caught. The small apparatus, No. 3, is even in excess of this value, inasmuch as over 3,000,000 nuclei per cubic centimeter are precipitated, while for equal

*Russel: Proc. Roy. Soc. London, LXI, 424, 1897; LXIII, 102, 1898.

values of $\delta p/p$, it is nearly twice as efficient as No. 1. What is particularly interesting is the definite occurrence of coronas of the first order, viz: the crimson c_1, and the red r_1, above the green g_2. The observer is left in doubt as to this, unless correlative measurements of aperture are made, which in case of table 13 was not feasible for so small apparatus. Such results are given, however, in table 14.

TABLE 13.—Comparison of large and small fog chambers. Dust-free air. Fog chamber No. 2, length 110 cm., diameter 14 to 22 cm.; fog chamber No. 3, length 16 cm., diameter 11 cm.

$\delta p/p$	s	$10^{-3}n$
Fog chamber No. 2.* Barometer 76.35 at 25°.		
0.202	....	....
.248	r	r
.287	2.6	4.5
.296	2.7	5.1
.340	4.0	19.2
.360	4.6	30.2
.405	6.2	80.6
.440	g b p 7.0	120.0
Fog chamber No. 3.† Barometer 76.43 at 25°.		
0.241	0	....
.262	1	0.2
.288	1	.2
.313	2	.3
.338	4	19
.360	c	106
.388	g	912
.410	v p	1560
.420	c	2200
.460	r	3000
.481	o-r	3000
.501	o-r	3130
.528	o-r	3220
Fog chamber No. 3. Barometer 76.69 at 27°.		
0.334	4	19
.348	g′ 5.2	40
.360	g 7.2	157
.370	9.7	440
.385	g 10.2	910
.396	b 10.5	1070
.364	c 9.0	310
Fog chamber No. 3, with wet cloth lining.		
0.335	1.9	2
.362	7.0	144
.385	10.8	910
.410	12.0	2200
.433	r	2900
.600	r	3470

*Not quite free from leak.
†Freshly put together, shows an internal source of nucleation throughout 10 or 20 successive exhaustions.

All fog chambers which have aged are free from internal sources of nuclei, whereas when freshly installed they may generate them throughout many successive exhaustions. Even after this, production of nuclei is still appreciable if long intervals of time elapse between the exhaustions. An endeavor was made to detect the nature of this phenomenon, but a satisfactory answer has not yet been reached beyond the surmise given above. The production is observed both in large and in small chambers and the nuclei are dust-like in size.

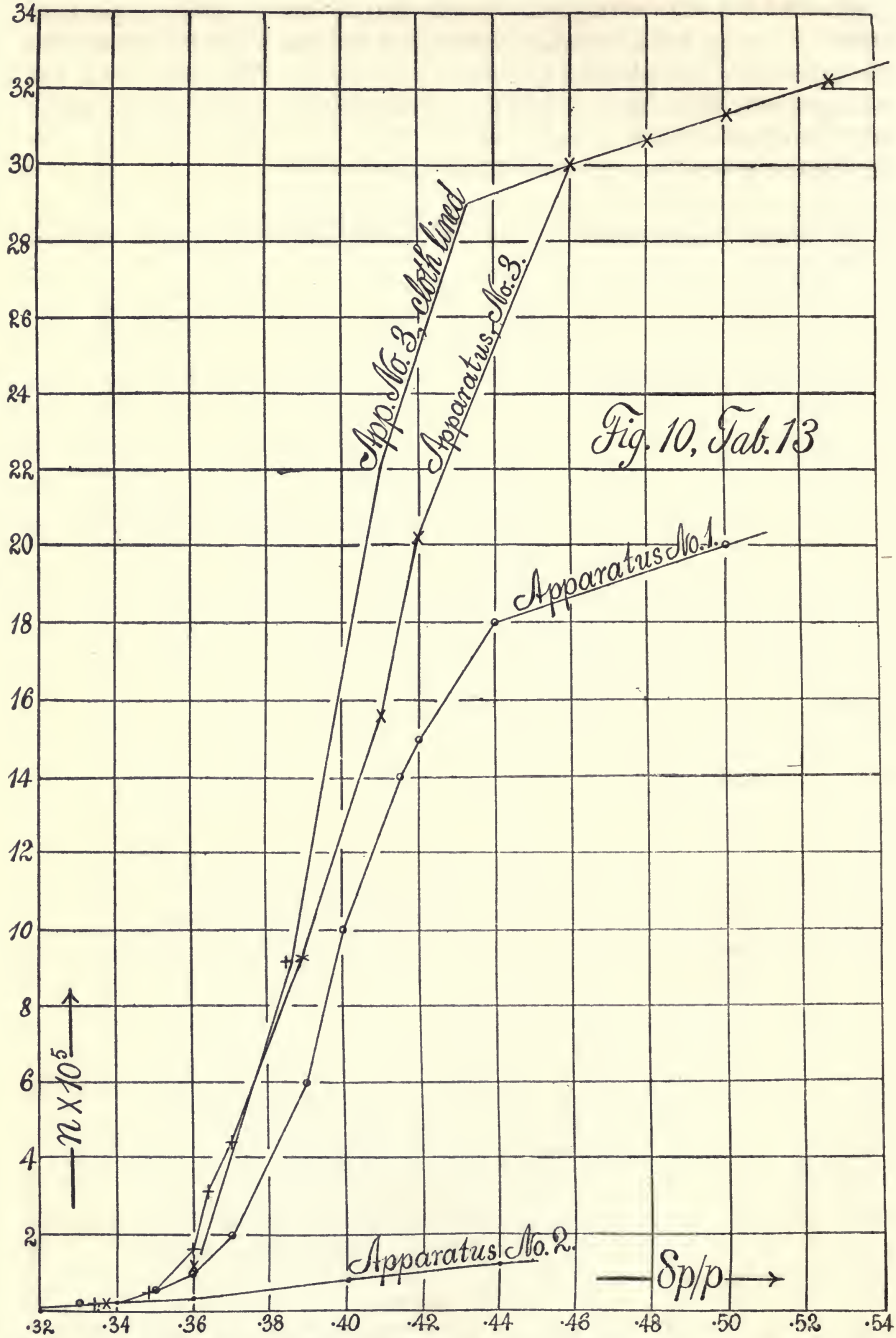

FIG. 10.—Condensational efficiency of large (1), intermediate (2), and small (3) fog chambers, as appearing in the number n of vapor nuclei of dust-free wet air caught on exhausting as far as $\delta p/p$.

29. Data for apertures.—To identify the coronas in case of the small vessel, No. 3, as to the order to which they belong, a special goniometer was constructed. In using this the eye is placed at the nearer wall of the fog chamber, while the two round vertical rods for defining the angular aperture are placed beyond the further wall, on a radius of 30 cm., the eye being the center. The inner edges of the rods determine the aperture by aid of a sliding scale passing across them. In this way very large coronas may be measured in relatively small apparatus. The angular

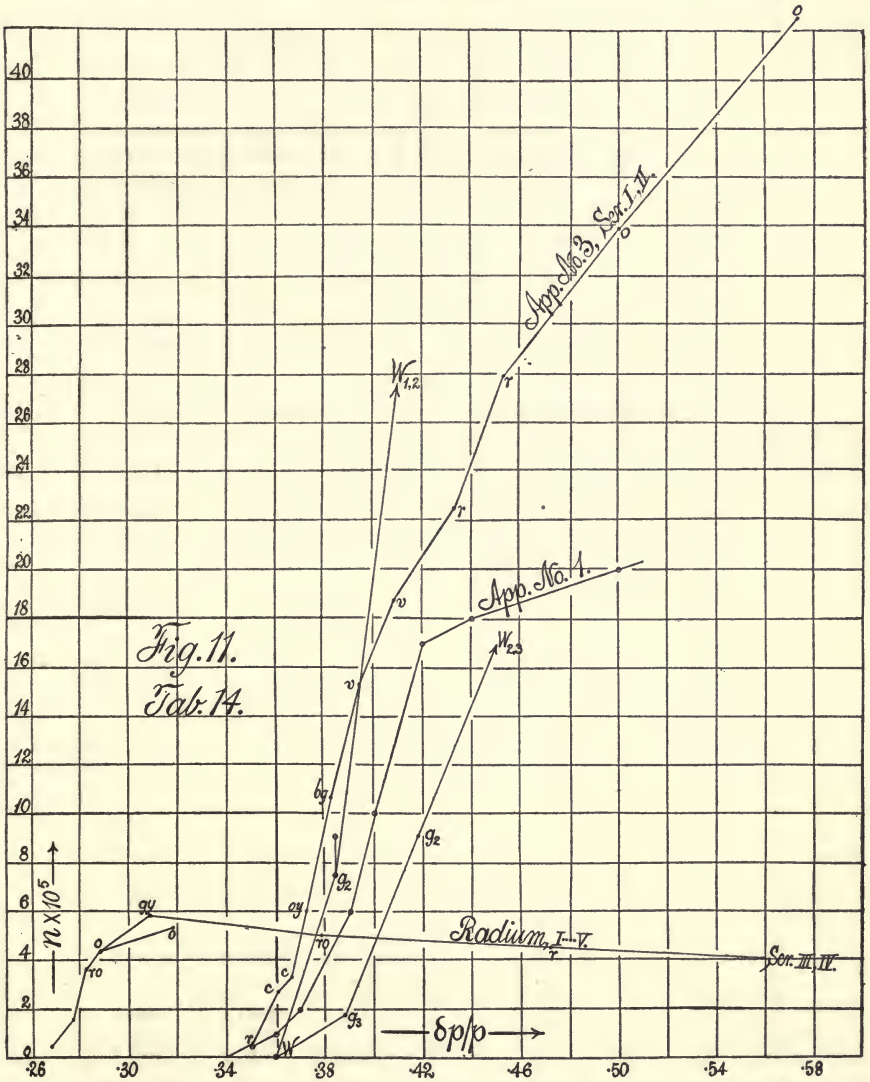

FIG. 11.—The same as fig. 10, obtained by goniometer measurement, including Wilson's colors and the effect of weak radium.

diameters are increased (*caet. par.*) and vision is at an advantage as to clearness. Test experiments made with definite coronas showed that the aperture s of the old goniometer was about equal to 0.9 s of the new, and with this number the reductions needed were made with the results given in table 14. The apparatus showed the same corona for the same $\delta p/p$ on a number of successive days, so that fixed conditions had been reached.

TABLE 14.—Efficiency of the small fog chamber, No. 3, with special goniometer. Length 16 cm., diameter 11 cm., 2-inch exhaustion pipe. Dust-free air and ionized air. Radium I . . . . V, axially placed.

Dust-free air.			Ionized air.		
$\delta p/p$	s	$10^{-3}n$	$\delta p/p$	s	$10^{-3}n$
I. Barometer 76.54 at 25°.			III. Barometer 76.54 at 25°.		
0.249	0	0	0.242	0	0
.261	.8	.06	.249	.6	.06
.273	1.0	.23	.251	1.1	.27
.285	1.1	.30	.255	1.5	.50
.300	1.4	.50	.268	6.5	48
.314	2.0	1.5	.282	12.5	360
.327	2.5	3.3	.288	13.5	436
.340	2.8	4.5	.318	14	537
II. Barometer 76.85 at 23°.			IV. Barometer 76.85 at 23°.		
0.340	3.0	5.6	0.277	9.7	159
.350	r 6.5	57.4	.308	g y 14.0	584
.361	c 10.8	278	.378	†r o 13.0	507
.366	*c 11.4	335	.472	†r 12.0	454
.372	o_1 y 16.0	599	.540	†c 11.5	416
.382	b_1 g 17.0	1070			
.394	v	1530	V. Radium II at 75 cm., observed at 50 cm. from exhaustion end in large fog chamber, No. 2, length 110 cm.; diameter 14 to 22 cm. Barometer 76.85 at 26°.		
.408	v	1870			
.433	r 18.5	2250			
.453	r	2790			
.500	o 21	3390			
.573	o	4320			
			0.194	....	....
			.217	....	....
			.238	1	0.2
			.260	3.5	10.6
			.281	g b p 7.2	97.2
			.326	b r 7.8	133
			.427	7.7	160
			VI. Barometer 76.35 at 25°.		
			.319	p 8.5	169
			.367	p 8.5	187
			.434	p 8.4	208

*Note different apertures for the same color.
†Coronas decreasing with increasing precipitation.

30. Results.—The results are constructed in fig. 11 in comparison with typical results for apparatus No. 1. The same high efficiency already recognized in case of this apparatus in table 13 is again exhibited, the nucleation caught actually reaching over 4,000,000 per cubic centimeter or invading the region of orange coronas, o_1, of the first order. It is now probable that with green monochromatic light the green corona, g_1, of the first order may actually be detected. With white light, however, the initial effect is a mere fog.

A number of trials with radium (I to V, within the chamber) exhibited the same terminal coronas as in the fog chamber No. 1. Ions are caught with the same facility in both chambers and about at the same $\delta p/p$. In other words, whereas vapor nuclei are caught in greater number by the more efficient small fog chamber, this is not the case with ions, as comparisons of the earlier records for No. 1 show, nor with the positions of the fog limit and rain limit. Moreover, in series 5 and 6, obtained with the excessively large apparatus, the ions are appreciably displaced after condensation has begun, showing that the supersaturation is excessive.

In series IV there is a pronounced decrease of the nucleation with increasing $\delta p/p$. From the maximum $n=584{,}000$ at $\delta p/p=0.31$, the nucleation drops uniformly to $n=416{,}000$ at $\delta p/p=0.54$. Inasmuch as the correction for increased precipitation has been applied (smaller coronas at high pressure-differences, because more water is precipitated), this result is to be associated with the greater removal of nuclei at high exhaustion. The coronas show the number of nuclei in the exhausted fog chamber.

The smaller nucleations in series V and VI are referable in part to the weaker radium used and in part to the exceptionally large vessel employed.

31. Conclusion.—The final question of interest is a revised comparison of these results with C. T. R. Wilson's disk colors, if his two extreme greens are interpreted as g_2 and g_1 instead of g_3 and g_2, as preferred in the preceding report.* In such a case the nucleations may be estimated as follows:

$\delta p/p$	Color.	$n\times 10^{-3}$	$d\times 10^{6}$
			cm.
0.360	Fog limit	0	....
.384	g	800	230
.418	g	7,000	120

*Am. Jour. Sci., XXIV, 1907, p. 309; Carnegie Institution of Washington Publication No. 96, 1908, sec. 35.

As far as $n = 1{,}500{,}000$ nuclei per cubic centimeter, this curve would still lie below the curve for the small apparatus. It then crosses and passes beyond it to a limit of over 7,000,000 nuclei, instead of 4,000,000 nuclei per cubic centimeter, estimated for the small fog chamber, No. 3. It is difficult, of course, without an actual measurement of aperture, to come to a conclusion as to the order of mere colors, but the possibility of reaching 10,000,000 nuclei per cubic centimeter does not now seem out of the question. The probability that the initial white fogs seen with ordinary light may be resolved with sufficient clearness for measurement when monochromatic light is used, has already been suggested. One may notice, however, in conclusion, that even in case of the extreme green, the diameter of particle would still be over twice the wave-length of light.

CHAPTER III.

REGIONS OF MAXIMUM IONIZATION, AND MISCELLANEOUS EXPERIMENTS.

REGIONS OF MAXIMUM IONIZATION DUE TO GAMMA RADIATION.

32. Introductory.—I have recently* standardized the fog chamber by the aid of Thomson's electron. The method (as will be shown in the following chapters) is not only expeditious, but leads by inversion, when my old values of the nucleations of the coronas are inserted, to values of e which agree with Thomson's and other estimates. This affords an incidental check on the broader bearings of the work. Before describing these experiments it will be expedient to refer to a number of incidental results bearing on the work, among which the displacement of ionization on rapid exhaustion is most important. This has been studied both in long and in short fog chambers.

33. Short fog chamber (see fig. 18, below).—The experiments themselves run smoothly and take but a few minutes each; but there is an *inherent* difficulty involved in the interpretation of the distributions of ionization observed in the fog chamber. The radium (10 mg., 100,000×, contained in a small, thin, sealed glass tube), is introduced into the inside of a cylindrical fog chamber, 45 cm. long, by aid of an aluminum tube (walls 1 mm. thick and about 0.25 inch in diameter), thrust axially from one end to the other of the horizontal chamber. The inner end of the aluminum tube is thoroughly sealed; the other end lies quite outside the fog chamber, is open, and serves for the introduction of the radium tube. In this way the latter may be moved axially from the glass end of the fog chamber on the right of the observer to the metal cap which closes the fog chamber on the left.

When the radium is placed successively at distances of about 11 cm. apart, within the available 45 cm. of the length of the fog chamber, the maximum nucleation (ionization) coincides with the position of the radium when both are near the glass end of the chamber (12 cm. in diameter). The nucleation then falls off rapidly and at first uniformly from the glass end to the metal end, where the coronas are strikingly smaller and the nucleation less than one-half of that observed at the glass end. Considered alone this would appear like the natural effect of an increasing distance from the source, except that the coronas near the distant end approach a constant diameter.

*Am. Jour. Sci., xxvi, pp. 87–90, 1908.

When the radium is moved about 12 cm. (one-quarter of the length of the fog chamber) from the glass end toward the metal end, the maximum nucleation, moving at a greater rate toward the brass end, has already outstripped the position of the radium and now lies near the middle of the chamber. The coronas and the corresponding nucleations, therefore, fall off rapidly toward both ends. In other words, the *maximum nucleation is seen where there is no radium.*

On moving the radium to the middle of the chamber, the position of the maximum nucleation coincides with the brass end, over 20 cm. beyond the radium. The coronas now fall off from left to right, to a uniform size near the glass end of the chamber, the ratio of the extreme nucleations being at least 200,000 to 100,000 per cubic centimeter in the cases examined. Finally, when the radium is placed in the brass cap of the chamber, the maximum still lies there and the nucleation falls off toward the glass end, but all nucleations are *reduced throughout* about one-half.

It is clear that the two ends of the chamber behave differently, but no simple hypothesis of the known properties of the rays, at least, will account for the occurrence and location of regions of maximum nucleation, nor for the high nucleation ratios specified. Moreover, plates of lead placed outside over the glass end of the chamber to modify the secondary radiation are quite without effect. Covering the aluminum tube with a thick lead pipe the phenomenon is slightly reduced in magnitude, but not in character. It follows that the gamma rays are chiefly concerned.

34. Behavior after removal of radium.—A final element of interest is the behavior of the axial aluminum tube after the radium (in small sealed glass or aluminum tubes) has been removed. The internally-sealed aluminum tube is distinctly radioactive for several hours, even though gamma rays alone have passed through it. The activity vanishes gradually, and more quickly if the ions are continually precipitated by exhaustion. The behavior of this residual nucleation is very peculiar; if the aluminum tube is pushed into the fog chamber, axially, from the glass end as far as the middle, the part of the chamber around the tube shows strong coronas on exhaustion, while the other half (toward the brass cap) is blank. Something, consisting of very slow-moving particles, gradually diffuses radially out of the aluminum tube. Of course it is difficult to deny with assurance that merest traces of emanation decaying within the aluminum tube may not possibly account for the activity; but what is remarkable in any case is the existence side by side of a region with nucleation and a region without it, in the absence of anything like a partition. The fog chamber itself must at all times be scrupulously free

from infection such as an emanation would produce, and anything of this kind is at once detected.

35. Long fog chamber.—After obtaining these results, the work was resumed with the aid of a larger fog chamber, *F F*, fig. 12, conical in shape, 110 cm. long, 22 cm. in diameter at the broad end, tapering down to 14 cm. at the small end, *E*, whence the exhaustion took place. It was so mounted as to place the axis slightly inclined above the horizontal, in order that an even depth of water, *w*, from end to end, might be stored. In the first experiments the large end was of glass, in the later of metal, but this difference is without appreciable effect upon the present results. In each case a hole *H*, 2 or 3 cm. in diameter, was available near the center of the large end for the introduction of an axial aluminum tube *AR* (walls 0.11 cm. thick), running from end to end of the chamber and closed at *R* within it. In the inside of this tube the sealed radium tubelets could be moved from place to place, in a way similar to the method followed in the preceding experiments. No wet-cloth lining was introduced, because the experiments had to be performed so slowly that saturation in case of a clean fog chamber, to which water adheres in an even film, was assured. The best method of cleaning is vigorous rubbing with a soft rubber probang, as for instance, a thick piece of rubber tubing at the end of a metal rod. Every part of the glass must be scoured.

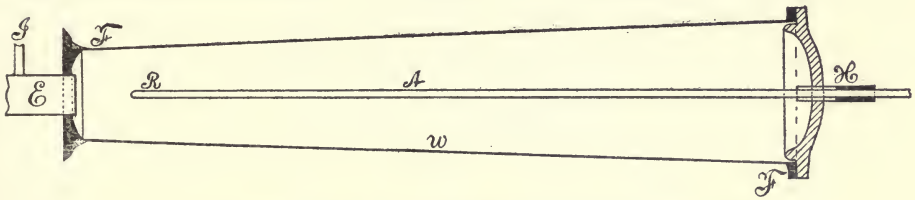

FIG. 12.—Section of long fog chamber with hollow aluminum core.

The chamber was too large to admit of the capture of as many ions for like conditions of exhaustion as was the case with the preceding smaller apparatus, but this difficiency is of no importance here. Filtered air is admitted through *I*.

36. Data.—Table 15 gives an example of typical results as obtained both with the glass and the metal capped fog chamber, the opposite (exhaustion) end being always of brass. In the first two parts of the table the chamber was not quite tight, but the leak was sufficiently insignificant to virtually filter the inflowing air, as was proved by the direct experiments and by the third part of the table, where the adjustment remained quite free from leak throughout. In the fourth part some miscellaneous experiments are added. Naturally the greatest care was taken to remove water nuclei.

TABLE 15.—Distribution of ionization. Fog chamber 110 cm. long, 12 to 20 cm. in diameter. $\delta p/p = 25/76 = 0.33$. Distance D from brass or exhaust end turned toward glass or closed end. Radium at d.

d	$D = 80$ cm.		$D = 50$ cm.		$D = 20$ cm.	
	s	$10^{-3}n$	s	$10^{-3}n$	s	$10^{-3}n$
			I.			
100	g b p 8.0	140	7.2	108	6.3	74
80	g b p 7.9	138	7.9	138	7.0	99
50	6.1	66	7.2	108	7.0	99
20	4.9	33	5.4	44	5.1	37
35	5.3	41	5.6	50	6.1	66
65	7.5	119	7.5	119	6.8	90
110	7.5	119	6.6	82	5.1	37
	II. Both ends of fog chamber of metal waxed.					
100	8.0	140	7.1	104	5.2	39
80	g b p 7.8	134	p 8.5	174	6.0	62
50	5.8	55	7.2	109	g b p 7.5	119
20	4.7	29	4.9	33	5.4	44
80	7.7	130	8.0	140	7.0	94
	III. The same; fog chamber quite free from leak.					
80	7.5	119	p 8.2	161	6.5	87
80	g b p 7.5	119	p 8.4	175	6.2	70
50	5.5	47	6.0	62	7.5	119
20	5.9	58	5.6	50	5.9	58
	IV. Miscellaneous experiments.					
*80	5.0	35	4.7	29	4.1	20
†80	8.0	140	9.0	200	7.8	135
‡80	8.2	155	9.0	200	7.5	119

*Core charged to 250 volts. †Core uncharged. ‡Influx at large end.

The results are also shown in the charts figs. 13, 14 and 15, the two latter being the more typical. The abscissas indicate the position of the axial radium tubelets measured in centimeters from the exhaustion end of the fog chamber, the ordinates the observed nucleation. The three curves correspond to three goniometers, placed at 20, 50, and 80 cm. from the exhaustion end, respectively. The results are seen to be of the same nature as those discussed above.

Fig. 14 shows particularly that the maximum always lies on the exhaust side of the position of the radium. Moreover, the ionization when the radium is near the exhaustion end is always small and nearly uniform throughout. The maxima are largest when seen in the middle ($D = 50$ cm.) and smallest when seen at the exhaustion end ($D = 20$ cm.).

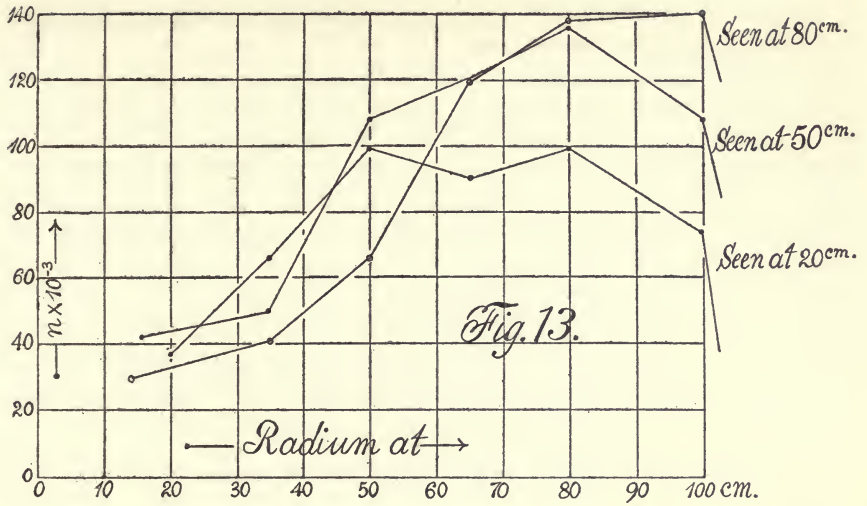

FIG. 13.—Ionization at different points along the axis of the fog chamber for different positions of the sealed radium tubelets within the aluminum core. Position of lines of sight shown on the curves.

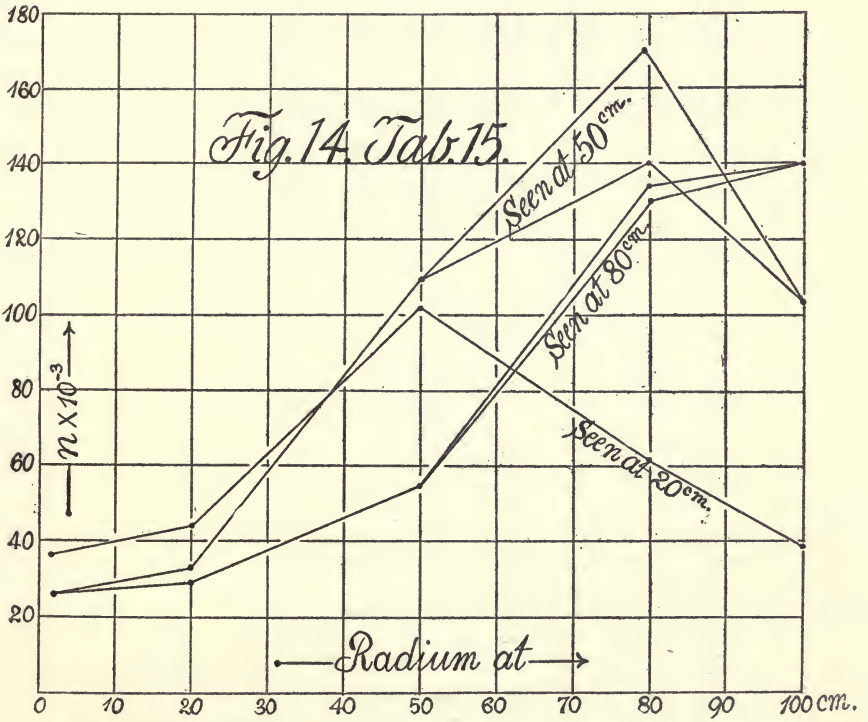

FIG. 14.—Ionization at different points along the axis of the fog chamber for different positions of the sealed radium tubelets within the aluminum core. Position of lines of sight shown on the curves.

In the third part of the table the occurrence of the maximum at 50 cm., for radium placed at 80 cm. from the exhaustion end, is again brought out. Furthermore, the destructive effects of electric charge on the insulated aluminum core extending from end to end of the fog chamber are clearly manifest, the number of ions being everywhere relatively very small. Specially favorable conditions obtaining in some of these experiments are accompanied by comparatively large ionizations with the uncharged core. This part of the table also contains an observation proving that if filtered air enters at either end of the fog chamber, the result is the same. Identical displacements were observed. In other words, there is no deficiency of saturation involved in the occurrence in the results in question, nor any difference between the freshly filtered air and the stagnant residue in the fog chamber, nor any effect attributable to parts of different material.

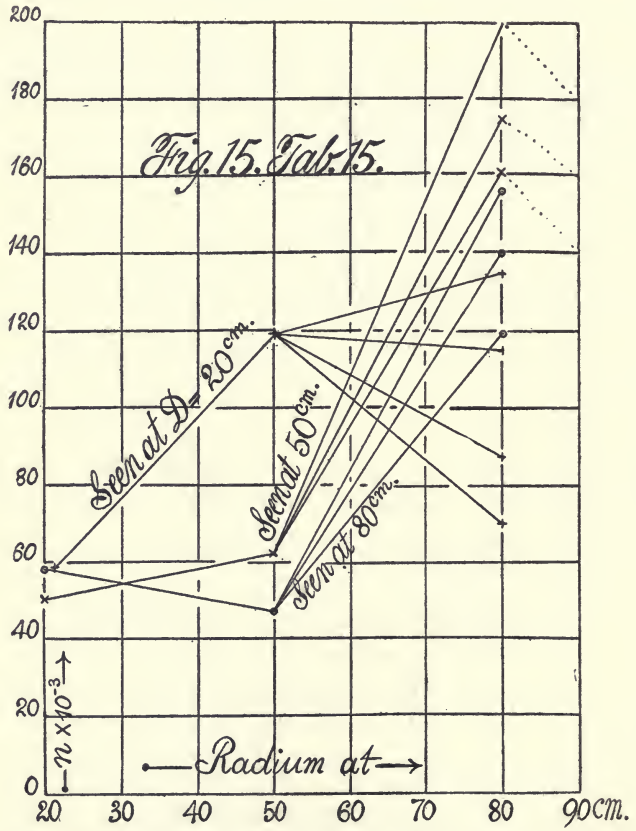

FIG. 15.—Ionization at different points along the axis of the fog chamber for different positions of the sealed radium tubelets within the aluminum core. Position of lines of sight shown on the curves.

37. Inferences.—At first sight one would conclude that in a region of maximum ionization there must either be a larger rate of production or a smaller coefficient of decay. The latter might be expected if in the given region the ions had largely the same sign. The frequent occurrence of the ionization ratio 2 to 1 in the earlier work lent some plausibility to this view, but the later experiments with a much longer fog chamber, and where much greater ratios occur in the ionizations of different parts of the chamber, quite disprove this surmise. The correlative view that the maximum might be referred to the superposition of primary and secondary radiations from different parts of the fog chamber is negatived by changing the character of these parts from glass to metal, or the reverse. Hence the maximum of ionization obtained must be *associated with the exhaustion itself* for in each case the displacement of the maximum is from the radium, wherever placed, to the exhaustion end of the fog chamber. And, in fact, since the exhaustion amounts to a volume ratio, v_1/v, if vapor pressures be neglected, and

$$\frac{v_1}{v} = \frac{p'^{(1-c/k)} p^{c/k} + [v/V]p}{p_3(1+[v/V])}$$

where $p' = 46$ cm. at the vacuum chamber, $p = 76$ cm. at the fog chamber, $p_3 = 51$ cm., the final common isothermal pressure when both chambers are in communication, and where the volume ratio of the chambers $[v/V] = 0.3$ nearly, the exhaustion is about $v_1/v = 1.33$. Hence the bodily displacement of air at the exhaust end would be 36 cm., and at the middle 18 cm. if the fog chamber were cylindrical. The conical form with the small end at the exhaust pipe would considerably enhance this bodily transfer of air from the closed to the exhaustion end of the chamber. Thus we infer, if the radium is at the closed end, that is, at the extreme distance from the exhaustion end, the maximum should lie there also, since there is no appreciable displacement of air. In proportion as the radium lies nearer the exhaustion end of the fog chamber, the displacement of maxima of ionization will be greater, compatibly with the greater bodily displacement of air, until in the case of the conical chamber, 110 cm. long, like the above, the displacement may exceed 40 cm. Furthermore, at the exhaustion end there will never be a proportionately large maximum, because the ionization has been removed into the vacuum chamber, and the whole series of coronas is of exceptionally small size throughout, due to increasing distance from the radium. In fact, it can hardly be said that any specific evidence of the occurrence of an appreciable secondary radiation has been adduced by the experiments.

In this way the above phenomena are at least qualitatively accounted for, as it must be acknowledged the displacement is often larger than the data here estimated, the reason for which is not sharply determinable

and may be due to turbulent motion immediately after the exhaustion. At higher exhaustions the distribution is often more uniform and other exceptional conditions supervene. For instance, with radium at $d=80$ cm. from the exhaustion end and $\delta p/p=0.43$, $n\times 10^{-3}=120$, 150, 140 at $D=20$, 50, 80 cm., respectively; with a tube containing six radium tubelets evenly distributed and extending from $d=65$ to 110 cm., the corresponding data at $\delta p/p=0.33$, were $n\times 10^{-3}=155$, 185, 240. In no case was more than a single maximum encountered.

Finally, the assumption has been made tacitly that the ions may be removed faster during the exhaustion and displacement than they can be reproduced by the presence of the radium, and that they may be caught before they appreciably decay. To take the example of the above cases: if the nucleation is equal to $N=500{,}000$ per cubic centimeter, the production would be $a=b\,N^2=10^{-6}\times 25\times 10^{10}=25\times 10^4$ or 250,000 nuclei per second per cubic centimeter, nearly. If the interval of displacement is between 0.01 second and 0.1 second, 2,500 to 25,000 nuclei should be produced to replace the 250,000 removed, which would at once imply a striking difference in the size of the coronas near the radium, such as has actually been observed.

In conclusion, therefore, the feature of great interest in these experiments is the definite proof contained that the ions may be displaced during the exhaustion at a rate much faster than they can be reproduced and that the maximum of ionization is therefore rarely found where it was generated.

MISCELLANEOUS EXPERIMENTS.

38. Experiments to detect the region of positive ions.—In table 16 a series of detailed experiments is recorded to determine the character of the relation between the drop of pressure and the number of ions captured in the fog chamber of the usual shape (No. 1, section 27). It was particularly desirable to locate the rather sudden flexure of the curve of distribution between its oblique and its horizontal branches and to see if any evidence could be found of a second region of flexure corresponding to the positive ions, by aid of a fog chamber like the one in question. The method of two independent sources was employed, the coronas being put in contact, S denoting the chord on radius of $R=250$ cm., or if 2θ is the angular diameter of the coronas, $S=2\,R\tan\theta$. It was not thought necessary to reduce S to the number of nuclei per cubic centimeter, as the former is in some respects a more convenient datum. There are two independent series (see fig. 16), in the first of which the sealed radium tubelet is on the outside of the chamber, in the other on the inside in the axial aluminum tube. In both cases the flexure of the curve lies at about $\delta p/p=0.285$, notwithstanding the decidedly greater nucleation in series 2.

The region of positive ions should begin at about $\delta p/p = 0.31$ cm., but neither curve shows the slightest suggestion of any increase in nucleation, though the drop in pressure has been intensified to an extreme case. Fog chambers of the above type thus refuse to admit the separate occurrence of positive ions. To this extent, therefore, the statement that negative ions only are captured would be justified.

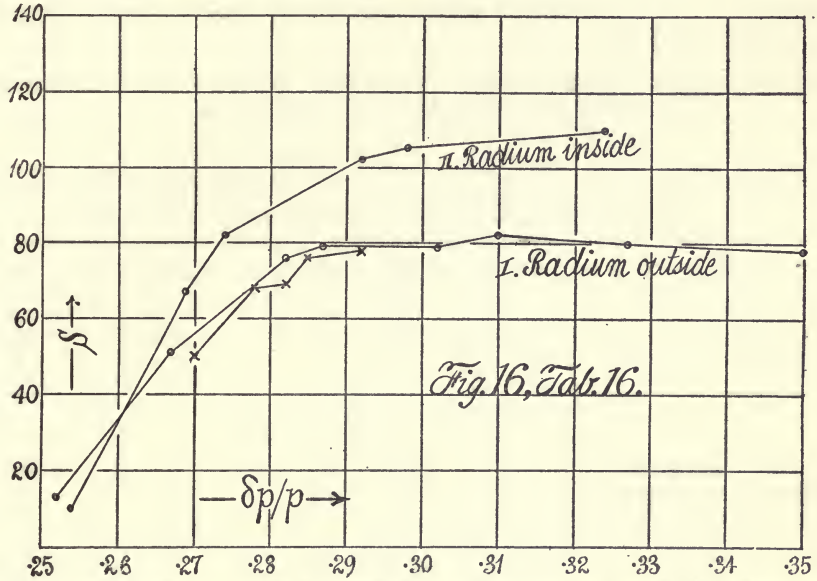

FIG. 16.—Absence of evidence for the region of positive ions beyond $\delta p/p = 0.31$, in case of a plug-cock fog chamber. Aperture S in terms of the exhaustion ratio $\delta p/p$.

TABLE 16.—Endeavor to find the region of positive ions in radium curve.

δp	$\delta p/p$	S	Corona.	δp	$\delta p/p$	S	Corona.
I. Barometer 75.9 cm.; temperature 26.0°. Radium I to V on top. $D = 7$ cm.				II. Radium I, inside of fog chamber. $D = 0$. Barometer 76.3 cm.; temperature 24°.			
26.6	0.350	78	g y	19.5	0.254	10	....
24.8	.327	80	g y	20.6	.268	67	o
23.5	.310	82	g y	21.0	.274	82	g
23.0	.302	79	g y	22.3	.292	102	o
21.9	.287	79	g y	22.8	.298	105	o
21.5	.282	76	o	24.8	.324	110	o
20.4	.267	51	o				
19.2	.252	13	....				
20.6	.270	50	o				
21.2	.278	68	r				
21.5	.282	69	r				
22.3	.292	78	g y				
21.7	.285	76	o				

39. Radium within the fog chamber. Sealed tubes.—An early series of experiments on the observed distribution of ionization within the chamber due to the presence of radium in different parts is given under special treatment in table 17. Coronas from two sources of light were put in contact, giving S. The radium was placed alternatively 12 cm. from the two ends of the fog chamber, 45 cm. apart. The lines of sight, I near the brass and II near the glass end, were 20 cm. apart in the middle of the available length.

TABLE 17.—Radium within chamber. Tubes I–V. Barometer 75.9; temperature 25.7°; air $S=1.0$; $\delta p_3=23.0$. $\delta p/p=0.303$.

	S	Corona.	$n\times10^{-3}$	$a\times10^{-3}=bn^2(1+b/cn)$
I. Radium* near brass-cap end. Observation lines 20 cm. apart.				
Observed near middle	84	w p	268	79
	82	w p	243	68
	83	w p	258	76
Observed at cap end	92	w r o	334	124
Observed at glass end	71	g	159	31
II. Radium near glass end.				
Observed near middle	106	w y	517	286
Observed at cap end	110	w y	580	356
Observed at glass end	91	w r	334	124

III. Fog limits.					
$\delta p_3=18.4$	0.9	1.0	$\delta p/p=0.2424$	$\delta p_0/p=0.240$	$v_1/v=1.215$
$\delta p_3=17.7$	.0	.0	.2332	.231	1.205

* Fog chamber cleaned with 3 exhaustions.

There was no vertical distribution of the ionizations, but the horizontal distribution was as usual very evident. Assuming that the number of ions produced per second, a, is given by $a=bn^2+cn$ where $b=10^{-6}$ is the decay constant and $c=0.036$ an absorption constant. The values of a are thus as follows:

	$10^{-3}n$	$10^{-3}a$
Radium at I (within fog chamber):		
Observed at I	334	124
Observed at II	159	31
Radium at II (within):		
Observed at I	334	124
Observed at II	550	320
Radium on top (outside)	175	37

A few rain limits were incidentally tested, as the opportunities were exceptionally good. These data are given in part III of the table. They have the usual values in my work, $\delta p/p = 0.23$ or $v_1/v = 1.21$, and lie below Wilson's values.

40. Distance effect.—A few experiments were incidentally made to determine the effects of the distance D of the radium from the fog chamber in terms of the numbers of ions produced per second, a, where $a = bn^2 + cn$, as above explained. The method of two sources (chord S) with the coronas in contact was used. Table 18 shows the chief results.

TABLE 18.—Distance effect. Radium I to V. Barometer 76.4; temperature 21.6°. D from axis of fog chamber. Air, $s = 1.0$. $\delta p_3 = 22.8$; $\delta p/p_3 = 0.298$; $b = 10^{-6}$; $c = 0.0356$.

D	S	$10^{-3} \times n$	$10^{-9} \times n^2D^2(1 + c/bn)$	D	S	$10^{-3} \times n$	$10^{-9} \times n^2D^2(1 + c/bn)$
*7.0	4	174	1784	100	30	13	4630
	73	167	1656		30	13	4630
	73	167	1656	200	22	4.6	7200
20	59	92	4720		22	4.6	7200
	61	104	5800	7	72	165	1612
50	45	41	7800				
	44	38	6975				

*Radium tube lies on the glass vessel, 7 cm. from the axis.

Inferring that $n^2D^2(1 + c/bn)$ should be constant, the following comparison results:

$D =$	7	20	50	100	200 cm.
$10^{-12} n^2D^2(1 + c/bn) =$	1.7	5.2	7.4	4.6	7.2

At $D = 7$ cm. the radium is too close for any law. The agreement thereafter is an attempt at constancy in so far as the small coronas beyond $D < 100$ cm. admit.

41. Attempt to calibrate the fog chamber with 5 separate sealed tubelets (I, II, III, IV, V) of radium.—These results are given in table 19. The tubes were placed in a gutter on the outside of the chamber at a distance D, or in a sealed aluminum tube within the chamber. The table gives the aperture S (two sources of light), the nucleation n computed therefrom and the number of ions a generated per second, where $a = bn^2 + cn$ as in the preceding instance.

TABLE 19.—Calibration with radium I to V.

Radium.	S	Corona.	$n \times 10^{-3}$	$10^{-3}a$	Computed $a \times 10^{-3}$
Part I. Barometer 75.9; temperature 25.7°; air, $S=1.0$; $\delta p=23.0$; $\delta p/p=0.303$. Radium I on top, each in its niche. $D=7$ cm.					
200,000×0.010 g.....II	65	....	122	19.2	....
20,000×.....V	56	....	78	8.8	....
10,000×.....I	61	....	102	14.0	....
(Mean).....I+II+V	74	w r	176	37.2	42.0
10,000×.....III	53	....	71	7.5	....
10,000×.....IV	55	....	74	8.1	....
I + . . . +V	74	g	176	37.2	57.6
Part II. Repeated. $D=7$ cm. Barometer 75.3; temperature 26.4°; $\delta p=23.0$; $\delta p/p=0.306$.					
II+V+I	68	g g	149	27.5	....
	72	g	169	34.6	....
	72	g y	169	34.6	....
Part III. Larger distance. $D=22$ cm. from axis. $\delta p/p=0.306$.					
II	49	....	55	5.00	....
V	41	....	32	2.16	....
I	47	....	50	4.27	....
III	37	....	25	1.52	....
IV	35	....	21	1.19	....
I+ . . . +V	60	....	103	14.2	14.1
I+ . . . +V	60	....	103	14.3	....
Part IV. Higher δp. $D=7$ cm. Air, $S=4.6$. Barometer 75.9; temperature 26.6°; $\delta p_3=26.6$; $\delta p/p=0.350$.					
II	61	....	113	16.8	....
V	56	....	87	10.7	....
I	63	....	125	20.0	....
III	54	....	78	8.9	....
IV	54	....	78	8.9	....
I . . . V	79	g y	238	65.1	65.3
Part V. Barometer 76.3; temperature 24°; $\delta p_3=23.0$; $\delta p/p=0.301$.					
II	115	o	400	174	....
V	99	r o	260	77	....
I	105	o	300	100	....
III	93	r	210	52	....
IV	95	r	225	59	....
I . . . V	130	y	570	344	461

The results in parts I and II are not satisfactory. Thus the separate determination of a for each tube added together are much larger than the corresponding datum for the tubes abreast:

I, II, V:		
Separately	$a=42{,}000$	ions per second.
Together	37,000	
I, II, III, IV, V:		
Separately	57,600	
Together	37,000	

With the tubes together, a certain number of ions apparently failed of capture, but this is not the case, as is shown in table 16, where all ions are caught for $\delta p/p=0.28$, much below the present datum.

The third part of the table, however, shows accordant results, giving 14,000 ions per second separately and 14,300 when the tubes are acting together, but the ionization is lower ($D=22$ cm.).

In part IV the drop in pressure is larger. The agreement is satisfactory, $a=65{,}000$ ions per second when the tubes act together and $a=65{,}000$ when their separate effects are added, but in other similar cases the results were not so good. Thus in the last series V, the separate and joint effects are 460,000 and 340,000; here, however, the high nucleation is due to the presence of radium within the chamber in sealed aluminum tubelets, and the diffuse coronas are hard to measure.

The method of graduation depending on the use of sealed batches of radium, together and separately, has not, therefore, given trustworthy results. The chief reason for this is that the rate of production a is as the sixth power of the aperture S

$$a/a'=S^6/S'^6$$

If the tubelets were equally strong their sum would be $\sqrt[6]{5}a=1.3\sqrt[6]{a}$, which is about the relation of aperture for contiguous crimson and green-yellow coronas. Hence small subjective differences play a large part in such experiments.

CHAPTER IV.

THE STANDARDIZATION OF THE FOG CHAMBER BY THE AID OF THOMSON'S ELECTRON.

THE CONSTANT *e*, EXPRESSED IN TERMS OF VELOCITIES OF THE IONS.

42. Advantages.—Of all the methods which I have tried to evaluate the coronas in terms of the number of nuclei which they represent under given conditions of exhaustion, the above method is the most expeditious and promising. A single experiment need take but a few minutes. Incidentally the observer learns whether negative and positive ions have been captured, for on using the table of coronas which I developed heretofore, the value of *e* may be computed and the result must coincide with Thomson's datum.

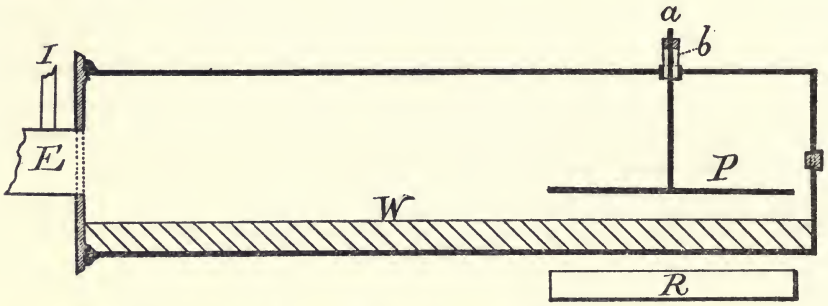

FIG. 17.—Fog chamber with plate electrical condenser.

43. Plate.—These experiments were of a tentative character and the condenser used was a plate of brass P, of area $A = 5 \times 15$ sq. cm. suspended at a distance of 1 cm. above the water W, and parallel to it. It was supposed under these circumstances the discharge current in the presence of radium in sealed aluminum tubes placed at R in fig. 17 would be largely confined to the narrow space between plate P and water W, which was earthed, but this proved not at all to be the case, as will be seen presently. In the absence of radium, the leakage was throughout negligible, the conductor a being sheathed by the hard rubber tube b, kept dry except during use. The fall of potential was measured by a graduated galvanoscope, whose capacity was in parallel with P. The number of ions n was found from the aperture of the coronas on condensation. We may therefore write for the charge per ion, if 1 is the distance of P above the water-surface W, and V the potential difference in volts

$$e = \frac{C l}{300 A U n} \frac{\dot{V}}{V}$$

where C is the total capacity and U the appropriate velocity of the ions in the field of 1 volt per centimeter, each ion carrying the charge e, in electrostatic units, positive or negative, depending on the charge on the plate.

While the apparatus as a whole apparently functioned very well, it was found that the removal of the plate made no difference whatever. Thus if D is the distance of the radium from the fog chamber:

Condenser plate P in place.			Condenser plate P removed.		
D	Leak.	$\dot{V}/V$	D	Leak.	$\dot{V}/V$
cm.	*Volt/cm.*		*cm.*	*Volt/cm.*	
40	0.00012	0.00286	40	0.00028	0.00242
	....	287		30	277
	....	289		29	260*
15	.00040	475	15	....	635
	21	547		....	808
	14	544		....	720
	....	435	0	....	.01015†
0	.00021	635		....	.00975
	....	703		....	995
	....	685		....	

*With two lead plates each 1 mm. thick covering the radium, $\dot{V}/V = .00298$.
†With two lead plates each 1 mm. thick covering the radium, $\dot{V}/V = .00800$.

The results (due to incidental reasons) are thus even larger in the absence of the plate P than when it is present, although the conduction-leaks are throughout *negligible*. It is therefore impossible to interpret the results obtained or to compute the e from them. When D was 15 cm., or larger, the effect of one or more thin lead plates over the radium was no apparent deduction. In the adjustment given, therefore, the whole region of the radium conducts and the fog chamber is merely effective as a part of the region.

44. Cylinder.—If the sealed radium tubelets rr are inserted by aid of a wider aluminum tube AR (closed at one end) into the axis of the cylindrical fog chamber FF, the closed end A projecting within as in fig. 18, the difficulties referred to are in a measure obviated. Nevertheless, in the present experiment it was thought preferable to use the fog chamber for measuring the number of ions only, while an independent condenser was installed for electrical measurements.

The cylindrical electrical condenser is employed as follows: A closed aluminum tube 0.62 cm. in diameter, 18 cm. long, containing weak radium in sealed tubelets equally distributed along its inside, is made the core of the condenser, the outer surface being 2.1 cm. in diameter and leaded to an inch or more in thickness beyond. The aluminum core in question is suspended axially from a fine wire leading to a sensitive

electrometer. The voltages here to be measured must of course be small, and hence all connecting wires are to be inclosed in earthed metal pipes.

The core in question is then removed from the electrical condenser and put into the axis of a dust-free fog chamber (fig. 18), where the nucleation (ionization) is found on condensation from the constants of the coronas, or *vice versa*. Here there are some outstanding difficulties, for the coronas are not the same throughout the length of the fog chamber, as discussed in Chapter III. Even immediately around the radium core a single corona may be green on one side and red on the other. In a fog chamber 45 cm. long, the coronas may vary from the glass end to the metal end of the chamber in a way to correspond to from 100,000 to 200,000 nuclei, respectively, while the radium core is fixed in the middle. Inferring secondary radiation, one might naturally expect to obtain still larger coronas near the metal end if the radium core, thoroughly sealed, is placed there instead of in the middle of the chamber. But this is not the case, the coronas being markedly smaller than before, decreasing uniformly in size toward the glass end. As the sealed aluminum tube is within the chamber, this behavior is clearly of great importance.

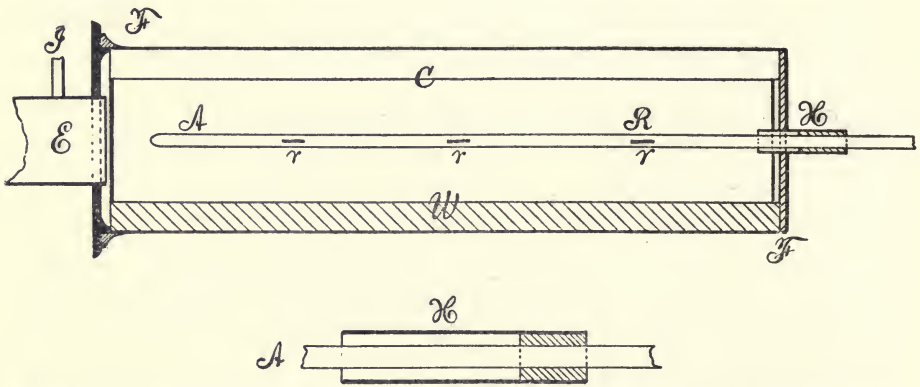

FIG. 18.—Fog chamber used as a cylindrical electrical condenser. *AR*, aluminum core.

These difficulties are inherent in the phenomenon and merely exhibited by the fog chamber. The latter has the great advantage that enormous nucleations, like millions per cubic centimeter, are not excluded. Under these circumstances the coronas alone are available for finding the nucleation, inasmuch as all the fog particles evaporate before subsidence. Finally, the occurrence of maxima of nucleation may in a large measure be obviated by distributing the radium along the axial tube.

45. The same. Preliminary data.—To test the efficiency of the fog chamber it is sufficient to make a preliminary measurement of Thomson's e. Let the radii of the electrical condenser be R_1 and R_2, its length

I; let C (electrostatic units) be the capacity of the electric system, condenser, and electrometer, together with such auxiliary capacity as may be inserted to get a leakage of proper value. Let U be the efficient* velocity of the ions, positive or negative as the case may be, in a field of 1 volt per centimeter, V the voltage and $\dot{V}$ the change of voltage per second. Finally, let N be the nucleation caught when the identical condenser core is placed in the fog chamber. Then for the cylindrical condenser (if natural logarithms be taken),

$$e = \frac{ClnR_1/R_2}{600\pi lUN}\frac{\dot{V}}{V}$$

If V is small enough to keep $\dot{V}/V$ constant, the curves show this at once. Rough tests, using the old data of my fog chamber, led to values about as shown in table 20, where the irregularities are in the electrometer, due it was supposed to the connecting wires, which were not at the time surrounded by earthed pipes. It has been assumed that relative ions only are caught in the fog chamber and that a negative current only is observed. The e so found is too large.

TABLE 20.—Preliminary values of e. Wires not surrounded by pipes.

$$e = \frac{ClnR_1/R_2}{600\pi lU}\frac{\dot{V}/V}{N}$$

$C = 130$; $U = 1.87$ cm./sec. (neg. ions); $V < 0.5$ volt; field 0.7 volt/cm.; $N = 210{,}000$ per cm³ (neg. ions); $2R_1 = 2.1$ cm.; $2R_2 = 0.62$ cm.; $l = 18.2$ cm.

$\dot{V}/V$	$e \times 10^{10}$	$\dot{V}/V$	$e \times 10^{10}$	$\dot{V}/V$	$e \times 10^{10}$
0.049	....	0.054	....	0.056	....
56	....	62	....	68	....
65	....	56	....	67	....
71	....	50	....	65	....
....	....	....	....	67	....
.060	7.3	0.56	6.9	.065	8.0
*0.05	6.4				

* Same with $N = 185{,}000$ per cm³ (neg. ions).

46. The same. Wires surrounded by earthed pipes.—In order to make use of the high sensitiveness of the Dolezalek electrometer, the wires were now surrounded, so far as possible, with pipes of galvanized iron, 2 inches in diameter, put to earth. Under these circumstances there was less irregularity, though the current still continued to be far from proportional to the voltage, even for low values of the latter. It will not, therefore, be worth while to give a detailed account of $\dot{V}/V$, and the mean value for a field of 1 volt per centimeter was taken, as found from

*If one shell of the condenser is put to earth, positive or negative currents only are measured and not the whole current.

five independent series of measurements of the fall of the potential of the core per second. The following is the summary, referring to the negative current, where C is 136 cm., $U=1.87$ cm./sec., $P=18.8$ cm., $2R_1=2.1$ cm., $2R_2=0.62$ cm.

$\overline{V}$	Field.	$\dot{V}/V$	(Negative ions) N	$e\times10^{10}$
Volt	*Volt/cm.*			*Els. units.*
0.7	1	0.04	150,000	6.6
.9	1.2	.14	570,000	5.9

When the condenser was disconnected there was no leakage, showing the piping to be nearly free from such currents as might result from irregular penetration of the gamma rays. The approach of the final values of e to those currently in use is no closer than before. It has again been assumed that negative ions only have been caught in the fog chamber, and that a negative current alone is in question when the core (connected with the electrometer) is charged positively and the shell of the condenser is put to earth.

47. Conclusion.—The values of e obtained under widely varied conditions in the present rough experiments, are of the same order and to this extent show that the present method is not unworthy of development, with a view to the further measurements of this important constant. For this purpose I have been at work on a redetermination of the nucleation values of the coronas (see Chapter II), using as a source of light the virtually monochromatic mercury lamp. This is sufficiently intense and the coronas admit of a more definite optical interpretation.

All of the e values are too high, however, when it is assumed that a negative current only is in question and that negative ions only are caught. The reason for this high value of e is probably referable to the aluminum-brass condenser, which contains an electromotive force not allowed for nor eliminated by commutation. Such a case would modify the ratio $\dot{V}/V$ in the above results by changing the zero-point of the electrometer. The experiments were abandoned at this point owing to the dampness of the summer season. They will be resumed in Chapter V.

THOMSON'S CONSTANT *e*, EXPRESSED IN TERMS OF THE DECAY CONSTANT OF IONS, WITHIN THE FOG CHAMBER.

48. Introductory.—In the last paper* an account is given of certain tentative experiments to determine Thomson's electron, by aid of the fog chamber and a separate well-leaded cylindrical electrical condenser. The results obtained were in keeping with the accepted values. It was presumed that the constants of coronas are determinable from purely optical considerations of diffraction and interference, and that the accuracy of the method may be enhanced by using the mercury lamp as a source of light for the coronas. There was, however, one grave misgiving, inasmuch as the distribution of ionization within the fog chamber varies in marked degree from place to place for any given position of a sealed radium tube, and that the mean value assumed was in a measure gratuitous. The results seen in the fog chamber are a complication of the effects of primary and secondary radiations, together with a very marked exhaustion displacement of the ions. The maximum ionization (Chapter III) does not coincide, as a rule, with the position of the radium, and there is no reason why the ionization in the fog chamber should be quite identical with the ionization produced by the same radium tube in the electrical condenser, unless both are one and the same apparatus. This is the case in the experiments of the present paper. The results also show that the same method may be applied under the circumstances of the last paper, where *e* was obtained in terms of the velocities of the ions.

49. The electrical condenser fog chamber.—It is therefore necessary to make a fog chamber itself the electrical condenser, and this is easily done, if the chamber is cylindrical, by installing a tubular core of aluminum closed in the inside of the chamber and running axially from end to end, as in fig. 18. This core is charged to a definite potential and made the inner surface of the condenser, while the scrupulously clean inner wall of the glass chamber (to which water adheres evenly) is the outer surface and put to earth. Finally, the radium, contained in small sealed tubelets of aluminum, is placed within the length of the axial aluminum tube or core in such a way as to make the ionization within the fog chamber uniform—a condition vouched for in case of the occurrence of uniform coronas on exhaustion, from end to end of the chamber.

There are thus three currents to be determined:

(1) The conduction current due to inevitable leakage between the condenser surfaces. This is made a minimum and nearly negligible in value by keeping the aluminum core out of the condenser when not in use and by sheathing it with an annular air-space beyond the condenser. It is found experimentally by direct measurement in the absence of radium.

*C. Barus: Am. Journ. Sci., xxvi, pp. 87–90, 1908.

(2) The current due to the ionization of the room air near the fog chamber and on the outside of it, due to gamma rays. This is made a minimum by allowing the thin wire communicating with the electrometer to run axially away from the fog chamber, for the gamma rays, in spite of their penetrating powers, are quickly reduced by distance. The current is found in the presence of radium within the axial tube by leaving all adjustments identically in place, but breaking the metallic connection between the aluminum core and the electroscope, etc., by a hard rubber insulator. If an auxiliary condenser is used, the measurement (1) must be made without it, as otherwise its leak would be counted twice. Fortunately the conduction current is quite negligible.

(3) The current due to ionization within the fog chamber. This is found by deducting from the total current found on connecting the charged aluminum core and the electrometer the two preceding currents.

50. Auxiliary condenser.—To vary the experiments to the extent that different speeds of leakage may be obtained, as well as to find the capacities of the electrometer and fog chamber, an auxiliary condenser must be inserted as a part of the electroscope. This condenser consisted in the present experiments of two plates of brass, having an area of 315 sq. cm., and usually kept at a distance of 0.32 cm. apart by outrigged feet of hard rubber, which stood on a plate of glass. By putting small glass plates under these feet the capacity could be varied at pleasure. The usual equation was corrected by aid of the factor

$$1+\left(d+d\ln 16\sqrt{A\pi}(d+\delta)/d^2+\delta\ln(d+\delta)/\delta\right)/\sqrt{A\pi}$$

where a is the area, d the distance apart, and δ the thickness of the plate of the auxiliary condenser. Naturally a guard ring condenser would have been preferable for standardization, but none was at hand.

To determine the very small capacity C of the electroscope-fog-chamber, two successive full charges from the lighting circuit, at a potential $V=250$ volts, were in turn imparted from C to the auxiliary condenser of capacity C'. If V'' be the potential observed after these two charges and $S=V''/(V-V'')$, $C=C'S/(1+\sqrt{1+S})$. It is curious that this method of successive charges leads to involved cubic, quartic, quintic equations, etc., which follow no simple rule. The ratios R of the potentials, after four and after two charges $R=V''''/V''$ is, however, still available for if $r=C'/C$, then $r=(R-1)\left(1+\sqrt{1+(2-R)/(R-1)}\right)/(2-R)$. Apart from these complications, the large deflections obtainable after many successive charges would, in the absence of conduction leakage in the condensers, make this method very satisfactory.

In the definite measurements, however, almost the whole capacity may be placed in the auxiliary condenser, so that the capacities of the

electrometer and fog chamber are of small importance. Ratios of $C'/C = 86/17$, $30/17$, $20/17$, and others, were tried.

51. Method.—In the preceding paper the value of e found was ultimately dependent upon the velocity of the ions in the unit electric field. In the present experiments a value will be found, based on the decay constant $b = 1.1 \times 10^{-6}$, of the ions. This method has the advantage that large-core potentials are admissable in the electrical condenser, so that an ordinary graduated Exner electroscope suffices for the measurement of current. The small capacities of the instrument make it necessary to insert an auxiliary condenser, as otherwise the discharges are too rapid for trustworthiness.

If a is the number of ions produced per second per cubic centimeter by the radium within the condenser core, n the number of nuclei per cubic centimeter in general, and N the number of nuclei (ions) found when the core is free from charge, $dn/dt = a - bn^2 = 0$, if $n = N$. Again, if n is the number of nuclei found when the core is charged and i the corrected current observed, e Thomson's constant, and v the effective volume of the fog-chamber condenser,

$$dn/dt = b(N^2 - n^2) - i/ev = 0 \qquad (1)$$

Hence if the capacity of the system is C and $\dot{V}$, the corrected fall of potential per second

$$e = C\dot{V} / \left(bv(N^2 - n^2)\right) \qquad (2)$$

Usually $\dot{V}$ is measured in volts, so that $\dot{V}/300$ replaces $\dot{V}$ in the equation. It is obvious that V must be large enough to keep the current $\dot{V}$ constant and the observations always show this at once.

If equation (1) is multiplied by $\frac{1}{2}$ throughout it will express the case for the negative ions alone and the negative current alone. Hence equation (2) is at once applicable here.

52. Data disregarding external gamma rays.—By the aluminum-foil electroscope it was made convenient to use the high potentials of the electric-lighting circuit (about 250 volts) for charging.

The number of nuclei (ions) found in the presence of the radium tubelets and in the *exhausted* fog chamber free from charge at its central core was $N = 474{,}000$. The number of nuclei found in the exhausted fog chamber when the core was charged 250 volts was $n' = 82{,}500$. Hence about 391,000 vanished in the presence of the electrical current, the original apertures of the coronas being reduced from about 22° to 13°. The drop of pressure, $\delta p/p = 0.30$ nearly, was taken high enough to catch all the available ions, but not so high as to catch the vapor nuclei of dust-free wet air.

The amount of exhaustion was equivalent to the volume ratio $v_1/v = 1.29$. Thus the number of ions in the fog chamber at atmospheric pressure was $N = 611{,}000$ per cubic centimeter for the uncharged core.

TABLE 21. — Fall of potential and currents. $\dot{V}'$ conduction leakage; $\dot{V}''$ due to presence of radium. Wires not piped. Four-second intervals between observations.

V'	$\dot{V}'$	V''	$\dot{V}''$	V''	$\dot{V}''$
$\dot{V} = 3.0$ volt/sec.; $C = 103$.				$\dot{V} = 5.8$ volt/sec.; $C = 47$.	
250	1.6	250	5.5	249	5.5
247	2.6	230	5.9	229	6.1
237	2.6	206	5.7	205	6.2
226	2.6	183	5.4	180	5.6
216	2.6	160	5.6	155	5.6
205		140		135	5.6
195		122		110	5.8
				90	
$\dot{V} = 6.4$ volt/sec.; $C = 47$.				$\dot{V} = 12.1$ volt/sec.; $C = 17$.	
250	3.6	250	9.4		
236	3.4	216	10.4	249	12.0
221	3.2	175	9.5	209	13.2
207	3.2	133	9.8	153	10.4
195	3.4	99		103	
182				249	12.0
168				207	13.0
				153	10.9
				103	
				249	12.3
				205	12.7
				151	12.1
				103	

The value of $b = 1.1 \times 10^6$ is taken from Professor Rutherford's book. The source of light for the coronas is part of a Welsbach mantle, as usual, and the old constants of coronas were used, since it is a part of the purpose of this paper to test those constants. The volume of the fog chamber was estimated at 51,000 c. cm. In the first experiments the effect of the gamma rays penetrating into the air on the outside of the fog chamber was neglected and the data, summarized from table 21, on using different condensers, were as follows, all data being given in electrostatic units. C denotes the capacity of the system, $\dot{V}$ the drop of potential per second, i the corrected current passing through the condenser-fog-chamber.

C	$\dot{V} \times 10^3$	$i \times 10^2$	$e \times 10^{10}$
103	10	103	5.1
47	21	101	5.0
47	19	92	4.5
17	40	70	3.4

The last observation being made without an auxiliary condenser. The current i was quite constant throughout the voltage interval (near 250 volts) of observation. Hence the effect of gamma-ray penetration has seriously increased the leakage, and e therefore appears too large, except in the last observation, where i is probably no longer measureable.

53. Further data.—In the following experiments the effect of the external gamma rays was eliminated as specified in section 49. The conduction current was usually quite negligible. The nucleations observed in the exhausted fog chamber were $n=82{,}000$ and $N'=506{,}000$, when the core was charged and uncharged, respectively. The exhaustion was again equivalent to a volume increase of $v_1/v=1.29$. Hence in the fog chamber full of air the respective nucleations are $N=653{,}000$ and $n=106{,}000$, whence $N^2-n^2=415\times10^9$. The drop of pressure $\delta p/p=0.30$ was about the same as before.

TABLE 22.—Fall of potential and currents. V' in the presence of radium; V'' due to γ rays; V leakage due to conduction; 4-sec. intervals. Wires in earthed pipes.

V'	$\dot{V}'$	V''	$\dot{V}''$	V'''	$\dot{V}'''$	V'	$\dot{V}'$	V''	$\dot{V}''$	$\dot{V}'''$
$\dot{V}=2.24$ volt/sec.; $C=103$.						$\dot{V}=5.88$ volt/sec.; $C=37$.				
245	3.4	244	1.5	247	0.9	240	8.1	241	2.5	1.1
232	3.6	236	1.0	243	.8	204	8.1	231	2.5	1.6
218	3.6	232	1.4	240	.6	175	8.1	221	2.0	1.7
203	3.6	228	1.4	237	.6	139	8.1	211	2.0	1.4
189	3.9	221	1.5	235	.6			205	2.2	1.6
174	4.1	217	1.5	232	.9			195	2.1	1.5
157	3.7	209	1.38	230				187	2.22	1.48
141						$\dot{V}=10.0$ volt/sec.; $C=17$.				
$\dot{V}=5.15$ volt/sec.; $C=47$.										
						248	15.9	245	4.5	0.21
245	7.0	244	1.9	....	1.4	180	13.8	226	4.4	.17
217	7.0	232	2.0	....	1.1	121	14.8	209	4.3	.19
189	6.9	225	1.8	....	.8	70	....	191	3.9	.19
161	6.97	217	1.8	....	1.3	248	14.7	175	4.4	
134		209	1.6	....	1.2	187	14.1			
		203	1.82	....	1.0	130	14.4			
		195		....	1.13	74				
		190		....						

The electrical measurements, if all data are given in electrostatic units, may be summarized from the data in table 22, as follows:

C	$\dot{V}\times10^3$	$i\times10^2$	$e\times10^{10}$
103	7.5	77	3.3
47	17.2	81	3.5
37	19.6	72	3.1
17	33	58	2.5

Thus, with a correction for the external gamma radiation, the data for e show reasonable values, in spite of the simplicity of the experiment. It follows, therefore, even in the case of such large numbers of ions as occur in these experiments (over 500,000), that the constants of coronas used heretofore are substantially correct. In case of the last value $e \times 10^{10} = 2.5$, for the small capacities of 17 cm., the aluminum leaves on the electroscope converge too rapidly for measurement, so that the air resistance may have produced an appreciable discrepancy. Hence both i and e are too small. No refinement has been attempted in these experiments, their chief purpose being to test the standardization of the fog chamber in terms of coronas and the degree to which positive and negative ions may be caught even at very high nucleation. One may note in conclusion that the currents $i = 77$ electrostatic units or 2.6×10^{10} amperes are already quite within the reach of the sensitive galvanometer.

CHAPTER V.

THE ELECTRON METHOD OF STANDARDIZING THE CORONAS OF CLOUDY CONDENSATION, IN TERMS OF THE VELOCITIES OF THE IONS.

54. Introductory.—In the following experiments I have returned to the measurements* of N in terms of e and the velocities of the ions, Chapter IV, modifying the method by using the cylindrical fog chamber both as an electrical condenser for the measurement of current, as well as for the specification of the number of ions in action by aid of the coronas of cloudy condensation. It is to be assumed that negative ions only are caught in the fog chamber.

55. Apparatus (fig. 19.)—This consists of a cylinder of glass CF, about 45 cm. long, 13.4 cm. internal diameter, closed at one end F, and provided with a brass cap C with exhaust E and influx attachments I, in the usual way. There is a layer of water w at the bottom. The glass must be scrupulously clean within, and this is best secured by scouring with a probang of soft rubber under water, until the water adheres as an even film on shaking. The fog chamber is put to earth.

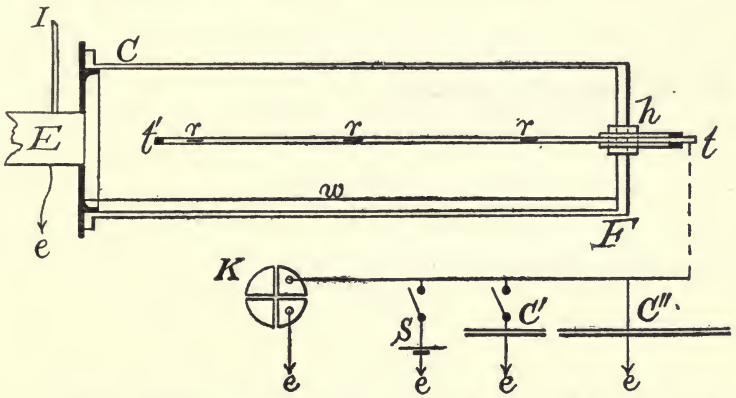

FIG. 19.—Electrical condenser and fog chamber combined, showing the disposition of the auxiliary condensers C' and C'', the Clarke cell S, and the electrometer K, diagrammatically. Earthed wires are shown at e.

The end F is perforated at h to receive the aluminum tube tt', closed at t' and open at t, 40 cm. long and 0.64 cm. external diameter. Sealed tubelets of radium rr may be placed at intervals within this tube to ionize the surrounding wet air. The walls being about 0.1 cm. thick, β and γ

*Amer. Journ. Sci., XXVI, 1908, p. 87; *idem.*, p. 324.

rays are wholly in question. Neither emanation nor α rays escaped the double thickness of aluminum. The tube tt' is grasped at t by a sheath of hard rubber with an annular air-space and fixed in place by a rubber cork. If care be taken to keep the tube in dry air except when in use, there is no conduction leakage of consequence.

The end t, moreover, is placed in connection with a Dolezalek electrometer, by aid of a thin wire running axially within an earthed tin drain pipe and away from the fog chamber, to escape the action of γ rays as much as possible. In fact, their combined effect does not exceed 2 per cent and is determined in special measurements.

The keys to the electrometer were all placed on pillars of hard rubber and actuated by long wooden rods from a distance. So far as possible the electrical wires of the room were surrounded by earthed pipes, but it was not practicable to carry this out completely, so that a method of correction appears in the tables below. Even when the electric-lighting circuit was completely cut out the electrostatic drift in question, supposed to be due to this cause, remained. It was afterwards found that the source of drift was due to an imperfection in the electrometer, but that it could be eliminated by commutation, as was done.

The measurements were standardized and the electric system charged by a Carhart-Clarke cell. The radium tubelets used were as follows: I, 100 mg., strength 10,000×; II, 10 mg., strength 200,000×; III, 100 mg., strength 10,000×; IV, 100 mg., strength 7,000×; V, 100 mg., strength 20,000×.

56. Auxiliary electrical condensers.—To give the fall of potential a suitably small value relatively to the period of the damped drop of the needle a number of auxiliary condensers (fig. 19), are needed. It suffices, however, to measure three capacities, viz: (1) that of the cored fog chamber alone, c; (2) that of a relatively large auxiliary condenser, including the electrometer, the piped wires, and the fog chamber, $C''+c$; (3) that of a standard condenser C' for reference.

In the present paper C' was computed by the equation

$$C'=\frac{A}{4\pi d}\left(1+\frac{1}{\sqrt{\pi A}}(d+d\ln\frac{16\sqrt{\pi A}(d+d')}{d^2}+d'\ln\frac{d+d'}{d}\right)$$

where A is the area, d the distance apart, and d' the thickness of the brass plates. Since A is equal 315 sq. cm., $d=0.082$ cm., $d'=0.67$ cm.,

$$C'=305.6(1+0.0784)=330 \text{ cm.}$$

This value will suffice for the present purposes, though it needs further correction by comparison with a standard condenser not now at hand.

A special key was provided whereby C' could be switched into the electrometer system or out of it and put to earth. Hence in a series of successive discharges

$$(C''+c)V=(C''+C'+c)V' \qquad (C''+c)V'=(C''+C'+c)V'', \text{ etc.,}$$

so that for n discharges, if the residual potential is V_n

$$V(C''+c)^n=V_n(C''+C'+c)^n$$

from which the total capacity $C=C''+C'+c$ is determinable in terms of C'. The results were

Positive charge.....	$C''+C'+c=$ 1445	1443	1422	
Negative charge.....	$C''+C'+c=$	1482	1480	
Mean.....	$C=$ 1459			

the experiments alternating from positive to negative charge, because of the marked drift by the electrometer system when isolated from the cell, as already specified. To measure the small capacities c of the fog chamber, the same method with *ten* discharges suffices, if C'' is excluded and C' retained. Thus the data were successively found,

+Charge.....	$c=$ 11.8	12.4	12.2	12.9
−Charge.....	$c=$ 10.8	10.4	11.1	11.5
Mean.....	$c=$ 11.3	11.4	11.6	11.2

eliminating the drift in the final mean $c=11.4$.

Since the capacity c in terms of the effective internal radius R_2 and external radius R_1 and lengths l of the cylindrical condenser may be written

$$\frac{1}{l}\log\frac{R_1}{R_2}=\frac{1}{2\times 2.3\times c}$$

the constant c furnishes a mean value for the factor on the left. The ratio of $4.6c$ to the measured value of $(\log R/R_2)/l$ was 0.568, a reduction factor used throughout the tables below.

57. Method pursued.—If C is equal to $C''+C'+c$ we may write the equation for the negative ionization N (positive charge)

$$N=\frac{C\ln R_1/R_2}{600\,\pi\, lve}\frac{d(\ln V)}{dt}=\kappa\frac{d(\ln V)}{dt}$$

where R_1, R_2, and l are the effective radii and length of the condenser, $10^{10}e=3.4$, $v=1.51$ cm./sec., and $u=1.37$ cm./sec., the velocity of the negative and positive ions in the unit field, volt/cm., and in case of moist air. The factor $(\ln R_1/R_2)/l$ is replaced by $C/2$, as specified in section 56,

which must here be regarded as an adequate correction for the ends and the imperfect cylindricity of the condenser fog chamber. Similarly the equation for the positive ionization is (negative charge)

$$N' = \frac{C \ln R_1/R_2}{600\ \pi l n e} \frac{d(\ln V')}{dt} = \kappa' \frac{d(lnV')}{dt}$$

and the total ionization is therefore $N + N'$.

The experiments below will show that even if the fog chamber is put to earth there is a drift towards negative potential sufficiently steady as to be eliminated in the mean results.

The drift is due to a high permanent voltage which has its seat in the electrometer and is not due to the lighting circuit of the building, for, even when this circuit is cut out, the effect remains with undiminished intensity. It will appear in Chapter VI that in the *absence* of radium and of initial charge in the condenser the equation $I_a = C\dot{V}_a$, where $\dot{V}_a$ for any given ionization is a constant quantity, of the same sign as the voltage of the needle, applies very closely within the limits of measureable $\dot{V}_a$ values. Hence in the presence of radium in the core of the cylindrical fog chamber and a positive charge

$$I_a + 600\ \pi\, lVNev/\ln R_1/R_2 = C\,\dot{V}$$

Thus in this case

$$VN = \kappa d(V - V_a)/dt \qquad -V'N' = \kappa' d(-V' - V_a)/dt$$

and for the same $V = V'$, to a first degree of approximation,

$$N + N' = d(\kappa \ln V + \kappa' \ln V')_{V=V'}/dt$$

numerically, as before. If the equation for N is integrated, and $N/\kappa = K$, since $I_a = C\dot{V}_a$, $\dot{V}_a$ being intrinsically negative for a negative needle,

$$V = \varepsilon^{-Kt}(V_0 - \dot{V}_a/K) + \dot{V}_a K \qquad V' = \varepsilon^{-K't}(V'_0 + \dot{V}_a/K') - \dot{V}_a/K'$$

where $\dot{V}_0$ and V'_0 are the initial positive and negative potentials. Both of these are of the form

$$V = V_0 e^{-Kt} + \left(\dot{V}_a(1 - kN)/K\right)(1 - c^{-Kt})$$

where k is a constant, considered in the next chapter. If $k = 0$, as in the present case, and $V = V'$, the correction would be $\frac{\dot{V}_a}{V}(\kappa' - \kappa)$, which shows that large values of V only are admissible.

58. Data. High ionization. Currents.—The following tables contain the mean potentials $\bar{V}$, the positive and negative logarithmic currents $d(\log V)/dt$ (apart from the constant), the apparent nucleation N positive and N' negative, computed from these data and the additional information at the head of the tables. In most of the cases the corresponding logarithmic currents due to rays outside the fog chamber was carefully measured in the same units by placing a short hard rubber rod between the end t of the aluminum tube (fig. 19) and the wire leading to the electrometer. This cuts out the fog chamber, but leaves the whole remaining circuit undisturbed.

Similarly the leak value of $d(\log V)/dt$ in the absence of radium and due to mere conduction of moist parts is always quite negligible. Thus in the first part of table 23, for relative logarithmic currents in the order of 0.035, the γ ray effect is 0.0010, the conduction leakage smaller than 0.0001. The other extreme, *i. e.*, the value of $d(\log V)/dt$ for the freely falling needle is about 0.1 in the same units. Hence it follows that in the first part of table 23 the needle falls faster than would be quite trustworthy, therefore the auxiliary capacity selected is too small.

Moreover, the negative current only is here measured, as the indispensable need of measuring both currents was not then apparent. Hence in the second part of table 23 the measurement of both currents is undertaken. At the same time the capacity of the condenser has been increased to give the needle the necessary slow descent. The time interval between observations for V is 4 seconds in both parts.

TABLE 23.—Number of ions per cm³. Cylindrical condenser fog chamber. Capacity of system: small auxiliary condenser, 330 cm.; electrometer and wire, 69 cm.; fog chamber, 11.4 cm.; total, 410 cm. Fog chamber: glass $2R_1=13.4$ cm.; aluminum core, $2R_2=0.635$ cm.; $l=39.5$ cm. Velocity of ions: $u=1.37$ cm./sec.; $v=1.51$ cm./sec. in field of volt/sec; $e=3.4\times10^{-10}$. Current due to γ-rays without: $d(\log V)/dt=0.001$; current due to conduction leakage $d(\log V)/dt=0.000081$. Accelerated free fall of needle, $d(\log V)/dt=0.06$ to 0.16 for corresponding deflections. Time interval 4 sec. Radium I+II+III+IV+IV′+V. $\kappa=76\times10^6$. Cm. of scale equivalent to 0.0585 volt.

$\bar{V}$	$d(\log V)/dt \times 10^4$	$N\times10^{-3}$ corrected.	$\bar{V}$	$d(\log V)/dt \times 10^4$	$N\times10^{-3}$ corrected.
I Charge+.			I Charge+ —Continued.		
1.32	145	621	0.37	518	2230
1.10	262	1130	.19	1360	5870
.83	355	1530	.06	1118	4850
.58	445	1910			

TABLE 23—Continued.

The same, with larger auxiliary condensers: Capacity of fog chamber, 11.4 cm.; C'', 1049 cm.; C', 330 cm.; wires and electrometer, 69 cm.; total, 1459 cm. Current due to gamma-rays without $d(\log V)/dt = 0.00021$ (pos. ch.) to 0.00022 (neg. ch.). Time interval 4 sec. Radium I–V. Charges positive and negative. Positive charge $\kappa = 289 \times 10^6$; cm. of scale equivalent to 0.0608 volt. Negative charge $\kappa' = 319 \times 10^6$; cm. of scale equivalent to 0.0613 volt.

$\bar{V}$	$d(\log V)/dt \times 10^4$	$N \times 10^{-3}$ corrected.	$\bar{V}$	$d(\log V)/dt \times 10^4$	$N \times 10^{-3}$ corrected.
II. Charge −.			III. Charge +.		
1.43	4	74	1.42	9	138
1.42	19	323	1.39	33	503
1.39	31	525	1.34	54	827
1.35	37	625	1.26	68	1040
1.30	41	694	1.18	86	1314
1.25	37	625	1.10	72	1102
1.21	35	599	1.03	71	1092
1.17	39	678	.97	75	1150
1.13	35	594	.91	66	1012
1.09	36	610	.85	78	1192
1.06	34	583	.79	84	1288
1.03	32	541	.73	72	1102
1.00	30	509	.68	88	1346
.97	31	525	.63	84	1293
.94	28	472	.58	91	1399
.92	32	541	.53	87	1330
.89	33	567	.49	94	1447
.87	27	456	....	....	....
.84	31	530	....	....	....
.82	32	541	....	....	....
.80	21	355	.37	107	1643
.78	34	578	.34	98	1505
.76	26	440	.30	131	2014
.74	27	456	.27	122	1876
.72	18	302	.24	137	2104
.71	28	472	.19	158	2427
.69	26	440	.18	145	2230

59. The same. Coronas.—Table 23 contains the data for the maxima obtainable with the radium tubelets I, II, III, IV, V, at my disposal. The corresponding corona was a large orange-yellow type, corresponding in my former reductions to 506,000 nuclei in the exhausted fog chamber. I have supposed this to be equivalent to 653,000 when the fog chamber is at atmospheric pressure, seeing that the coronas are actually displaced during exhaustion; *i. e.*, at the maximum ionization does not coincide in the position with the largest corona on exhaustion,* but is displaced in the direction of the exhaust currents. This would seem to mean that exhaustion is more rapid than the reproduction of ions to restock the region of dilatation. In general this inherent discrepancy of a marked

*See Chapter III; also Science, XXVIII, p. 26, 1908.

distribution of ionization increasing from end to end of the fog chamber is still outstanding. It is partially allowed for, since the observations are made near the middle of the chamber, where the average conditions supervene.

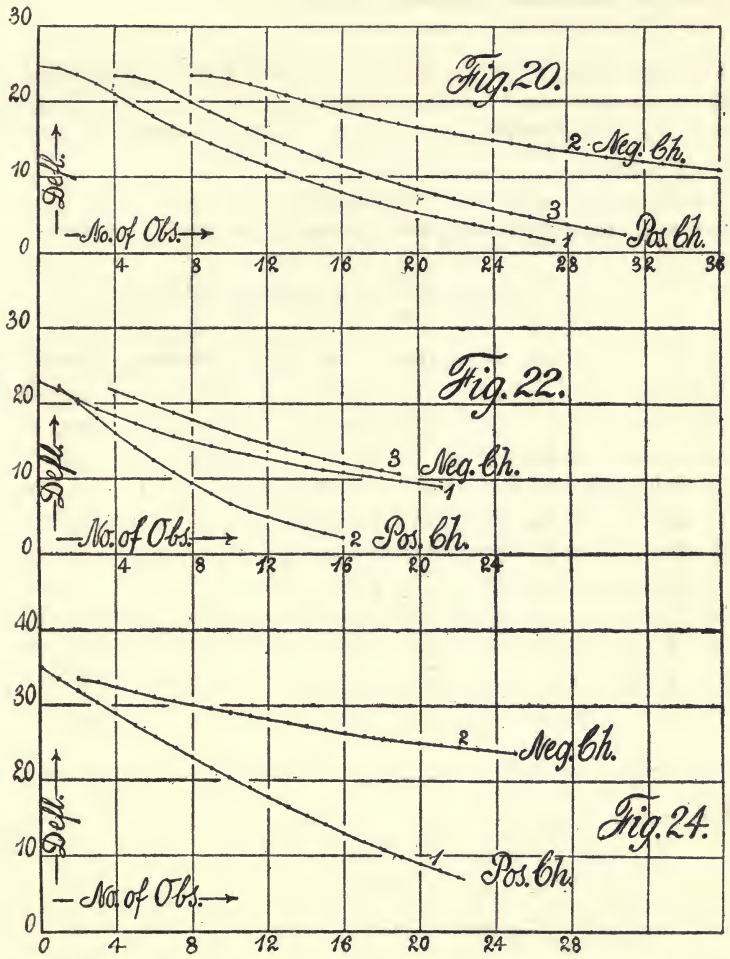

FIGS. 20, 22, 24.—Deflection at the electrometer in successive observations 4 seconds apart, for successive negative and positive charges in the orders of the numbers on the curves.

60. The same. Summary.—The data of table 23 are given in figs. 20 and 21; fig. 20 merely shows the fall of potential in scale readings in the successive observations 4 seconds apart, for positive and negative charges. Fig. 21 gives the corresponding positive and negative *apparent*

ionizations. If the two curves between 0.8 and 1.2 volts be considered, the mean ionization of each is

Apparent positive ions, negative charge	$N =$ 540,000
Apparent negative ions, positive charge	$N' =$ 1,164,000
Total true ionization	$N + N' =$ 1,704,000
Total nuclei caught	650,000

It will be seen that $N+N'$ is the true total ionization positive and negative, if $10^{10}e = 3.4$. Only 65/170, or about 38 per cent, of this is actually caught in the given fog chamber on exhaustion, provided the old coronal values are correct.

If, however, it is assumed that negative ions only are caught during exhaustion in the fog chamber in question, then the value of the electron would be

$$10^{10}e = 3.4 \times 2.62 \times \frac{1}{2} = 4.4 \text{ electrostatic units.}$$

61. Data. Moderate ionization. Electrical currents.—These results were obtained by placing but one radium tubelet, No. IV, in the aluminum tube tt' of the condenser fog chamber (fig. 19). The data were assembled in the same way as the above, $N = \kappa d(\log V)/dt$, as usual, but they are here withdrawn, as they are sufficiently reproduced in the curves (figs. 22 and 23). In the first and second parts of the table positive charges only are treated and the results show the apparent negative ionization. In the third part of table 23, however, both currents are observed in succession and the true total ionization is $N+N'$ as before. Moreover, in parts 1 and 2 the capacity of the condensers is widely varied, 410 to 1459 cm., without showing serious divergence; though to bring this effect out fully both positive and negative currents should have been averaged.

62. The same. Coronas.—At a fall of pressure of 21 cm. or $\delta p/p = 0.27$, the nucleation was stationary and equal to $N = 113{,}000$ in the exhausted fog chamber. At atmospheric pressure, therefore, $113{,}000 \times 1.37 = 154{,}000$ nuclei should have been present. The effect of a charge on the core of the condenser did not appreciably diminish the nucleation or at least the estimate could not be pushed below about 140,000.

63. The same. Summary.—For the case of the third and fourth parts of table in question the successive observations at intervals of 30 seconds apart are shown in fig. 22, the slopes only being of interest. The apparent values of N are given (fig. 23). Though the positive and negative currents are both taken in one section only, parts 3 and 4, all the four series show about the same drift, even though taken many days apart. The condenser effect (excessive rapidity of needle) may be considered eliminated for capacities greater than 500 cm.

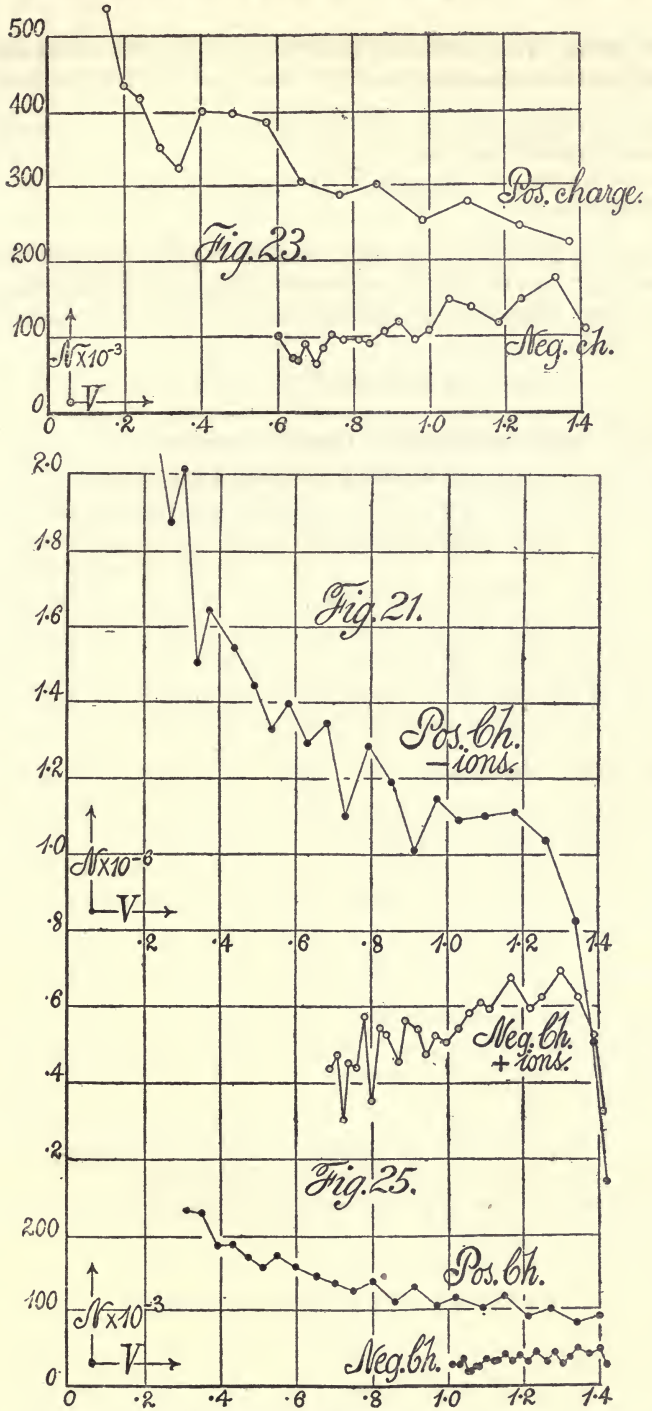

FIGS. 21, 23, 25.—Apparent ionization, N per cu. cm., corresponding to the different voltages, V.

By averaging the ionizations between $\overline{V}=0.6$ and $\overline{V}=1.24$ in both parts 3 and 4 of the experiments made, the data found are as follows:

Apparent negative ions	$N=278{,}000$
Apparent positive ions	$N'=107{,}000$
True total ions	$N+N'=385{,}000$
Total nuclei	180,000

Hence about 47 per cent of all the ions were caught on exhaustion if the values of u, v, e, N, inserted, are correct. Supposing that negative ions only are caught in the above fog chamber the value of the electron would be

$$10^{10}e=3.4\times 2.14\times\frac{1}{2}=3.6 \text{ els. units.}$$

64. Data. Small ionizations. Electric currents.—In the next series the aluminum tt', fig. 19, was surrounded by a lead tube with walls 0.117 cm. thick, leaving the γ rays only effective and these much reduced in intensity. The data are given in figs. 24 and 25.

65. The same. Coronas.—The coronas found at a drop of pressure similar to the above, $\delta p/p=0.300$, corresponded in my reductions to 46,200 nuclei in the exhausted fog chamber. Hence at atmospheric pressure there should have been 64,000. The effect of charging the core was not clear; the reduction could be estimated at 51,000 at the uttermost.

66. The same. Summary.—The drop of potential in scale parts in successive intervals 30 cm. apart is given in fig. 24, showing how much more slowly the negative charges are lost than the positive charges. The apparent values of N are given in fig. 25, to which remarks similar to those already made are applicable. There is the usual drift and the usual temporary fluctuation.

If the mean data be taken between $V=1.1$ and 1.4 volts the results are

Apparent positive ions	$N'=$ 37,000
Apparent negative ions	$N=$ 98,000
True total ionization	$N+N'=135{,}000$
Total nuclei caught	60,000

It follows, then, that about 44 per cent of the total ionization computed from $10^{10}e=3.4$, u and v, is caught on condensation.

If we suppose the negative ions only are caught in the above fog chamber, the electron value is

$$e\times 10^{10}=3.4\times 2.3\times\frac{1}{2}=3.9 \text{ els. units.}$$

67. Conclusion.—Supposing the electron value to be $10^{10}e = 3.4$ electrostatic units as before, the normal velocities of the ions in wet air to be $u = 1.37$, $v = 1.51$ cm./sec. in the volt/cm. field, the coronal value of the ions caught in the above fog chamber is in the several cases

Total ions, 1,700,000	Total nuclei, 38 per cent.
385,000	47 per cent.
135,000	44 per cent.

When N is 1,700,000 the coronas are too diffuse for sharp specification. If it is assumed that negative ions only are caught, and if the nucleations corresponding to the coronas seen in the given fog chamber be taken as developed in my earlier work, then for $N + N' = 1{,}700{,}000$, 385,000, and 135,000, the electron values are $10^{10}e = 4.4$, 3.6, and 3.9 electrostatic units.

With regard to the two parts of this paper that need revision the first, the comparison of the computed condenser capacity C' with a standard, is a minor matter, but the other, *i. e.*, the marked distribution of ionization along the axis of the fog chamber, will need further inquiry. In the direction of the exhaustion the amount of ionization may vary in the ratio of more than 1 to 2, in a fog chamber of about 0.5 meter of length, and this under conditions where there should apparently be no variations and irrespective of the production of radiation from within or from outside of the fog chamber. The final question relating to the drift, and the asymmetry of the curves will be considered in all its bearings in the next chapter.

CHAPTER VI.

THE ELECTROMETRIC MEASUREMENT OF THE VOLTAIC POTENTIAL DIFFERENCE BETWEEN THE TWO CONDUCTORS OF A CONDENSER, SEPARATED BY AN IONIZED MEDIUM.

68. Introductory.—The difficulties encountered in the preceding paper (Chapter V, section 57), were made the subject of direct investigation by replacing the fog chamber with a metallic cylindrical condenser, the core of which was an aluminum tube 50 cm. long and 0.63 cm. in diameter, the shell a brass tube 50 cm. long and 2.1 cm. in diameter, coaxial with the former. Sealed radium tubelets could be placed within the aluminum tube or withdrawn from it. Moreover, either the outer coat or the core of the condenser could be joined in turn with the Dolezalek electrometer, the other being put to earth. The conducting system now appears as shown in fig. 26, C being the outer coat or brass shell, A the aluminum core, and r the radium tubes in the cylindrical core. Conductors are earthed at e. BB show the metallic connections with the auxiliary condensers C' C'', E is one of the insulated quadrants of the electrometer with the highly charged needle N, E being virtually also a condenser.

A Clark standard cell S may be inserted for standardization, but it is otherwise withdrawn.

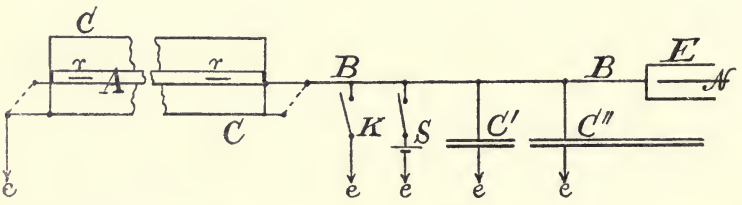

FIG. 26.—Disposition of cylindrical condenser C, auxiliary condensers C' C'', key to earth K, electrometer E, standard cell S. All earthed at e Diagram.

Direct experiment showed the self-charging tendencies to come apparently from the highly charged needle N, or at least to arise in the electrometer E. Positive ions are lodged into the conductor $EBBA$ for a positive needle, negative ions for a negative needle. In addition to this, however, there is a *voltaic* difference, aluminum-brass, at AC when radium is in place and the medium therefore highly ionized. The latter potentials are usually negligible. These are the chief electromotive forces, the first

very high (150 volts) and in a weakly ionized medium, the other low (0.2 volt), but in an intensely ionized medium, but they may eventually produce equal currents. Effectively this is the case. Other voltages such as the room potential may be operative, but their effect proved to be secondary. If the capacities $C'C''$, are successively removed, the electrometer current increases proportionately, showing its origin to be directed from the needle or the electrometer case toward the insulated or non-earthed pair of quadrants.

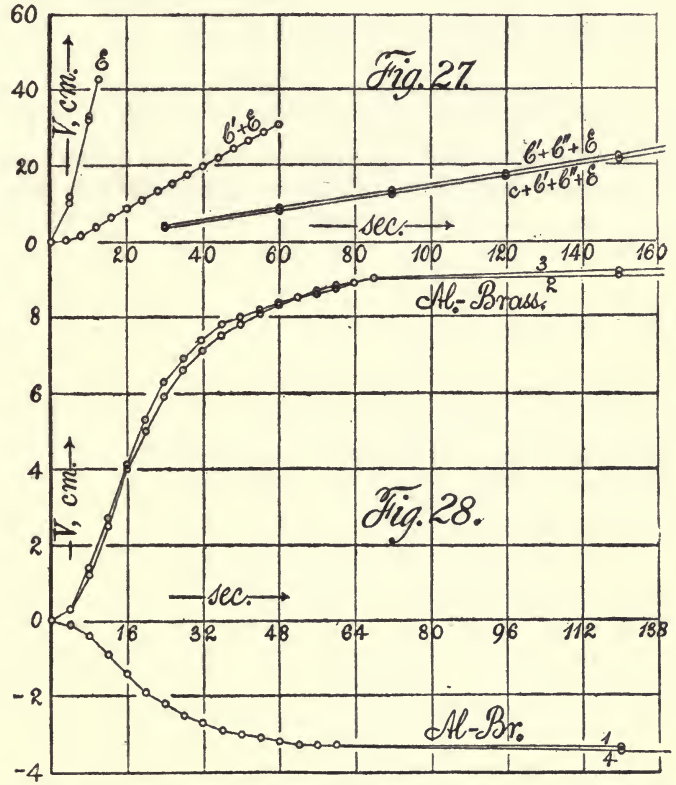

FIG. 27.—Increment of potential (cm. of scale), in the lapse of time (seconds), when the auxiliary condensers are successively removed.

FIG. 28.—Variation of potential V (cm. of scale), in the lapse of time (seconds), when the aluminum core or the brass shell of the electrical condenser are alternately put to earth. Subscript zeros indicate the earthed metal.

If the electrometer metals are reversed (see fig. 26), the voltaic couple is reversed. This makes it possible to obtain both the voltaic contact potential and the ionization in the cylindrical condenser C, from a pair of commutated measurements. If the sign of the charge of the electrometer needle is reversed, the deflection of the needle is not reversed, but

continues to grow indefinitely in the lapse of time in an invariable direction. Hence there must be a source of current in the electrometer, as intimated.

69. Theory.—Let V_n be the potential of the needle, V_c the voltaic potential difference of the two metals of the condenser, the shell being put to earth, V the potential of the insulated conductor BB, measured by the electrometer. Let n be the *apparent* ionization in the electrometer, N the (radium) ionization in the condenser (length I, radii R_1R_2). Let C be the total capacity of the systems $CBBE$. Then

$$\dot{V} = A(V_n - V)n - \frac{600\ \pi l N e v}{C \ln R_1/R_2}(V - V_c)$$

where A is a constant, u and v the normal velocities of the positive and negative ions, e the charge of the electron. The needle is supposed to be positively charged. This may be written

$$\dot{V} = \dot{V}_a - K(V - V_c)$$

where for $N = 0$, $K = 0$, or

$$\dot{V} = \dot{V}_a = A(V_n - V)n$$

i. e., the current in the electrometer, observed in the absence of radium, from needle to quadrants. This is directly measurable with accuracy. It is nearly proportional to V_n since V is much within 1 per cent of V_n.

The integral of this equation is, t being the time,

$$V = (\dot{V}_a/K)(1 - KV_c/\dot{V}_a)(1 - e^{-Kt})$$

the sign of V is negative if $\dot{V}_a < KV_c$, which is the case below. If there is an initial potential V_0 imparted by the standard cell, which is then removed,

$$V = V_0 e^{-Kt} + (\dot{V}_a/K)(1 - KV_c/\dot{V}_a)(1 - e^{-Kt})$$

If, now, the needle is left positively charged, but the condenser metals exchanged (commutated), so that the aluminum core is earthed and the shell now put in contact with the electrometer (see figure), the equation becomes

$$V' = (\dot{V}_a/K)(1 + KV_c/\dot{V}_a)(1 - e^{-Kt})$$

Here K refers to the negative current or normal velocity of negative ions v. Similarly let K' refer to the normal velocity of positive ions u. Also let $\kappa = N/K$ and $\kappa' = N/K'$. Then if $k = V_c/\kappa\dot{V}_a$, and $k' = V_c/\kappa'\dot{V}_a$

$$\dot{V} = \dot{V}_a(1 - kN)e^{-Kt} \qquad \dot{V}' = \dot{V}_a(1 + kN)e^{-Kt}$$

If the potential $V = V_\infty$ at $t = \infty$,

$$V_\infty = \kappa \dot{V}_a / N - V_c \qquad V'_\infty = \kappa \dot{V}_a / N + V_c$$

two equations from which both N and V_c may be found, if the limiting potentials V_∞, V'_∞ and the electrometer current $\dot{V}_a$ are severally observed. If V_∞ is not obtainable, it may be computed from observations at t and $t_1 = 2t$ as

$$V_\infty = (2V - V_1)/V^2 \text{ and } V'_\infty = (2V' - V'_1)/V''^2$$

Here, however, there is a difficulty, as the curves begin with a double inflection not yet explained. The times $t_1 = 2t$ must therefore be estimated from the observations beyond the double inflections, or the rearward prolongation of the curve for those observations, to meet the time axis. The initial tangents may be found in the same way, but this is not necessary, since their values are, respectively,

$$\dot{V}_0 = \dot{V}_a(1 - kN) \text{ and } \dot{V}_a(1 + kN)$$

while

$$V = \dot{V}_a(1 - kN)\frac{1 - e^{-Kt}}{K}, \text{ etc.}$$

A few other relations are often useful, as, for instance,

$$N = \kappa \dot{V}_0 / V_\infty, \; k = \frac{V_\infty}{\kappa}\left(\frac{1}{\dot{V}_a} - \frac{1}{\dot{V}_0}\right)$$

$$\dot{V}_0 = \dot{V}_a \frac{V_\infty}{V_\infty - V_c}, \; V_c = V_\infty(1 - \dot{V}_a/\dot{V}_0)$$

all of which, however, have limited application because of the initial double inflection of the curves.

To solve the transcendental equations the times of two observations may be chosen, so that if V and t, V' and t' correspond, $t' = 2t$. Thus,

$$e^{-Kt} = \frac{V' - V}{V}$$

from which $N = \kappa K$ follows. Similarly,

$$\frac{1}{V_\infty} = \frac{2V - V'}{V^2}$$

If $t' = 2t$ and $t'_1 = 2t_1$, the initial double inflection may in a measure be ignored in

$$e^{-K(t - t_1)} = \frac{V - V'}{V_1 - V'_1}\frac{V_1}{V'}$$

70. Data. Origin of the electrometer current.—The seat of the chief electromotive force or charging current in the electrometer follows from the following data, summarized in fig. 27, in which the capacities C, C', C'', fig. 26, are successively removed. The currents increase in the same ratio as the reduction of capacities, E being that of the electrometer. The data are, potentials in scale parts (where 1 cm. is equivalent to 0.0595 volt), $\dot{V}_a$ being the fall per second:

Capacities.	$\dot{V}_a$ in cm.	$\dot{V}_a$ in volts per sec.
$C+C'+C''+E$	0.14	0.0083
$C'+C''+E$	.15	.0089
$C'+E$	.58	.0345
E	4.3	.256

The change of voltage throughout the main contours of the curves is almost a linear variation with the lapse of time, except that at the beginning the motion is accelerated from rest as usual; for instance:

Time.....	0	4	8	12	16	20	24	28	32	.....60 sec.
V_a.....	0	.3	1.5	3.7	6.1	8.7	11.0	13.4	15.5	.....31.0 cm.

It is the linear character of these curves that greatly simplifies the following measurements.

TABLE 24.—Measurement of ionization N, and voltaic contact difference V_c. Time intervals 4 sec. Aluminum-brass condenser. $l=50$ cm., $2R_1=2.01$ cm., $2R_2=0.634$ cm. Scale part cm.=0.0588 volt. Radium I, II, III, IV, V in aluminum tube. $N=1{,}750{,}000$; $V_c=6.37$ cm. or 0.375 volt.

Deflection.			
(1) Aluminum to electrometer, brass to earth.	(2) Aluminum to earth, brass to electrometer.	(3) Aluminum to earth, brass to electrometer.	(4) Aluminum to electrometer, brass to earth.
0.0	+0.0	0.0	−0.0
− .1	.3	.3	− .1
− .4	1.2	1.4	− .4
− .9	2.5	2.7	− .9
−1.4	4.0	4.1	−1.4
−1.9	5.0	5.3	−1.9
−2.2	5.9	6.3	−2.3
−2.5	6.6	6.9	−2.6
−2.7	7.1	7.4	−2.8
−2.9	7.5	7.8	−2.9
−3.0	7.8	8.0	−3.0
−3.1	8.1	8.2	−3.1
−3.2	8.3	8.4	−3.2
−3.2	8.5	8.5	−3.3
−3.3	8.7	8.6	−3.3
−3.3	8.8	8.7	*−3.5
*−3.4	8.9	*9.2	*−3.6
	9.0	*9.4	
	*9.0		
	*9.2		

* After additional 60 sec.

TABLE 25.—Voltaic contacts, Al-Zn, Al-Cu, Al-Al. Four-sec. intervals (usually) between observations for V. Scale part cm. = 0.092 volt. $Va = 0.0454$ cm. Positive needle. Radium I to V. $K = 36.1 \times 10^{+6}$.

V for Al-Zn.			V for Al-Cu.			V for Al-Al.		
Zn to earth.	Al to earth.	Zn to earth.	Cu to earth.	Al to earth.	Cu to earth.	Shell to earth.	Core to earth.	Shell to earth.
−0.0	0.0	−0.0	0.0	0.0	0.0	+0.0	+0.0	+0.0
− .0	.0	− .0	− .1	.1	− .1	.0	.0	.0
− .2	.4	− .1	− .5	.7	− .5	.0	.1	.0
− .3	.8	− .3	−1.2	1.6	−1.3	.0	.3	.1
− .5	1.3	− .3	−2.0	2.6	−1.9	.1	.6	.2
− .7	1.7	− .5	−2.7	3.5	−2.6	.2	.8	.3
− .9	2.0	− .6	−3.2	4.2	−3.1	.3	.9	.4
−1.0	2.2	− .7	−3.7	4.7	−3.5	.3	1.1	.4
−1.0	2.4	− .7	−4.0	5.1	−3.8	.4	1.2	.5
−1.1	2.5	− .8	−4.2	5.4	−4.1	.4	1.3	.5
−1.1	2.7	− .8	−4.4	5.7	−4.3	.5	1.5	.5
−1.1	2.8	− .9	−4.6	5.9	−4.4	.5	1.6	.6
−1.2	2.8	− .9	−4.7	6.1	−4.5	.6	1.7	.6
−1.2	2.8	− .9	−4.8	6.3	−4.7	.6	1.8	.6
−1.2	2.9	− .9	−4.9	6.5	−4.8	.6	1.9	.6
−1.3	2.9	− .9	−5.0	6.6	−4.8	*.6	1.9	.6
*−1.3	*3.0	−1.0	*5.3	*6.9	*−5.2		1.9	*.8
		*1.1	*5.3	*6.9	*−5.2		*2.1	.8

* After further 60 sec.

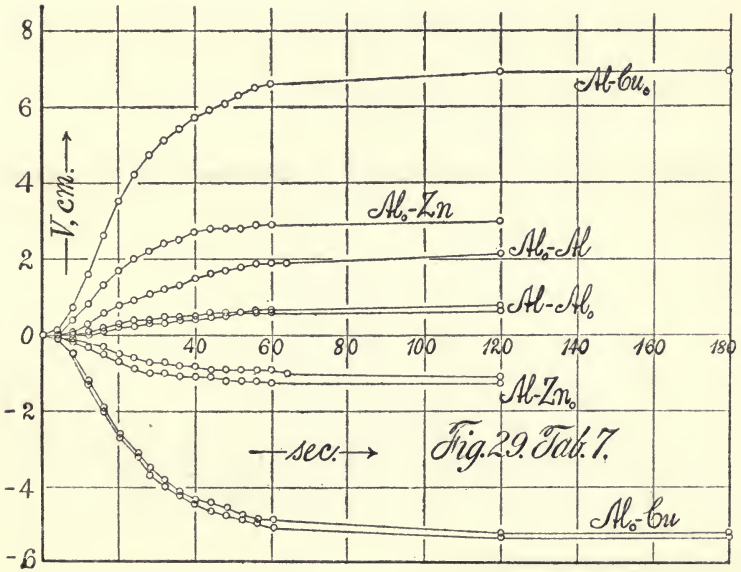

FIG. 29.—Variation of potential (cm. of scale) in the lapse of seconds for aluminum-copper, aluminum-zinc, and aluminum-aluminum condensers. Subscript zeros show the earthed metal.

71. Aluminum core charged with radium tubelets I-V. Data.—The air in the condenser C is now highly ionized and its voltage becomes appreciable. The data obtained are given in table 24 and fig. 28. The needle is positively charged thus (virtually) impelling positive ions toward the quadrants of the condenser. In the four series of data observed the aluminum core of the condenser is twice joined to the electrometer, the brass shell being put to earth (series 1 and 4) and twice commutated (aluminum to earth series 2 and 3). The results are identical, except that in series 3 the insulation was perhaps better. The accelerated march of the needle from rest is obvious in both curves and is thus independent of the sign of the limiting voltage V_∞. It may be mere inertia, but it is of less consequence here because the initial data are not needed in the computation of table 25.

72. Results. Ionization N. Voltaic contact potential difference V_c.—The equations

$$V_c = \kappa \dot{V}_a / N - V_\infty \qquad -V_c = \kappa \dot{V}_a / N - V'_\infty$$

may now be used to compute N and V_c. The constants are numerically (all in scale parts, 1 cm. equivalent to 0.0595 volt)

$$\kappa = 36.1 \times 10^6 \quad V_\infty = -3.45 \quad \dot{V}_a = 0.142 \quad \kappa' = 39.7 \times 10^6 \quad V'_\infty = +9.3$$

Hence

$N = 1{,}750{,}000$ ions, either positive or negative.
$V_c = 6.37$ cm., or 0.38 volt.

73. Voltaic contacts: aluminum-zinc, aluminum-copper, aluminum-aluminum.—The results obtained for aluminum-brass made it desirable to investigate similar cases for other metals and zinc; copper and aluminum suggested themselves. These were used in form of thin sheets of the metal, bent into cylindrical shells about as large as the above brass shell. No special care was here taken to secure accurate diameters, nor to prepare the metal surfaces. The aluminum core with the radium tubelets (I to V) within, was the same as heretofore. The data are shown in table 25 and in fig. 29. All potentials are given in scale parts where 1 cm. is equivalent to 0.092 volt. The charging current for the electrometer, found in the absence of radium before and after these experiments, was $\dot{V}_a = 0.0454$ cm.

Since we may write algebraically

$$N = \dot{V}_a \cdot 2\kappa / (V'_\infty + V_\infty)$$

and

$$V_c = \kappa \dot{V}_a / N - V_\infty = V'_\infty - \kappa \dot{V}_a / N$$

remembering that V_∞ is negative, while V'_∞ is positive, the following data appear:

Couple.	N	V_c	V_∞	V'_∞
		Volt.	*cm.*	*cm.*
Al-Cu	5,050,000	0.558	−5.25	+6.90
Al-Zn	1,790,000	.191	−1.17	3.00
Al-Al	1,140,000	.065	+0.73	2.15

The large nucleation obtained here for copper remains unexplained. It was somewhat reduced in other similar experiments, but remained high. Since $V'_\infty + V_\infty = 1.65$, slight differences in contact would produce a serious effect. From these data it follows, finally, that the voltaic contact zinc-copper is 0.367 volt. After cleansing with acids data like Al-Cu = 0.58 volt, Al-Zn = 0.06 volt, or Zn-Cu = 0.52 volt were obtained, which varied again after other treatment.

74. Further experiments. Conclusion.—In addition to the above experiments, a great variety were made, as, for instance, with weaker radium (single tubelets) in the core of the condenser; with radium inside and outside of the condenser; with the metal surfaces cleansed with acids, or polished, or aged, etc. A few data may be referred to here.

The highest nucleation for an aluminum core charged with radium tubelets occurs in case of a copper envelope for the condenser. Somewhat smaller values occur for zinc and brass, and the smallest for aluminum shells. The agreement is usually unsatisfactory. The voltaic contacts are such as to place zinc-copper at 0.4 to 0.6 volt. The data for groups of radium tubes are larger than the values computed from individual tubes, $N = \sqrt{N_1^2 + N_2^2 + \ldots}$, probably from the effect of secondary radiation and non-uniform ionization. We may also ascribe the high ionization in a copper shell as compared with a low ionization in an aluminum shell to the same cause. If the radium is placed without the condenser the voltaic contacts do not appreciably differ from the values found when the radium tubelets lie in the core. One may note that even in the aluminum-aluminum condenser the voltaic contact is not zero but about 0.05 volt. In other instances non-commutated electromotive forces often appear. The contact Al-Zn is peculiarly variable even as to sign.

As a whole these experiments lead to no general conclusion of relevancy here and they have therefore been withheld from detailed consideration.

Finally, to detect the source of the electromotive force in the electrometer, this was replaced by another instrument, No. 2, of the same kind,

as soon as it could be obtained. The absence of electric current $\dot{V}_a = 0$ in the new instrument and its presence in the old electrometer made it necessary to overhaul the latter. It was eventually found that the brass case had been insufficiently earthed,* so that a current from the Zamboni cell, breaking through the hard rubber insulation at the top of the quartz-fiber suspension kept the case charged to a high-constant potential. This charge thereupon gradually leaked into the insulated quadrant through the amber insulators, producing the current $\dot{V}_a$ corresponding to the sign of the electrode of the Zamboni pile and of the electrometer needle. On providing the case of the old electrometer with a well-earthed clamp, the current $\dot{V}_a$ vanished. The new electrometer did not show this defect even when the case was not specially earthed, whereas any insulation of the old electrometer immediately restored $\dot{V}_a$.

Fortunately, however, $\dot{V}_a$ is so remarkably constant that it can actually be used in the measurements with advantage, as was done in the present chapter, or eliminated by commutation, as was done in Chapter V.

*Probably owing to a thin film of varnish which had escaped detection. The room was so dry that no discharge occurred through the feet of the instrument.

7 DAY USE
RETURN TO DESK FROM WHICH BORROWED

PHYSICS LIBRARY

This publication is due on the LAST DATE stamped below.

MAY 16 1988

RB 17–60m-8,'60
(B3395s10)4188

General Library
University of California
Berkeley

QC9
B37
Phys
Lib.